A STUDY ON FIRE SUPPRESSION MECHANISM IN TALL HALLS BY LONG-THROW SPRINKLER

DONG XUE

Ph.D

The Hong Kong Polytechnic University

2016

The Hong Kong Polytechnic University

Department of Building Services Engineering

A STUDY ON FIRE SUPPRESSION MECHANISM IN TALL HALLS BY LONG-THROW SPRINKLER

DONG XUE

A thesis submitted in partial fulfillment of the
requirements for the Degree of Doctor of Philosophy

August 2015

CERTIFICATE OF ORIGINALITY

I hereby declare that this thesis is my own work and that, to the best of my knowledge and belief, it reproduces no material previously published or written, nor material which has been accepted for the award of any other degree or diploma, except where due acknowledgement has been made in the text.

(Signed)

(Name of student) DONG XUE

Department of Building Services Engineering

The Hong Kong Polytechnic University

Hong Kong, China

August, 2015

Abstract

Abstract of the dissertation entitled:

A study on fire suppression mechanism in tall halls by long-throw sprinkler

Submitted by DONG Xue

for the degree of Doctor of Philosophy in Fire and Safety Engineering

at The Hong Kong Polytechnic University in August 2015.

Designing fire suppression in tall and large spaces is a challenge. Tall and large spaces typically contain large fire loads that can lead to a rapid increase in temperatures during an accidental fire. Conventional fire suppression systems are not able to extinguish fires in tall and large atria. The water droplets distinguished from sprinkler systems can either be vaporized or carried away by the fire-induced hot air currents in tall and large spaces. In this thesis, the fundamental principles of rapid and effective fire extinguishment, the major findings and limitations of existing sprinkler systems widely used were identified first. A side-wall long-throw sprinkler system is then proposed. The characteristics of the system including their structure, flow coefficient, operating pressure, sprinkler head distance and installation height were then studied.

The experimental portion of the study was started by establishing the key experiment parameters for the long-throw sprinkler, including the use of a 10 MW fire. Appropriate wood cribs were selected as the experimental fire in this study. The heat release rate characteristics for different arrangements of wood cribs with different numbers of wood cribs and placements were explored. Tests were conducted on the

water distribution qualities of sprinklers in a hall with different installation heights of 6 m, 8 m and 10 m under operating pressures of 0.2 MPa, 0.35 MPa, and 0.5 MPa respectively. The results were used to justify numerical simulations. Experimental results are then correlated with the most desirable water distribution characteristics for proposing design practices.

The Computational Fluid Dynamics (CFD) model Fire Dynamics Simulator (FDS) was then used to study the performance of proposed side-wall long-throw sprinkler systems. Two sets of four scenarios on sprinkler fire were adopted for CFD-FDS simulation. The size distribution of water droplets, sprinkler flow effectiveness, sprinkler head design, fire extinguishing system activation time and heat transfer characteristics between smoke and sprinkler water droplets were studied. For medium hazard classes, sprinklers with flow coefficients 115 and 161, installation heights higher than 10 m and operating pressure of 0.5 MPa are found to be appropriate for extinguishing fires.

Full-scale experiments were conducted on sprinkler fire for justifying CFD-FDS predictions. Important technical requirements for designing sprinkler for tall and large halls are the proportion of large water droplets discharged from the sprinkler system reaching the fire. The concept of Actual Delivered Density and Required Delivered Density were applied to evaluate the performance of sprinkler systems. Results from full-scale experiments are consistent with those from the mathematical models.

Keywords: tall and large halls, automatic sprinkler fire extinguishing mechanism, water distribution, side-wall long-throw sprinklers, penetration of water droplets

Acknowledgment

I would like to express my sincere thanks to my Chief Supervisor, Professor W.K. Chow, for his enthusiastic and patient guidance, continuous kind support and invaluable advices on this research.

I wish to thank my Co-supervisor Dr Geoffrey Y.K. Shea, who has always offered his strong support and invaluable suggestions to me. Thanks are also due to Zhou Xiangyi, Director of Jin Dun Fire Laboratory for giving me this valuable opportunity to join their study and their kind support to the laboratory work.

Last but not least, I would like to thank my family for their continuous and wonderful support, encouragement and understanding. Special thanks to my university, academic staff at the Department of Building Services Engineering and all my fellow classmates for their support and providing me a good study environment.

Table of Contents

List of Figures

List of Tables

Chapter 1 Introduction

1.1 Overview

With continued economic advancement and the improvement of technology, various buildings with tall halls have emerged. These tall halls are found in shopping malls, public transport terminals, hotels, cargo terminals and banks constructed all over the world since 1980 (Chow 1989). This type of construction causes difficulty in creating different fire zones, rendering traditional fire detection and fire extinguishment methods to be severely limited. Fire prevention, control and safety techniques for areas with tall halls are considered increasingly important around the world.

Areas with tall halls are typically located in places with high population density, such as exhibition centres, large integrated shopping centres with catering and entertainment facilities such as restaurants and cinemas. According to fire statistics compiled up to first half of 2009 (Central People's Government of the People's Republic of China 2009), there were 7,899 fire disasters in mainland China in areas with high population density, losing RMB 114 M. Casualties and injury tolls amounted to 94 and 77 respectively, in which 53 casualties were in shopping malls and cinemas, and 20 were in entertainment centres. Casualties amounted to 56.4% and 21.3% of casualties in areas with high population density. As areas of tall halls contain relatively large spaces, they are able to accommodate more people and store more objects. As a result, in the event of a fire disaster, an inability to quickly extinguish or control the

situation will result in grave consequences for the country and for society.

Fire suppression equipment used for fighting early-stage building fires typically include fire hydrant systems, fire water gun system and automatic sprinkler systems. Hydrant systems are conventional fire suppression facilities. In the event of a fire, they require on-site manual operation, with effectiveness limited by the time taken to sound and respond to the fire alarm, situation onsite, status of fire suppression equipment, and other factors. Using hydrant systems is not the main technique to fight fires in areas with tall fire halls. Traditional fire safety equipment is heavy and cumbersome, and do not come with the ability to detect and position the source of fire. Extinguishing fires using this method not only requires manual operation, but also requires a lot of water, with the risks of flooding. Thus, fire hydrants cannot be the only suppression system in such tall halls.

However, some halls are observed to store high amounts of combustibles as in Figure 1.1. Burning such combustibles would give a big hazardous fire (Chow and Wong 1993, Chow 2012a, 2012b, 2009b; Chow and Lo 2008). It is difficult to protect these halls by sprinklers as raised years ago (Chow 1996, 2009b, 2012c, 2012d, 2012e).

Recently, smart fire extinguishing systems called ‘water guns’ are increasingly used. The system can locate the fire and sound the fire alarm system known as homing fire extinguishing systems. This type of product comes with automatic positioning and firing systems, with water levels typically greater than 16 L/s, with some in the range of 10 L/s to 16 L/s, as shown in Figure 1.2. But these systems have weaknesses in splashing out of fire extinguishing water flow. Therefore, the ability to distribute water

is poor and inefficient, they cannot be blocked by objects in the way, and not yet intelligent enough to locate the fire source accurately. Thus, these systems have to be monitored by fire safety management personnel due to their ineffectiveness. Water guns with an infra-red ray scanning fire detection and interlocking controller system were used in huge space fire suppression with flame sensors (Yamada 1995). Although appropriate design can give a wide water coverage area, their effectiveness in controlling a fire (Chow et al. 2004) should be further explored to demonstrate suppression capability and reliability.

As the first choice of automatic fire extinguishing method since its invention over 200 years ago, automatic sprinkler systems are widely used in many different locations, with different types of sprinkler heads and system types, and have been continuously improved over time. However, areas with many objects, high clear height, significant use of decorations and furniture might result in a large fire base, high fire load, increase in rate of temperature rise, fast expansion of fire disasters, high heat release rate, early appearance of flashover, high emissions of smoke, high potential for harm, difficulty in expelling, high fire disaster danger rate, and other distinguishing characteristics. Traditional automatic sprinklers have difficulty in bringing water to the surface of combustible objects, and thus controlling fires.

It is important to modify the traditional techniques toward automatic sprinkler systems starting from fire extinguishment principles to develop systems to quickly detect temperature rise in a fire. Appropriate action should be taken at the early stage of the fire. The system should not only distribute water evenly by effective water discharge rate, but also allow water to penetrate upward hot currents.

Side-wall long-throw sprinklers at height activated by a fire detection system are therefore recommended (Chow et al. 2006, 2011; Hung and Chow 2001, Chow 2012c, 2012d, 2012e) as an appropriate system for tall halls unlikely to store large quantities of combustibles. As demonstrated by the preliminary field tests (Chow et al. 2006, 2013), water distribution density required in acceptable standards can be provided in the protected coverage areas, though there are some challenges. Performance of the long-throw system will be evaluated thoroughly in this thesis. Technical problems related to effectively control and extinguish fires in tall and large halls will be pointed out first. Experiments were carried out to observe the sprinkler-fire interaction phenomenon, using experimental evidence to validate theoretical principles, and consolidated related technical analysis. Full-scale experiments that meet the standard requirements of fire extinguishing experiments were performed to validate the results from mathematical modeling. The results compiled will give guidelines in developing automatic sprinkler techniques for extinguishing fires in tall and large halls.

1.2 Other Studies Related to this Topic

Experimental data on wood crib fires were studied by Smith and Thomas (1970). Results collected from prior experiments demonstrated that the burning rates of wood cribs can be correlated by empirical formula.

The heat of combustion during the growth phase of wood cribs made of sugar pine was investigated by Heskestad (2006). These measurements were generalized to any combustible object. The convection value was found to be almost constant in the growth phase, doubling value in the decay phase.

Experiments were conducted by Croce and Xin (2003) to evaluate a scheme for quasi-steady wood crib fires in enclosures. Modeling schemes such as Froude modeling, pressure modeling and radiation modeling were included. The results suggested that appropriate model was used to predict the fire environment and burning rate in enclosure fires. The burning rate, gas temperature and wall temperature correlated well with experimental data. However, the combustion product concentration and radiative heat flux were not correlated well.

The heat release rate of various objects were calculated by Hansen and Ingason (2011) using three methods results. Results are compared with experimental results wood cribs placed at equal distance from one another. One of the methods used the critical heat flux, and the other two used the ignition temperature as the ignition criteria. Experimental results showed that the first method gave the heat estimation agreed well with the theoretical conclusions.

A series of cone calorimeter tests were conducted by Xu et al. (2008) to examine the combustion behavior of small-scale wood cribs. Wood cribs frequently used in fire experiments gave consistent heat release rates. Their behavior also resembles closer to the development in real fires. The heat release curves of small wood cribs are different due to the porosity. A marked difference is noted between large-scale wood cribs and small-scale wood cribs. For large-scale wood cribs, the surface char formation effect is greater. Small-wood cribs are easier to burn away completely.

1.3 Outline of the Thesis

In Chapter 1 and 2, starting from the fire and safety questions associated with tall and large halls and through the analysis of the special fire characteristics of buildings with tall and large halls, early detection and rapid and effective fire extinguishing were pointed out as the key operating principle. With conventional fire sprinkler systems, the water droplets discharged may be vaporized in the air currents created by smoke in tall and large halls, thereby being unable to control the fire expansion. Automatic fire sprinkler system research needs to address this critical problem. Through research on automatic sprinkler system developments and fire extinguishing systems related to this type of fire disasters, the main type of system and technical parameters to focus on, key sprinkler structures, mathematical modeling and real-life experiments were proposed to evaluate the heat release rate of various typical combustion materials. The appropriate real-life fire disaster experimental model was confirmed. The basic requirements for automatic sprinkler systems were proposed. An experiment platform for automatic fire extinguishing sprinkler systems was created and research on the water distribution qualities of typical sprinklers were conducted. The Computational Fluid Dynamics (CFD) software Fire Dynamics Simulator (FDS) (McGrattan 2005) was commonly used to conduct research on the interaction between fire load and sprinkler operations, and real-life experiments were conducted to validate the modeling results (Chow et al. 2011). The critical factors affecting the effectiveness of fire extinguishing sprinklers were confirmed, and appropriate sprinkler structures and basic operating parameters (flow coefficient, operating pressure, sprinkler head distance, installation height) were proposed.

The basic testing and experimental study was described in Chapters 3, 4, 5 and 7. First, the heat release rate in a fire disaster and the selection criteria for typical combustion materials were described, and the principles for measuring heat release rate based on the oxygen consumption principle were detailed. Past research on the heat release rate of various types of combustible materials were revisited, and appropriate criteria to select broadly applicable combustion materials that can substitute for combustion materials in real fire disasters were devised.

Wood crib fires (DiNenno et al. 2002; Bill 1993; Nam 1996, 1999; Song and Li 2013) will be used in experimental studies in this thesis. The measurement requirements of the 10 MW large thermal system were introduced. Heat release rates achieved in burning one, two, three or four wood cribs placed in a straight line, one on top/two below, or stacked placement methods were measured. Various heat release rate changes and phases of change were obtained and the key characteristics of the subject materials in the stable burning phase were identified, establishing a sound basis for subsequent research in full-scale experiments. Through analysis of the fire extinguishing areas of tall and large spaces, fire extinguishing requirements were identified. The use of side-wall long-throw sprinklers in tall and large spaces, and the open fire extinguishing system were innovatively proposed. Based on related standard requirements, an experiment platform was built for the testing of sprinkler water distribution characteristics, and research were conducted on the water distribution qualities of sprinklers at installation heights of 6 m, 8 m and 10 m, and under operating pressures of 0.2 MPa, 0.35 MPa and 0.5 MPa. Based on the water distribution experimental results, three types of sprinkler numbers and sprinkler related techniques giving the best water distribution characteristics were identified.

Chapter 6 and 8 focused on the mathematical modeling of a typical fire disaster scenario and full-scale experiment validation work. First, the theoretical basis was introduced for choosing the FDS (Chow and Yin 2002) fire extinguishing modeling software: basic control processes, combustion models and radiation models provided the typical FDS use case scenario. Then, from the size of the water distribution of water droplets, sprinkler flow effectiveness, sprinkler head design and fire extinguishing activation time set up, heat transfer between fire disasters, smoke and sprinkler water droplets, the basic theoretical basis for sprinkler water distribution was described. Based on these, the main operating parameters for the mathematical models were established, including the fire source effectiveness and experimental conditions for the fire extinguishing system. The threshold conditions were innovatively enriched and models were made that allowed FDS (Zhang et al. 2002) to be suitable for modeling side-wall sprinkler systems. Two sets of four typical application scenarios were designed for the purposes of mathematical modeling. Through the modeling results, the fire control and extinguishing results under three types of side-wall sprinklers with three different flow coefficients were obtained. It is concluded that sprinkler heads with flow coefficients 115 and 161, at installation heights above 10 m and operating pressure of 0.5 MPa, are capable of extinguishing medium danger fires.

This thesis initiated research on the use of side-wall long-throw sprinklers in tall and large halls. Full-scale experiments for validation were conducted that can innovate in the areas of the operating principles, application height, design parameters and fire load selection. The requirements for fire extinguishing system, sprinkler choice, and fire extinguishing and control are the same as those for the mathematical model. The validation results are also consistent with the results from the mathematical models. In

the use of sprinkler extinguishing techniques in tall and large halls, there are also higher requirements for the proportion of large water droplets in the sprinkler emissions compared to ordinary height areas. Actual Delivered Density (ADD) and Required Delivered Density (RDD) will be studied with fire experiment set up matching with the fire load requirements. Through collection of the water discharged by the sprinkler head that can penetrate the fire plume and hot air currents and reach the surface of the combustion materials, the water sprinkler distribution density was measured and the results under similar water distribution scenarios were compared. Preliminary research on the penetrability of sprinkler water droplets was conducted. The results from the full-scale experiment are again consistent with those by the mathematical model.

The key research areas of this thesis and areas of innovation were concluded in Chapter 9, with areas suggested for future research.

Chapter 2 Research Background

2.1 Tall Halls

With rapid economic development, tall buildings and large spaces have become the distinguishing characteristics of cities' industrial and commercial developments. In today's cities, commercial centres, exhibition centres, logistics centres and other large spaces have emerged. These buildings can be classified in two types. The first type is buildings that occupy a large area and have a high clear height. This type of building typically comprises high plot ratio buildings, with heights 8 m to 20 m. For example, large-scale department store, food and beverage and entertainment integrated centres, indoor sporting centres, cinemas, airports, etc., are illustrated in Figures 2.1 and 2.2. The second type is buildings that occupy a limited area but have very high clear height, as indicated in Figures 2.3 and 2.4.

2.2 Fire Hazards of Tall and Large Halls

Fire hazards in buildings with tall and large spaces are different from ordinary buildings in several ways with at least three distinguishing characteristics. Firstly, interior spaces relatively large and connected, thus creating varied and complex assortments of combustible objects and environments. Air supply for ventilation would support the fire development, causing the easy creation of large amounts of smoke, creating difficulties in evacuation and extinguishing of fires. It is very important to

emphasize early detection and rapid extinguishing of fires in tall and large spaces. Secondly, traditional fire detection techniques do not meet the requirements of fire detection in tall and large spaces. Due to the height and width of the spaces in question, the smoke created is diluted by the circulation of air flow and the reduction in temperature at greater heights. This creates difficulties in smoke detection, making it easy to miss the most opportune time to start fire extinguishing. Lastly, water discharged from ordinary sprinklers evaporate easily due to convection currents, making it difficult for the water to land on the surface of the fire. Even if part of the water may be able to penetrate the smoke and land on the fire surface, the weakened concentration renders it unable to stem the expansion of the fire.

How these fire hazards can be controlled by automatic fire extinguishing techniques in tall and large halls will be investigated in this thesis.

2.3 Overseas Automatic Sprinkler Systems

Sprinkler systems are one of the most widely applicable and effective automatic fire extinguishing systems in the world. The first sprinkler system was used in 1812 in the Royal Theatre of England (Yang 2012). Sprinklers to date span more than 200 years of history. Through one DN250 main pipe, water flow is directed to three branching pipes, with 2000 emission heads 15 mm in diameter. Valves are used to separate the system into many protection zones, and they are manually activated depending on the location of the fire site.

Sprinklers were first used (Song and Yang 2008) in the United States in 1852, initially only used to protect factories and textile mills, later expanded to protect scotching, carding and spinning workshops. Sprinkler heads are 0.25 mm in diameter, each separated with a distance of 220 mm, with fixed locations beneath the ceiling. When extinguishing fires, water is discharged towards the ceiling, which then lands on the combustible objects and the floor. However, this type of system has two fatal weaknesses. First, due to limitations in water distribution, water use is unduly large. Second, if the sprinkler heads are congested by dust or other sediments, there is a high likelihood of system failure, rendering it unable to extinguish fires.

The Harrison sprinkler head (Song and Yang 2008) was produced in 1864 with copper. It consists of multiple emission points, spanning 50 mm to 75 mm, with a piston connecting the top of the shell to the bottom, and a soft rubber valve near the sprinkler heads, suspended by thin ropes, as shown in Figure 2.5. It operates based on the following principle: in case of fire, the thin rope will be burned, causing the piston to drop, opening the valve, causing water to emit from the shell of the sprinkler, and covering the fire site.

As reviewed by Williams (1993), in 1847 in the United States, Parmelee invented a sprinkler that activates automatically through the use of fusible alloy as a temperature detection device. This was the earliest automatic sprinkler that was widely used. More than 100,000 of this type of sprinklers were manufactured, and used in 19 fire disasters in mills, demonstrating the potential for the wide use and development of sprinkler systems. Parmelee’s invention provided the essential technique behind automatic sprinkler activation in the event of increase in heat of the surroundings. This had a

seminal impact on the subsequent development of automatic sprinkler systems, and the basic principles are still being used today.

Sprinklers in Parmelee's times were relatively cumbersome and heavy. Some sprinkler heads were as heavy as 1.3 kg. Furthermore, sprinkler sealability and water distribution ability remained undesirable. In 1882, American Grinnell invented fusible alloy strut-type nozzles (Williams 1993), crystalizing another leap forward in the development of automatic sprinklers. Grinnell's sprinkler crystalized the distance between water and fusible alloys, significantly reducing the heat transferability between water and fusible alloy, increasing the heat sensitivity of the sprinklers.

Glass bulb sprinklers were originated in 1922 as reviewed by (Williams 1993). Initially, the main change was to replace fusible alloy with working fluid glass bulbs. It was only 10 years later that there were significant improvements. Glass bulbs and the combination of cushions and adjustable screws ensured the security of the sprinkler. A representative Grinnell glass bulb sprinkler is shown in Figure 2.6. The conventional sprinkler, spray sprinkler and side-wall sprinkler are shown in Figure 2.7.

Early stage automatic sprinklers can only control the opening of the sprinkler and volume of water discharged, but not the distribution of water. Through longstanding experimental research and application, users discovered that sprinkler effectiveness does not only rest upon water throughput, but also the even distribution of water. In 1953, after incorporating the ability to control the even distribution of water, today's standard sprinkler that is used widely around the world was invented (Figure 2.8).

Standard sprinkler technique was standardized (Si 2004; National Fire Protection Association 2002) in the United States in 1953. In the 1960s, the needs of a number of new fire sites, along with the introduction of closed-type sprinkler systems and techniques to analyze the sprinkler Response Time Index (Si 2004; National Fire Protection Association 2002) spurred the rapid development of automatic sprinkler systems in three directions. First, sprinklers capable of penetrating high stock piles and large drop sprinklers were developed. Second, Fast Response sprinklers were designed to meet the requirement to protect human lives. Third, for aesthetic purposes, small bulb sprinklers with a diameter no wider than 5 mm were developed. With the development and wide use of plastic chemicals and increase in building heights, the American United Plant Laboratory initiated specialized research on large drop sprinklers, with the requirement to have sufficient water pressure to penetrate the strong upward air currents in strong fires. In the 1980s, early suppression fast response sprinklers were developed. This sprinkler not only provides early response, but also increases the ability to extinguish fires even with small numbers of sprinklers.

Nonetheless, the availability of sprinklers in the event of a fire is also very important. Hauptmanns et al. (2008) used fault tree analysis to evaluate the availability of fixed wet sprinkler systems and proposed an approach for assigning a numerical value on the availability of the system. The team identified certain measures that could be implemented that would improve the availability of the system by a factor of 10 without needing changes to the hardware.

2.4 Development of Automatic Sprinkler Techniques in China

Towards the end of 1920s, garment factories and public facilities in Shanghai, China started having wet systems installed (China National Standard 2005b). For example, the No. 17 factory in Shanghai built in 1926 had wet systems installed in the office, garage and storage rooms. The Shanghai International Hotel built in 1934 also had wet systems installed in guest rooms, kitchens and restaurants. In the 1950s, factories helped built by the Soviet Union in China also contained wet systems.

From the 1970s onwards, research and development in automatic sprinkler systems was started (Gao and Xu 2003) at the Sichuan Fire Institute, Tianjin Fire Institute and related enterprises. In the 1980s, the glass valve sprinkler was developed (Song and Yang 2008). In the mid-1990s, the early suppression fast response (ESFR) sprinklers, camouflaged sprinklers and other new products were also developed (China National Standard 2005b). This rapidly transformed the previous reliance on imports for fire and safety systems. The fire system safety standards developed by the Tianjin Fire Institute started being widely adopted in the late 1990s. In 2002, the China Certification Center for Fire Products (CCCF) started (Hu and Yu 2010) using identifiers for all fire and safety related products sold in China, as the industry started developing at a rapid pace. According to some studies, as of 2013, the number of automatic sprinklers manufactured each year exceeded 45 million, with more than 100 different types and 30 million units used. Traditional specialized valves produced also exceed 1 million units. China has become the world’s largest manufacturer and user of automatic sprinkler systems.

At the same time, China also initiated research (Song and Li 2013; Liu et al. 2014) on related techniques: closed-end sprinklers' response time index testing devices, oxygen consumption calorimeters at MW level, automatic sprinkler systems, ESFR automatic sprinkler techniques, and effectiveness of automatic sprinkler use in typical locations such as high rack warehouses and tall buildings.

Hong Kong is the location in the world with the most widespread use of automatic sprinkler systems. Since the start of the last century, Hong Kong has already adopted English standards to install and use such systems.

2.5 Long-throw Sprinkler System

Long-throw sprinklers were installed at height to protect tall halls which are unlikely to store high amounts of combustibles. Water coverage at the protected area was demonstrated to be adequate. However, the performance of long-throw sprinkler installation in tall halls with high combustible contents should be evaluated. The large buoyancy of hot gases from the big fires with long burning duration would induce much stronger turbulent airflow. The long distance travelled by the water droplets in the sprinkler spray discharged in a tall hall would experience much stronger air dragging effect. Air entrainment towards the fire plume and sprinkler water spray would be entirely different from that for a small fire. Ruffino and diMarzo (2004) simulated a fire sprinkler's thermal response in the presence of water droplets. When a sprinkler nearest to the position of the fire is activated, the water droplets may be entrained by the flow of hot smoke and air, potentially cooling adjacent sprinklers and delaying the activation of those sprinklers. The researchers proposed the concept of

equivalent cylindrical links as a means of quantifying thermal response of sprinklers in the event of a fire.

Chow and co-workers (Chow 2011a, 2011b; Chow et al. 2004, 2009) discussed the use of sprinkler systems in green or sustainable buildings. Ordinary sprinkler systems may not be suitable for use in buildings with a tall hall because too much water can hamper evacuation efforts, resulting in damage to the property and too much waste from the excessive water. Chow et al. (2004) evaluated alternative sprinkler systems such as water guns, intelligent fire detection systems and water mist fire suppression systems.

Similarly, Nam et al. (2003) conducted five large-scale fire tests to evaluate the protection requirements in areas with tall halls (floor-to-ceiling height up to 18.3 m). The team found that the sprinklers would be able to provide sufficient protection even with a clearance height of 16.6 m above the combustion materials.

Note that there are deep concerns on having so many big post-flashover fires. As raised previously after the big Fa Yuen Street fire, projects with difficulties to comply with prescriptive fire codes should be watched (Chow 2012b). Projects going through fire engineering approach (FEA) in Hong Kong, in fact performance-based design (PBD), must include intervention of fire services, impact on firefighting and rescue strategies, and potential safety and health effect to firefighters. This was pointed out and discussed in a railway conference (Korea Railroad Research Institute & SFPE Korean Chapter 2011). For example, asking firemen to walk through a much longer travel distance must be watched. Their equipped portable breathing apparatus can only operate for 30 minutes, might not be appropriate for taking actions in places with

extended travel distances. Very few FEA/PBD reports include vigorous analysis on safety and health of firefighters; warning them to upgrade their equipment in very hazardous environment and revising their normal training schedule in suppressing big fires. It is good to learn that the fire authority in Hong Kong (Lo 2011) is taking appropriate actions in watching all FEA projects approved after 1998. This thesis focused on how to effectively use long-throw sprinkler systems in typical tall and large buildings.

Two concerns were pointed out on long-throw sprinkler installation at height (Cheung 2012; Chow 2012c, 2012d) in halls storing high amounts of combustibles as in Figure 1.1. These are on aerodynamics resulted from sprinkler-fire interactions and hence control of heat release rate.

2.6 Aerodynamics Resulted

Under a big fire with high heat release rate, the resultant air flow due to dragging of water spray and fire-induced buoyancy will be very strong. Smoke might fill up the whole hall space due to the turbulent motion. Consequently, a clear two-layer pattern would not form in a very tall hall (and even in an hall with a normal ceiling height of 3 m) under a bigger fire. Smoke cannot be kept at sufficiently high positions, affecting occupants and firefighters staying below. Occupants might be able to leave the hall as indicated by the results from evacuation simulation in a reasonably short time (Chow and Chow 2005; Chow 2011b; Chow et al. 2007). However, robotic motion assumed (Babrauskas et al. 2010) in the simulations should be justified. Perhaps, orderly

evacuation can be ensured by directing movement by security guards with firefighting experience. Further, evacuation packages were developed without including appropriate human behavior in the Far East (Chow 2011a). In addition, health effect of firefighters is a deep concern. Firemen must upgrade their personal protection equipment under such fire scenario. Very few in-depth studies on this special issue were carried out. However, the performance of the portable breathing apparatus were only evaluated (Chow 2009a) under small fires and without water action. Further, the performance of the smoke exhaust system, particularly static smoke exhaust in tall halls, will be affected. Integrating long-throw sprinklers at height with static smoke exhaust system should be further justified, particularly for those railway stations located deep underground (Chow 2011b). It is very dangerous for firemen moving down to deep space. The maximum depth of an underground car park might be 7 levels in Korea. Any depth over 20 m should be watched.

Chung and Tung (2004) presented a modified smoke filling time calculation method that allows for the precise measurement of the smoke layer height and demonstrated that smoke volume increases after the activation of sprinkler systems. They also conducted a full-scale experiment to evaluate the applicability of the proposed method and proposed appropriate sprinkler activation times that limit the possibility of smoke blocking the exits for occupants being evacuated.

2.7 Control of Heat Release Rate

It is difficult to control the combustible content inside a big hall. Putting in festival

decorations such as tall Christmas trees as in Figure 1.1 made of materials not passing the non-combustibility test would give high heat release rates upon ignition. The possible heat release rate upon burning combustibles in a tall hall was complied with some guides. However, results (Hong Kong Airport Authority 2011) are not supported by full-scale burning tests and some approaches are even taking average heat release rate as peak heat release rate (Chow 2012a). Overseas results suggested that burning a normal small domestic tree would give at least 7 MW (Madrzykowski 2008). A plastic tree ten times taller than that might give 70 MW! Igniting adjacent combustibles of the tall tree would give very different fire phenomena (Chow and Han 2011; Chow et al. 2011). Consequently, it is difficult to suppress the fire and control the heat release rate to the expected value, say 2 MW, even if water coverage of long-throw sprinkler satisfied the acceptable design rule (Loss Prevention Council 1987). That is why the observed arrangement as in Fig. 1 is a deep concern to fire officers (Lo 2011). Firemen have to stay inside the hall with hazardous environment to rescue trapped and hurt occupants, and fight against the big fire!

2.8 Problems to be Studied in this Thesis

Both concerns reported in the above section suggested that more full-scale burning tests on long-throw sprinklers in tall halls under big fires have to be carried out. Apart from studying the water coverage of the protected area, there are still no in-depth systematic studies using appropriate numerical simulations nor in-depth experimental studies to address these two points reported in the literature. These two points on resultant aerodynamics and heat release rate will be addressed in this thesis.

Fire hazards due to storing combustible objects and the typical heat release rate in large and tall spaces will be surveyed. Fundamental issues such as water droplet kinetics discharged from sprinkler heads with regard to sprinkler type, structure and design will be studied to have a better understanding on water distribution effects and water droplet penetration effects.

CFD-FDS will be applied to study the interacting effects of sprinkler and fire. Full-scale burning test results with appropriate sprinkler pressures and flow rates in different fire scenarios and fire sources will be compared.

The fire hazards of different kinds of tall and large halls were discussed in this chapter. The history of using automatic sprinkler systems was studied. The development of automatic sprinkler techniques in China was also mentioned, as experiments in this thesis were carried out in Mainland China. The performance of long-throw sprinkler systems in controlling fires in tall and large halls will be studied in this thesis. Controlling the heat release rate is an important issue. Problems to be studied in this thesis are also summarized to give a clear picture.

Chapter 3 Burning Objects

3.1 Introduction

In order to study how effective a long-throw sprinkler can put out fires experimentally, a test fire composed of combustible objects is needed. Heat release rate is one of the most important parameter in fire hazard assessment. Different wood crib arrangements will be studied in this paper. Importance of heat release rate and measurement using the oxygen consumption method will be discussed.

3.2 Heat Release Rates

Heat release rate (HRR) is the heat released by combustible objects in a unit of time (Karlsson and Quintiere 2000; Zhao et al. 2002). During the combustion process, most combustible objects will have different HRRs over time. Through heat release rates, it is possible to define the dimensions of the fire site. It is also possible to use HRR to describe other related factors, including the concentration of smoke and poisonous substances (Babrauskas and Grayson 1992; Peacock et al. 1991).Thus, HRR has always been considered the most important factor in describing a fire scene and the process of a fire disaster.

There are two ways to obtain the HRR of combustible objects: through full-scale fire tests or by modeling experiments. The scale of full-scale fire tests cannot be too large

due to cost considerations. Modeling experiments produce the HRRs through small-scale physical models and mathematical calculations. As the equations used to calculate the HRR requires a lot of experimental data, coupled with the rough nature of the modeling equations and the complexity of the fire disaster (for example, the type of combustible objects, scale and nature of combustible objects, placement of objects, air flow situation, etc.), the mathematical calculations and projections involve a number of boundary conditions that are difficult to understand. Most calculations are based on a large number of restrictions and assumptions, and typically contain relatively large omissions (Jones et al. 2005). Thus, experiments remain the basic method of obtaining HRRs (Xi et al. 1999).

Under the same radiation levels, different materials can generate different HRRs. Even with the same materials, HRR can be different under different experimental conditions and with different ways of handling the materials. Thus, in order to compare the HRRs of different materials, it is important to control the environmental factors and vary only the radiation levels when conducting the experiments. Only then will the HRRs produced be comparable. If the dimensions of the objects used in the experiment are comparable to those in actual conditions, then the combination of single experimental objects in small quantities can be termed large-scale experiments (Wang et al. 2004). Large-scale experiments can determine a more realistic response of combustible objects in fire disasters, and allow for the testing of changes in environmental factors.

To assess the scaling law for temperature, Chow and Lo (2011) conducted scale-modeling on smoke filling in an atrium naturally. They used a facility built in China to conduct 50 hot smoke tests, and determined that the equations on time and heat release

rate are useful in expressing the process of smoke-filling. However, the scaling law of temperature described in Froude modeling was found to require further examination and research.

3.3 Oxygen Consumption Calorimetry

The oxygen consumption principle is the most developed method of calculating HRR. Thorton discovered (Chow et al. 2004) that when many organic liquids and gases undergo combustion, there is a linear relationship between every 1 kg of oxygen consumption and heat release rates. Huggett (1980) also proved that this relationship applies not only for organic liquids and gases, but also for common combustible objects found in buildings. At the same time, Huggett (1980) determined that the average of this coefficient is 13.1MJ per kg of oxygen, with more than ±5% accuracy. Incomplete combustion and different combustible materials only have a small impact on the result.

Oxygen consumption derived based on volume flow and mass flow is given by:

$$Q = E^1 \cdot V \cdot X_{O_2}^{\alpha} \cdot [\frac{\Phi}{\Phi(\alpha - 1) + 1}] \qquad (3\text{-}1)$$

In the above equation, E^1 refers to heat released per unit volume of oxygen. Under 25℃ sample combustion $E^1 = 17.2 \times 103$ kJ/m^3; V refers to the gas volume flow in the exhaust pipe, m^3/s; α refers to the oxygen diffusion coefficient in an air combustion reaction; $X_{O_2}^{\alpha}$ refers to the oxygen concentration in the oxygen-containing vapor environment,

$X_{O_2}^{\alpha} = X_{O_2}^{0}(1 - X_{H_2O}^{0})$, $X_{H_2O}^{0}$ refers to the vapor concentration in the environment; and Φ refers to the oxygen coefficient as derived by:

$$\Phi = \frac{X_{O_2}^{0}(1 - X_{CO_2} - X_{CO}) - X_{O_2}(1 - X_{CO_2}^{0})}{X_{O_2}^{0}(1 - X_{CO_2} - X_{O_2} - X_{CO})} \quad (3\text{-}2)$$

In the above equation, $X_{O_2}^{0}$ refers to the initial molar concentration of oxygen measured in the oxygen analyzer; X_{O_2} refers to the molar concentration of the oxygen measured in the exhaust pipe during the experiment; $X_{CO_2}^{0}$ refers to the initial carbon dioxide molar concentration, while X_{CO} refers to the molar concentration of carbon monoxide measured by the carbon monoxide analyzer in the exhaust pipe.

3.4 Different Combustibles

During fire disaster research, building a fire test model is an important part of the experiment. With respect to liquid and gas fire disasters, it is possible to choose the actual combustible liquid or gas to conduct the experiment. But with regard to solid fire disasters, the combustible objects in different places are complex. Thus, multiple research institutions are focused on choosing combustible objects that are universal and placed in actual test centres, to model the actual fire situation as much as possible. In recent years, Song and Li (2013) and Liu et al. (2014) from Tianjin Fire Research Institute chose and confirmed two types of standard combustible objects in fire disasters, which can be used to model different fire loads and levels of fire disasters

(See Figures 3.1 and 3.2).

Cardboard paper of dimensions 500 mm by 500 mm by 500 mm, weight 2.7 kg, thickness 4 mm, water absorption level controlled at 5% to 8%; paper cuts made of pulp, 10 g each, volume 550 ml, water absorption level controlled at 3% to 5%; plastic cup made of pure polystyrene resin, weight 30 kg, volume 450 ml were used. Plastic and paper cups were placed in a standard cardboard box with 5 layers, 25 on each level, separated by corrugated cardboard. This honeycomb structure allows a quicker development of fire levels and HRRs.

Song and Li (2013) selected 20 random samples amongst a population of 1,000 different two-type combustible objects to conduct the fire test. The HRR of the ignition source was 10 kW. The starting point for increasing combustion was when the HRR reached 10 kW. The HRR is indicated in Figures 3.3 and 3.4.

Using t^2 to fit the HRR curve and calculations to derive the average fire growth, the plastic cup combination produced an average value of 0.0073 between slow fire speeds (0.00277) and medium fire speeds (0.0111). The paper cup combination produced an average of 0.00164 and was considered slow fire.

However, as prototypes for Class A experimental materials, the two combinations of combustible objects contain significant limitations. This is because the above combustible objects are unable to fully reflect the basic characteristic of most Class A combustible materials: steady, sustained combustion.

Zhao et al. (2008) carried out research on wooden cribs, and tested combustible objects chosen from composite wooden combustible materials, with gasoline as the ignition material, to test the HRR under different combustion scenarios. Through comparison and analysis of experimental results, the team attempted to advance research on materials for study fire disaster research (See Figure 3.5).

For wooden box 1, the combustion spread from one corner to the whole of the wooden box, and was of a relatively long duration. In the early stages, only the gasoline was burning, and the HRR was low. Once the wooden crib was ignited, a peak was created as a result of rapid combustion of the combustible objects. As the wood turned to ash, due to the isolating function of the ash, the HRR reduced. As the charring increased, the wooden support collapsed, and a large volume of air entered the crib, again fueling the combustion process and increasing the HRR, creating the second peak. At the same time, the burning of the ashes also contributed to the increase in HRR. Because of the limited thickness of the composite panel of the crib and the combustion speed, the HRR curve did not present a stable phase.

For wooden box 2, the ignition of freely spilled gasoline resulted in a rapid increase in HRR. As the gasoline was fully used, the crib was ignited, and the HRR declined rapidly. As the inside of the wooden crib was hollow, the heat radiation generated by the combustion caused the four panels to burn at the same time. The top surface, once burned through, allowed the entry of fresh air, which speeded up the combustion of the wooden crib, increasing the HRR, creating a significant peak, and resulting in an overall shorter combustion period.

In the experiment described above, the different direction and speed of the early stages of the fire cause a difference in radiation and intensity. At the same time, the burning of different substances causes differences in the combustion process, and is the fundamental reason for the difference in peak values and maximum HRRs when varying the fire ignition point but using the same wooden crib.

Liu et al. (2002) conducted research on HRR of PMMA (polymethyl methacrylate) and pine wood under different external heating intensities. Results are shown in Figure 3.6.

Experimental results show that firstly, differences in ignition amounts create significant differences in the combustion properties. Secondly, when in solid state, HRR of PMMA is relatively flat and stable in the early stages. Once liquefied, the PMMA combustion properties become similar to liquid combustible objects, the controlling factors affecting the combustion characteristics is the evaporation rate. The increase in temperature causes the increase in HRR, reaching a peak. In the extinguishing phase, the combustion is controlled by the amount of combustible materials, causing a rapid decline in HRR. HRRs of the pine wood samples show two clear peaks, creating a saddle shape. This is closely related to the combustion properties of pine wood. As pine wood is ignited, a large amount of combustible gas is released, creating a strong chemical reaction and creating the first peak. As the dissolution of the pine wood speeds up, the surface turns to ash, creating a relatively long period of low steady combustion. As the temperature increases, the ash layer breaks, increasing the HRR and creating the second peak.

3.5 Observations

Based on the above results, the following are observed:

When choosing combustible objects, it is important to fully reflect the main characteristics of the combustion process and cover a broad spectrum (Vcakatcsh et al. 1997). Different materials and different external factors (ignition agent, experiment environment, etc.) create significant differences in HRR and affect the design of the fire model. As wood is commonly found in Class A combustible materials with steady burning process, this material is suitable for fire extinguishing experiments. Therefore, wood cribs arrangement is selected in this study.

Results with changes in the placement of the combustible objects and amount of combustible objects will be further explored in the following chapters of the thesis.

Chapter 4 Experimental Study on Wood Crib Fires

4.1 Introduction

Wood crib fires are selected for studying suppression by long-throw sprinkler. Heat release rates of wood crib arrangement measured by a 10 MW calorimeter are shown in Figure 4.1. The system comprises a pipe, a measuring section, a hood, a fan and other components, with a height of 11.9 m. The system complies with ISO9705 requirements. The supporting facilities include a lift truck to arrange wood cribs and put them at different positions, and a camera to produce experimental records. Detailed arrangement is shown in Figure 4.2.

The experimental facility is located at Tianjin Fire Research Institute.

The combustible object used is pine wood crib. Dimensions and structure are shown in Figure 4.3a to c. The material testing parameters are shown in Table 4-1.

The following experiments were carried out on wood cribs fires:

- Experiment W1

Experiment model is one wooden crib, placed as in Figure 4.4. To ensure that the smoke released can be fully covered by the hood, the wooden crib are lifted by lift trucks to a height of 10.2 m, with a distance of 0.7 m from the hood, as shown in Figure 4.5. During tests W1 to W5 with details described below, the distance from wood crib

to hood are all the same as 0.7 m.

Combustion method: Wood crib placed on a steel supporting structure of height (400 ±10) mm as shown in Figure 4.6. The experiment ignition material is N-heptane. Beneath the wood crib is a 500 mm by 500 mm oil tray, within which is placed 5 cm height of water, with 1.5 L of N-heptane.

- Experiment W2

Experiment model is two wooden cribs distanced at 15 cm apart and placed as in Figure 4.7, lifted to a height as in Figure 4.8, with the same ignition method as the above. The amount of N-heptane in each oil tray is 1.5 L, totaling 3 L.

- Experiment W3

Placement of four wooden cribs in a square distanced at 15 cm apart and placed as in Figure 4.9, lifted by the lift truck as in Figure 4.10. Combustion method is the same as in above. The amount of N-heptane in each oil tray is 1.5 L, totaling 6 L.

- Experiment W4

Experiment W4 comprises four wood cribs stacked in two layers, each layer with two wood cribs, 15 cm apart, and placed as in Figure 4.11. The wood cribs are lifted using a lift truck as shown in Figure 4.12. Same ignition method as in above. The amount of N-heptane is 1.5 L in each oil tray, total 3 L.

- Experiment W5

The setup comprises six wood cribs placed with one layer, three on each side, 15 cm

apart, as shown in Figure 4.13. The wood cribs are lifted using a wood crib as shown in Figure 4.14. Same ignition method as in above. N-heptane level is 1.5 L in each oil tray, totaling 9 L.

4.2 Experiment Process

There are two parts on ignition test and wood crib test.

4.2.1 Ignition test

In order to distinguish the impact on HRRs of the ignition of n-heptane versus the ignition of wood cribs, it is necessary to separately ignite the oil trays and measure the HRRs, as shown in Figure 4.15(a) to Figure 4.15(c). Relevant results are shown in Table 4-2.

4.2.2 Wood crib test

From experiment W1 to W5, the experiment process can be seen in Figures 4.15(d) to (f) and Figure 4.16(g) to (k). The process is shown as: ignition of the oil tray, fully ignited, oil tray extinguished, peak heat release rate, stable heat release rate, end of stable heat release phase, decline in heat release rate, and end of combustion. Typical processes are shown in Table 4-3 to Table 4-7.

In summary, Table 4-3 describes the typical combustion process in experiment W1. At time 0s, the oil tray was ignited. At time 77s, the heat release rate reached a peak value of 1.73 MW (N-heptane combustion). At time 121s, the oil tray was extinguished and

heat release rate reached 0.77 MW (wood crib ignition). At time 650s, heat release rate started to decline and heat release rate reached 0.56 MW. At time 1620s, the wood crib was fully extinguished and heat release rate averaged 0.18 MW. Table 4-4 describes the typical combustion process in experiment W2. At time 0s, the oil tray was ignited. At time 86s, the heat release rate reached a peak value of 3.47 MW (N-heptane combustion). At time 139s, the oil tray was extinguished and heat release rate reached 1.39 MW (wood crib ignition). At time 662s, heat release rate started to decline and heat release rate reached 0.94 MW. At time 1621s, the wood crib was fully extinguished and heat release rate averaged 0.25 MW. Table 4-5 describes the typical combustion process in experiment W3. At time 0s, the oil tray was ignited. At time 96s, the heat release rate reached a peak value of 5.88 MW (N-heptane combustion). At time 129 s, the oil tray was extinguished and heat release rate reached 3.11 MW (wood crib ignition). At time 600 s, the heat release rate started to decline and heat release rate reached 2.45 MW. At time 1623 s, the wood crib was fully extinguished and heat release rate averaged 0.35 MW. Table 4-6 describes the typical combustion process in experiment W4. At time 0s, the oil tray was ignited. At time 131 s, the heat release rate reached a peak value of 4.12 MW (N-heptane combustion). At time 151 s, the oil tray was extinguished and heat release rate reached 2.93 MW (wood crib ignition). At time 879 s, the wood crib collapsed, heat release rate started to decline and heat release rate reached 1.97 MW. At time 1387 s, the wood crib was fully extinguished and heat release rate averaged 0.44 MW. Table 4-7 describes the typical combustion process in experiment W5. At time 0s, the oil tray was ignited. At time 89s, due to excess heat (170℃), the lift truck was started to lower down manually, with heat release rate at 8.51 MW (N-heptane combustion). At time 91 s, the heat release rate reached a peak value of 8.56 MW (N-heptane combustion). At time 139 s, the oil

tray was extinguished and heat release rate reached 4.41 MW (wood crib ignition). At time 649s, the heat release rate started to decline and heat release rate reached 3.56 MW. At time 1250 s, the wood crib was fully extinguished and heat release rate averaged 0.72 MW.

4.3 Analysis of Results

4.3.1 Experiment W1

The HRR of wood crib and total heat released are shown in Figures 4.17 and 4.18. The total heat release rate of wood cribs are shown in Figure 4.18, which is the total heat release rate measured from the experiments on burning wood cribs. The total heat release rate of wood cribs are the total heat release rate measured after removing the total heat release rate of the oil in the oil tray. The total HRR was calculated by integrating the HRR curve over the burning duration of experiment W1. The experimental process can be divided into the oil tray combustion phase, wood crib stable combustion phase, and wood crib extinguishment phase. At 150 s after igniting the fire, the setup entered the stable heat combustion phase, with HRR maintained at 0.61 MW to 0.73 MW, average combustion time not less than 420 s. The HRR of wood crib at 610 s started to decline until the wood crib was fully burnt by 1621 s. Experiment total heat release level is 608.2 MJ. Subtracting the oil tray heat release of 40.0 MJ, the wood crib heat release is 568.2 MJ.

4.3.2 Experiment W2

The HRR of wood crib and total heat released are shown in Figures 4.19 and 4.20. The total heat release rate of wood cribs are shown in Figure 4.20, which is the total

heat release rate measured from the experiments on burning wood cribs. The total heat release rate of wood cribs are the total heat release rate measured after removing the total heat release rate of the oil in the oil tray. The total HRR was calculated by integrating the HRR curve over the burning duration of experiment W2. The experimental process can be divided into the oil tray combustion phase, wood crib stable combustion phase, and wood crib extinguishment phase. 139s after igniting the fire, the setup entered the stable heat combustion phase, with HRR maintained at 1.06 MW to 0.42 MW, average combustion time not less than 360 s. 610 s later, the HRR of wood crib started to decline until the wood crib was fully burnt by 1620 s. Experiment total heat release is 1,214.8 MJ. Subtracting the oil tray heat release of 79.8 MJ, the wood crib heat release is 1135.8 MJ.

4.3.3 Experiment W3

The HRR of wood crib and total heat released are shown in Figures 4.21 and 4.22. The total heat release rate of wood cribs are shown in Figure 4.22, which is the total heat release rate measured from the experiments on burning wood cribs. The total heat release rate of wood cribs are the total heat release rate measured after removing the total heat release rate of the oil in the oil tray. The total HRR was calculated by integrating the HRR curve over the burning duration of experiment W3. The experimental process can be divided into the oil tray combustion phase, wood crib stable combustion phase, and wood crib extinguishment phase. 129 s after igniting the fire, the setup entered the stable heat combustion phase, with HRR maintained at 2.2 MW to 3.0 MW. 600 s later, the HRR of wood crib started to decline until the wood crib was fully burnt by 1623 s. Experiment total heat release is 2443.2 MJ. Subtracting

the oil tray heat release of 171.2 MJ, the wood crib heat release is 2,272.0 MJ.

4.3.4 Experiment W4

The HRR of wood crib and total heat released are shown in Figures 4.23 and 4.24. The total heat release rate of wood cribs are shown in Figure 4.24, which is the total heat release rate measured from the experiments on burning wood cribs. The total heat release rate of wood cribs are the total heat release rate measured after removing the total heat release rate of the oil in the oil tray. The total HRR was calculated by integrating the HRR curve over the burning duration of experiment W4. The experimental process can be divided into the oil tray combustion phase, wood crib stable combustion phase, and wood crib extinguishment phase. 151s after igniting the fire, the setup entered the stable heat combustion phase, with HRR maintained at 1.9 MW to 2.6 MW. 861 s later, the wood crib collapsed, creating an inflection point, the HRR of wood crib started to decline until the wood crib was fully burnt by 1623s. Experiment total heat release is 2,306.0 MJ. Subtracting the oil tray heat release of 148.4 MJ, the wood crib heat release is 2158.6 MJ.

4.3.5 Experiment W5

The HRR of wood crib and total heat released are shown in Figures 4.25 and 4.26. The total heat release rate of wood cribs are shown in Figure 4.26, which is the total heat release rate measured from the experiments on burning wood cribs. The total heat release rate of wood cribs are the total heat release rate measured after removing the total heat release rate of the oil in the oil tray. The total HRR was calculated by

integrating the HRR curve over the burning duration of experiment W5. The experimental process can be divided into the oil tray combustion phase, wood crib stable combustion phase, and wood crib extinguishment phase. 139 s after igniting the fire, the setup entered the stable heat combustion phase, with HRR maintained at 3.4 MW.

4.4 Findings

Using oil trays to ignite different wood crib setups resulted in three typical phases: the oil tray combustion phase, wood crib combustion phase and the extinguishment phase:

(1) The HRR stabilization across the five tests is very obvious, typically lasting 6 minutes or more, establishing a basis for future fire test models.

(2) On one hand, the stable HRR in experiments W2 and W3 are 1.3 MW and 2.6 MW respectively. These works are suitable for modeling early and growth stage fires. On the other hand, from the result of experiment W4, the vertical arrangement of wood cribs would facilitate flame spread. The HRR under steady burning is about 2.0 MW. Therefore, it is necessary to increase the supplementary tests with the wood cribs number and arrangement, including the vertical arrangement of wood cribs as in Figure 4.27.and the arrangement of three wood cribs as in Figure 4.28.

(3) In experiment W5, oil tray area and N-heptane used are the largest, as is the peak HRR, reaching 8.55 MW. The stable HRR reaches as high as 3.5 MW, and can be used

as a model for mid-stage fire disasters.

(4) Wood crib placement in experiment W4 would facilitate fire spread, an important characteristic to pay attention to assessing fire hazard. The wood crib collapsed during the phase of the experiment, causing a sudden decline in heat release rate, creating an inflection point in the curve and affecting the experimental results.

(5) The heat released by a single crib is steady at 540 MJ to 568 MJ.

The five large-scale crib calorimeter test results are listed in Table 4-8.

(6) Supplementary experiment results

Based on the requirements in section 4 of the reference (Karlsson and Quintiere 2000), the supplementary heat measurement provides the below conclusions:

Details can be seen for HRR curve and total heat released of two wood cribs stacked up in Figures 4.29 and 4.30; and HRR curve and total heat released of three wood cribs placed one on top, two below in Figures 4.31and 4.32.

The above diagrams and comparison with the previous experiments show that different placement methods would affect the time taken to reach the maximum HRR, time taken to enter to stable combustion phase and time of the stable combustion phase.

This type of placement method increases the rate of combustion. That is because different placement will have different air flow around the wood cribs. If the number of wood cribs are the same, supplying more air would accelerate the rate of burning.

From the experiment, the ‘one on top/two below’ placement gave the best performance of the rate of combustion, which in line with the hypothesis above.

The 10 MW calorimeter and basic experiment requirements were introduced in this chapter. Scenarios under one, two, three, four wood cribs placed horizontally, vertically, and stacked one on top/two below were analyzed. The heat release rate and total heat released were measured in each scenario. Transient heat release rate curves were different for each scenario. In particular, knowing the burning characteristics of object under the stabilization phase will be useful for carrying out the subsequent full-scale experiment research.

Chapter 5 Long-throw Sprinkler and Fire Experiments

5.1 Introduction

The performance of long-throw sprinkler systems in large and tall halls will be studied experimentally. Results will be reported in later chapters. Experimental studies were performed at Shanghai. Designing fire extinguishment systems based on actual conditions is a critical problem to be solved.

5.2 Fire Hazard Scenarios

Current design trends favor the use of natural ventilation, lighting, and the creation of public spaces. In the densely populated Hong Kong, in particular, this creates distinguishing characteristics of spaces with tall atria: tall height, complex structure, and when plot ratio exceeds a certain level, the provision of only exhaust systems. According to Spadafora (2012) notes, an atrium refers to a large open space typically located near the main entrance of a large multi-storey building. Atria help augment the perception of space and lighting within structures, and are very popular in many architectural designs. According to building codes such as the International Building Code, an atrium refers to an opening closed at the top that connects at least two storeys. Internal fire load conditions vary with the environment, and typically have a number of uncertain factors. In large malls and exhibition centres, during holidays or marketing periods, large quantities of easily flammable and combustible decorations will be positioned temporarily, as shown in Figures 5.1 to 5.4, thus increasing the fire risks.

Under normal circumstances in closed sprinkler systems, sprinklers are usually installed at the top or layered top part of the building. For tall buildings, however, even though it may be theoretically possible to install sprinklers in a ceiling more than 10 m (but not more than 18 m) high, and the sprinkler contains a fast thermal response function, the tall and large space will affect the ability of hot smoke to flow upwards. Thus, the activation of closed sprinklers will be slower than in normal buildings. In buildings where there is a rapidly growing fire disaster, once the early opportunity to extinguish the fire is missed, the difficulty in extinguishing the fire will increase significantly. Chow and Fong (1992) conducted research on the performance of sprinklers in tall atria and assessed three points: first, the ability to actuate the sprinklers; second, the sprinkler head thermal response; third, the water and smoke layer interaction. They then performed a numerical experiment to calculate the airflow, temperature and smoke concentration contours. With a 5 MW fire in an atrium taller than 20 m, the sprinkler will not be actuated as the ceiling temperature will not be high enough. Furthermore, even if a sprinkler is actuated through an early-suppression fast-response system, the water spray discharged will lower air temperature and reduce the buoyancy of the smoke layer. The air drag from the water droplets will also pull the air along with the smoke downwards, creating a situation adverse to the occupants trapped in the atrium. The results suggest that ceiling sprinklers are ineffective in atrium spaces with high-headroom. Similarly, Chow (1996) evaluated the performance of sprinklers that are installed in the roof of an atrium based on three criteria: water requirement, thermal response and the ability to activate the sprinkler head. Chow (1996) calculated the water droplet trajectories to evaluate the water requirement, while DETACT software was used to determine the sprinkler head activation time for

sprinklers installed at different ceiling heights.

Farquhar (2002) also examined the fire protection risks in shopping malls and proposed recommendations for risk assessment, engineering review and building design. As pointed out by Farquhar (2002), special occasions such as exhibitions or seasonal decorations must be carefully scrutinized for fire safety related issues. Proposed approaches include the use of software evacuation models and dynamic fire and smoke models to determine fire spread. Farquhar (2002) also pointed out the difficulty of fire protection in spaces with large atria, as smoke can stratify at heights below the ceiling height.

Furthermore, it is commonly seen in buildings in Hong Kong that there may be no sprinklers above the easily combustible objects, as shown in Figures 5.5 and 5.6. Burning this type of combustibles would give high HRR upon ignition. Fire will spread rapidly and give large amounts of smoke. Regardless of whether smoke is naturally and mechanically exhausted, the smoke cannot be maintained at a high enough position. This will be fatal from the evacuation or fire rescue perspective. Chow and Wong (1988) studied a modern atrium located in a large department store in the Melbourne city centre and noted a number of fire safety issues. Suggestions proposed include installing smoke extraction systems and the removal of sprinklers at the high canopy, as modeling studies suggested that it would be difficult to activate these sprinklers.

Thus, addressing the issues associated with extinguishing fires requires appropriate selection, careful sprinkler system design and sprinkler distribution based on effective

and practical principles.

5.3 Long-throw Sprinkler

Two methods of discharging water from the sprinkler are shown in Figure 5.7. One shows a sprinkler head positioned near the top, the other shows the sprinkler head positioned by the side-wall. As shown in Figure 5.8, long-throw (side-wall) sprinkler has the following advantages:

(1) With regard to high clear height situations, this can effectively lower the sprinkler positioning height. This is especially suited for protection in the cases of Figures 5.5 and 5.6.

(2) In order to realize the objective of extinguishing fires early, protected areas can be set to use standalone, open-ended drainage pour systems. These systems are more convenient and simple than closed systems in the areas of mounting height, pipe network layout and system activation.

This thesis focused on the fire load of tall and large buildings as indicated in Figures 5.1 to 5.6, and investigated the use of side-wall sprinklers to extinguish fires in the early stages of the fire.

With regard to large spaces, this technique has higher requirements on sprinkler intensity and ability of water droplets to penetrate upward flowing air currents. The penetration ability of water depends on the momentum of the water droplets. Through

increasing the speed with which water flows downwards and water droplet quality, it is possible to increase the penetration ability. Other related factors include sprinkler head structure and system use cases.

It is commonly thought that the use of side-wall sprinklers contain relatively more limitations. According to NFPA-13 regulations (NFPA 2002), this type of sprinkler head can only be used in low danger situations, and only used in medium danger situations with special authorization. China's Automatic Sprinkler System Design Standards GB50067-2001 (2005 edition) (China National Standard 2005a) classifies this type of sprinkler as a side-wall sprinkler. The standards also state that side-wall sprinklers are only suitable for low to medium danger situations. Prasad et. al (2001) studied the use of water-mist suppression on fires in large scale compartment fires. Using computational physics and fluid dynamics Eulerian equations, the team described the gas phase and the water-mist and quantified the impact of parameters such as the diameter of water droplets, velocity, orientation, and density of mist injection, and location of sprinkler nozzles. The researchers proposed that water-mist injection through side, front or rear walls may be less efficient than injection through the top.

However, the multi-varied nature of present-day buildings necessitate the continuous innovation of simple, easy to use side-wall sprinklers. Because the protection area of typical sprinklers is limited, in recent years, large impulse, spray sprinklers are increasingly used in various office buildings, hotels, shopping centres and other buildings. This type of sprinkler has already been used in many tall and large buildings in Hong Kong with the typical danger III rating, with installation heights as tall as 15.5

m (Chow et al. 2006; Chow 2012c, 2012d; Loss Prevention Council 1987). Support can be found in English standards BS 5306: Part II (British Standard Institution 1990). Figure 2.38.1 shows a typical side-wall large impulse sprinkler head.

Large Impulse Sprinkler Heads are also known as side-wall long-throw sprinkler heads, and refer to sprinkler heads with a flow coefficient K greater than or equal to 115. Typically, there is a requirement for maximum protection area, along with the nozzle spacing on the pipe, and distance between the sprinkler head and the wall and related factors, to be able to wet the opposite wall and deflector wall 1.2 m and below. Furthermore, the water density within the scope of protection should be able to fulfill the fire sprinkler intensity level requirements.

However, with regard to the use of side-wall long-throw sprinklers in large and tall spaces, the location of the sprinkler will be significantly different from that in the typical office or hotel room. The sprinkler installation height will be much taller than in typical situations, and the main consideration would not be so called the “ability to wet walls”. The following problems have to be focused on:

(1) According to the related standards, when using side-wall long-throw sprinklers beyond limits, it is necessary to evaluate through experiments. The basis for this type of evaluation is the actual fire load condition.

(2) In the type of location indicated in Figures 5.5 and, in a fire disaster, the fire situation will be significantly different from that of typical combustible objects. Early stage HRR predictions can exceed 2 MW. Even though sprinkler and systems are

abided by typical allowed requirements, the safety of use remains in doubt.

(3) From the requirement of extinguishing fires quickly, when using side-wall sprinklers in tall and large spaces, it is necessary and more reliable to select early detection systems rather than using multiple open style sprinklers.

5.4 Sprinkler Water Distribution

With regard to automatic sprinkler systems, the water distribution performance of sprinklers is one of the most important determinants of the fire control and suppression ability; whether it is as the designed sprinkler watering shape and meets the minimum protection area in design standards (dimension: mm/min, termed water emission); and whether the sprinklers are possible to effectively extinguish fires, control fires or cooling. Water distribution performance of the entire sprinkler system can play a key role in extinguishing fires. The requirements of installation height, nozzle spacing and the working area are all related to water distribution performance.

Chow and Shek (1993) conducted research on K80 sprinklers. The results show that under certain operating pressure and nozzle mounting height, water density varies with radial distance and azimuth. Through changing the size of the nozzle body, nozzle diameter and depth deflector tooth, Gao et al. (2013) identified factors in nozzle structure that affect the sprinkler's water distribution properties. These factors include the diameter of the sprinkler head frame, the length from the sprinkler nozzle to the splash plate, the sprinkler method, and the depth of the water pan. Of these, the frame head diameter has the most significant impact. The most suitable length is 8.5 mm.

In order to investigate the impact of operating pressure and installation height on sprinkler water distribution in spaces, Ni et al. (2014) conducted 12 comparison experiments using K161 large diameter downward facing sprinkler heads, at installation heights of 8 m, 12 m and 18 m, under four different operating pressures. The conclusions are that the sprinkler ability to concentrate water (measuring sprinkler water intensity) is minimally impacted by installation height, and as water pressure increases, measured water intensity also increases, which is in-line with the theoretical calculation result, but on average slightly below. Sprinkler water distribution is minimally affected by the installation height. However, the higher the water supply pressure, the poorer the evenness of the water distribution. Although water distribution ability is not the same as sprinkler water distribution ability, but the impact on safety cannot be overlooked. For example in LPC regulations, typical danger (III) level sprinkler intensity can be no less than 5mm/min (LPC 1987). If water distribution level within the sprinkler coverage area cannot reach this requirement, the system will not be able to extinguish fires.

This study proposes the use of side-wall long-throw sprinklers installed in spaces with tall and large atria, with operating pressure, installation height and related distribution impact determined through experiments. This forms the basis for sprinkler selection and determines the structure, and is relatively appropriate.

5.5 Tests

With regard to the tests of sprinkler water distribution ability, similar to other automatic fire extinguishing products, the US FM, UL, LPCB are at present the world's most advanced and influential organizations. In recent years, the Tianjin Fire Research Institute has also advanced significant research in this area, for example, GB50067-2001 (2005 edition) (China National Standard 2005a) was edited by them. See Figure 5.9.

Although experimental result principles are similar, the standards used in different experimental laboratories are different. In order to unify the experimental results and standards, this study uses LPC related rules (LPC 1987) to conduct experimental research.

5.6 Complying with the Nominal Water Discharge Density

Water distribution density and sprinkler nominal discharge density are related. For example, the LPC stipulated medium (III) danger water discharge density cannot be less than 5mm/min, LPS1039 (2002) LPC (1987). If the water distribution ability of the sprinklers used in the operating area does not reach this requirement, they will not be able to extinguish the fire.

The nominal discharge density (NDD) is expressed as:

$$NDD = \frac{Q_f}{A_c} \quad (5\text{-}3)$$

In the above equation, Q_f refers to the flow of the sprinkler within the operating area (under stipulated design conditions, the maximum protection area of one sprinkler), with units being L/min; A_c refers to the operating area, with units m^2. Thus, with regard to the designated fire load water application rates, using the water distribution quality as the basis, deriving the NDD is plausible. This is also the basic reason why this thesis needs to conduct experimental research on water distribution ability.

On-site measurement of water distribution does not pertain to a particular sprinkler. The focus is rather the water flow. With regard to two sprinklers installed at designated distances, water distribution along the radial and axial distances requires investigation. The standards in the United Kingdom, United States and China all follow this requirement. The basic experimental condition for water distribution is as follows: each sprinkler has a minimum water flow of 131 L/min and minimum water pressure of 0.2 MPa (2 bar). The ideal sprinkler at least fulfills the below requirement: within the protection zone, the water distribution box with distribution volume less than 1.125 mm/min does not exceed 10% of the total, with the minimum average water distribution density no less than 5mm/min.

Considering the side-wall sprinkler standards in different countries, consolidating the research results of practical experiments by Jackman (1992) and Kung et al. (1982). It could be designated that the distance between two sprinkler heads as 2.5 m.

5.7 Experiments on Nominal Discharge Density

5.7.1 Experimental Setup

The following were selected:

(1) Pump units. Use 90 kW DC variable speed motor pumps, with nominal flow rate of 100 m^3/h, head 200 m. The pump unit can continuously supply water, and the water supply can meet the experiment's various water volume requirements.

(2) Flow measurement apparatus. Use a LW-50 turbine flow meter (measuring range: 66.67L/min ~ 666.67L/min).

(3) Pressure testing device. Test a variety of nozzle pressure settings: 0.2 MPa, 0.35 MPa, and 0.5 MPa. In order to measure the pressure of each sprinkler head, apart from pipeline pressure gauges, it is also important to install pressure sensors with measuring area 0~1.6 MPa, 0.2 level precision.

(4) Test pipeline. Designed in accordance with standard requirements. Nozzle diameter 25 mm, main water pipe diameter DN100 mm. The main pipe design installation and maintenance gate DN100 mm, turbine flowmeter DN50 mm and DN100 mm deluge valve membrane (water pipeline overall control), diameter DN100 mm pressure sensor: range 1.0 MPa, with drainage pipes installed in the trunk with an electric valve (DN 50 mm). The main water supply pipe diagram is shown in Figures 5.10, 5.11 and 5.12.

(5) Water catchment box

Made of galvanized steel, with dimensions 0.5m*0.5m*0.5m (L*H*B), as shown in

Figure 5.13.

5.7.2 Selection of Automatic Valve on Main Water Supply Pipe

The valve on the water supply pipe typically uses the gate valve or the butterfly valve, it is not convenient with respect to the DN100 pipe operations, particularly, in order to minimize post-experiment excessive water drip. The distance between the valve and the sprinkler head should be as far as possible, therefore in the pipe design, the valve is installed at the ceiling, creating even greater inconvenience when operating. Furthermore, for automatic valves installed on the main pipe, their activation switch controls the overall water flow. The opening and closing of the valve needs to be on-time, precise, with minimal resistance, and easily operated. According to the above requirements, electric ball valves, electric gate valves, magnetic valves and diaphragm valves are compared. The results show that electric ball valves and electric gate valves have overly long time requirements to go from a closed to open state. A 100 mm diameter valve typically requires 40 s. Magnetic valves have much lesser time requirements, typically within 1 s, and achieve the goals of being on-time and easily operated, but the loss in resistance is significant. Furthermore, large diameter magnetic valves have poor sealability, typically after installing for some time, sealing open-close operations of the valve are difficult to guarantee. Diaphragm valves when opening and closing have precise and reliable movements, minimal resistance loss and are easily operated. Relatively speaking, they fit the technical requirements more. Furthermore, when applying the results of this research, a large part of the consideration is for an open form. Hence, diaphragm valves are selected to be used as the main means of controlling the pipelines.

At the end of the experiment, the excess water in the pipe network will fall into the collection pan directly below, and is one of the factors impacting the accuracy of the measurements. Thus, drainage pipes are designed on which electric drainage valves have been installed. This electric valve complements the diaphragm valve; when the diaphragm valve is activated, the drainage valve is closed; when the drainage valve is open, the diaphragm valve is closed. The drainage pipes are installed at the lowest point of the pipe network.

5.7.3 Choice of Sprinkler Head

First, two sprinklers of the same standard model are used, installed as shown in Figures 5.14 and 5.15. Table 5-1 lists the related technical characteristics of the seven types of sprinkler heads used for the water distribution experiment. In order to ascertain the impact of the K series on water distribution reliability once the installation height is increased, side-wall long-throw sprinklers of K=80, 112, 160 are chosen.

5.7.4 Experiment Precision

To measure sprinkler distribution performance, technical parameters include flow, volume, time and pressure (reference value). The time measurement device used is precise to 0.1 s; turbine flowmeter accurate to 0.5%; pressure sensor accurate to 0.2, with a range of 1.6 MPa; single level ruler range 1000 mm and measurement sensitive to 0.1 mm. All these meet the standard accuracy requirements.

5.7.5 Experiment Requirements

Water distribution data can be collected using the following scenarios:

- Sprinkler installation height 6 m, working pressure 0.2 MPa, 0.35 MPa and 0.5 MPa.
- Sprinkler installation height 8 m, working pressure 0.2 MPa, 0.35 MPa and 0.5 MPa.
- Sprinkler installation height 10 m, working pressure 0.2 MPa, 0.35 MPa and 0.5 MPa.

5.8 Results

Water discharging time is 3 minutes, with experiments conducted on each type of sprinkler 9 times. The working situation of the water distribution experiment are shown in Figures 5.14, 5.15 and 5.16.

The experimental results of seven different sprinklers at different installation heights and operating pressures are listed in Table 5-1 to 5-43.

The water distribution density of each water collection pan is calculated by:

$$\rho = Q / (t \cdot S^2) \qquad (5\text{-}1)$$

In the above equation, ρ is the individual water collection pan water distribution density, mm/min; Q is the individual water collection pan volume of water collected,

mm^3; t is the water distribution time, min; and S is the individual water collection pan collection area, mm^2.

It can be expressed in terms of the water collection pan water height H, mm:

$$\rho = H/t \quad (5\text{-}2)$$

The water volume in each water collection pan was measured and each collection pan's water distribution density, the average and the minimum density across all pans were calculated and used as the basis for measuring water distribution.

5.9 Analysis

5.9.1 Water Distribution Ability under Different Flow Coefficients

This experiment used flow coefficients K=80, K=115 and K=161, and seven side-wall sprinklers with different splash plate structures and frame structures. According to the results in Tables 5-2 to 5-43, for sprinkler no. 5, 6 and 7 with K=80, under different installation heights and different operating pressures, the water distribution ability is worse than large impulse (extended coverage) K=115, K=161 sprinklers. Furthermore, water distribution ability is very poor at installation heights higher than 8 m. This demonstrates that flow coefficient K=80 sprinklers are not suitable for use in tall and large atria. Thereafter, related fire extinguishing experiments should use the four types of sprinklers with flow coefficients larger than 80. The following analysis focuses on these four types of sprinklers.

5.9.2 Comparison of Water Distribution Ability under Different Operating Pressures but Same Installation Height

Taking the installation height of 6 m as an example, when the sprinkler operating pressure is relatively low (0.2 MPa), the water distribution ability does not vary significantly among sprinkler no. 1 to 4, and are relatively similar. As operating pressure increases to 0.35 MPa, water distribution ability declines. However, when operating pressures further increases to 0.5 MPa, water distribution ability does not change significantly.

5.9.3 Comparison of Water Distribution Ability under Different Operating Pressures at an Increased Installation Height

As installation height and operating pressure increases, most sprinklers of no. 1 to 4 exhibit a decline in water distribution ability. This is in-line with the situation described previously with regard to tall and large spaces. However, some of the sprinklers also exhibit good water distribution ability under certain installation heights. See Table 5-44.

Table 5-44 shows that with regard to sprinklers of different structures, there is an appropriate installation height and operating pressure. Considering the availability, installation height and fire extinguishing requirements, sprinkler no. 1, 2 and 4 are selected to conduct the next stage of analysis.

The diagrams and orifice sizes of the three splash pans are shown in Figures 5.17, 5.18 and 5.19.

5.10 Summary

Real conditions in fires in large and tall halls and the corresponding fire extinguishment requirements are analyzed in this Chapter. The use of side-wall long-throw sprinkler systems in large and tall halls was proposed as an Open-type fire extinguishing systems. Based on the requirements, an experimental study to evaluate the performance of side-wall long-throw sprinkler systems was proposed. At heights of 6 m, 8 m and 10 m, sprinklers with operating pressures 0.2 MPa, 0.35 MPa and 0.5 MPa were tested on their water distribution ability. Based on the water distribution results, the three sprinkler types and related sprinkler techniques with the best water distribution characteristics in large and tall halls were identified.

Chapter 6 Numerical Simulation

6.1 Mathematical Models

This chapter focuses on two types of work. First, selecting FDS fire simulation software (Fire Dynamics Simulator, the field simulation software, which was developed by National Institute of Standards and Technology) to model gas flow associated with indoor sprinklers in tall and large atria with regard to different situations. Second, selecting a typical fire extinguishing scene to validate the model.

FDS includes two types of modeling methods as reviewed (e.g. Chow 1995): Large Eddy Simulation (LES) and Direct Numerical Simulation (DNS). DNS is mainly used in small-size flame structure analysis; LES describes the turbulent mixing of fuel and combustion products with the surrounding air. The basic idea on applying FDS for sprinkler fire, particularly on gas flow, was reported (e.g. Chow and Yin 2002). As there are limitations on computer hardware, only LES is used in this study.

The FDS program on simulating gas flows is divided into two modules (Zhang et al. 2002). The first module is to solve differential equations for the main program and describe specific parameters of the fire scene. The second module SMOKEVIEW is a drawing program that can visualize the fire development. Figure 6.1 shows a typical FDS application flow.

To begin, first confirm the target object’s detailed information (target object

dimensions, internal structure, opening, wind flow, fire control facilities). Next, establish the FDS data file by entering target object structure, calculation area, fire source effectiveness and boundary conditions. Next, execute the FDS application. Monitor the convergence of FDS and use Smokeview to confirm execution. Finally, use Smokeview to see the modeling result and confirm the appropriateness of the result.

6.2 Gas Flow Simulation

FDS uses a similar N-S equation suitable for a low Mach Number. NS equation approximation includes a filtering, and only considers the temperature and pressure of large eddy components. This equation has oval features, and is suitable for low speed, thermal convective processes. The basic FDS equation is as follows:

1) Mass Conservation Equation

$$\frac{\partial \rho}{\partial t} + \nabla \cdot \rho u = 0 \tag{6-1}$$

2) Momentum Equation (Newton's Second Law)

$$\frac{\partial}{\partial t}(\rho u) + \nabla \cdot \rho u u + \nabla p = \rho f + \nabla \cdot \tau_{ij} \tag{6-2}$$

The volume force term f in the equation includes gravity and other external forces such as spray water resistance.

3) Energy Conservation Equation (First Law of Thermodynamics)

$$\frac{\partial}{\partial t}(\rho h)+\nabla\cdot\rho hu=\frac{Dp}{Dt}+\dot{q}'''-\nabla\cdot q+\Phi \tag{6-3}$$

4) Ideal Gas Equation

$$\rho = \rho RT/M \tag{6-4}$$

5) Subgrid Scale Turbulent Viscosity Component Equation

$$\frac{\partial}{\partial t}(\rho Y_i)+\nabla\cdot\rho Y_i u=\nabla\cdot\rho D_i\nabla Y_i+\dot{m}_i''' \tag{6-5}$$

In the above equation, Y_i is the mass fraction of the i^{th} component, m_i^m is the production rate (or loss ratio) of the i^{th} component by unit volume, $D_{i\ is}$ the diffusion coefficient of the i^{th} component. Summing all the above five equations together, then the total mass conservation equation can be obtained. Also, equation (6-6) can be obtained.

$$\sum Y_i=1;\sum\dot{m}_i'''=0;\sum\rho D_i\nabla Y_i=0 \tag{6-6}$$

Combustion Model and Thermal Radiation Model

FDS sets up DNS and LES simulation of two combustion models for large eddy simulation, because it is difficult to directly solve the mixing of fuel and oxygen diffusion process, which uses a mixture fraction combustion model by Chow (2002) and Kang and Ma (2010).

(1) Mixture Fraction Combustion Model

The model for large-scale convection and radiation phenomena directly simulates time for small-scale approximation of physical phenomena. Assuming control of the combustion process, the required components can be expressed with a mixed fraction of Z, x and t. z is a conserved function that indicates the proportion of a substance to share at point x in the combustion gas mixture. The relationship between the components is called the “state relationship”. The general form of the combustion reaction is:

$$v_F Fuel + v_o o_2 \rightarrow \sum_i v_{pj} \,\mathrm{Pr}\, oducts \tag{6-7}$$

V_i refers to the stoichiometric coefficient, while the subscripts F, O, P refer to fuel, oxygen and products respectively.

Mixed Fraction z is defined:

$$Z = \frac{sY_F - (Y_O - Y_O^\infty)}{sY_F^1 - Y_O^\infty}; s = \frac{v_O M_O}{v_F M_F} \tag{6-8}$$

The range of Z starts from Z=1 (indicating the region only contains fuel). Y_f^i indicates the share of fuel combustion gas mixture mass fraction. M_F, M_O refer to the molecular weight of fuel and oxygen respectively.

(2) Thermal Radiation Model

It comprises a gas diffusion surface radiation heat transfer and radiation heat transfer model.

Absorption, emission and scattering radiation transport equation is defined as show in

equation (6-9) below:

Radiative Transport Equation (RTE)

$$s\nabla I_{\lambda}(x,s) = -[k(x,\lambda)+\sigma_s(x,\lambda)]I(x,s) + B(x,\lambda) + \frac{\sigma_s(x,\lambda)}{4\pi}\int_{4\pi}\Phi(s,s^{'})I_{\lambda}(x,\lambda^{'})d\Omega^{'} \quad (6\text{-}9)$$

Within the equation I_λ (x, s) is the intensity of the radiation at the wavelength λ, s is the direction vector of the radiation intensity, k(x,λ) and σ_s(x,λ) are the local absorption and scattering coefficients respectively. B(x,λ) is the emission source. The integral equation represents incident scattering items from various directions. Ω is the solid angle.

Diffuse radiation intensity gray surface boundary conditions are defined as:

$$I_w(s) = \varepsilon I_{bw} + \frac{1-\varepsilon}{\pi}\int_{s^{'}\cdot n=0} I_w(s^{'})\,|\,s^{'}n_w\,|\,d\Omega \quad (6\text{-}10)$$

In the equation, I_w refers to the object surface radiation intensity, ε refers to the emissivity, and I_{bw} refers to the blackbody radiation intensity of the surface.

6.3 Sprinkler Spray Simulations

Fire sprinkler flow field research began in the 1950s, mostly in the form of real-site experiments. Factory Mutual Research Corporation (FMRC) in 1956 conducted

research in this area, and chose a long, wide space 36.6 m by 18.3 m, using field test results to derive a theoretical basis for flue gas flow patterns. On this basis, other research institutions such as Fire Research Station (FRS), Underwriters Laboratories Inc. (UL) and Illinois Institute of Technology Research Institute (IITRI), conducted similar research. In the early 90's, British Standards Institution (BSI) conducted many field experiments, through different fire scenes to examine the interaction of sprinkler and a real-life experiment method to obtain the interaction of the sprinkler and smoke layers. In 1998, National Institute of Standards and Technology (NIST) conducted many full-scale experiments to study the effects of smoke flow of water spray in high-rise buildings and tall spaces, thereby revising and improving the computer simulation software FDS using experimental results.

Using modeling methods to examine the impact of sprinklers on a fire, obtain the fire heat release rate and various modeling parameters is one of the most important research areas in present day fire and safety research. Through experimental methods, Madrzykowski and Vettori (1992) obtained the experiential equation for water sprinkler systems. Through analyzing the experimental results, Evans (1993) proposed corrections to Madrzykowski's proposed equations, and applied these changes using the CFAST software. In research from 1995 to 2000, the mathematical model for water sprinkler systems was obtained by Cooper (1995, 2000).

Nam (1996, 1999) further conducted simulations on the use of water sprinkler systems in various fire extinguishing scenarios, and in comparing and analyzing the theoretical conclusions versus experimental results, good experimental support for the mathematical model was found. Nam (2003) conducted research on the actuating of

sprinklers at clearance facilities with high ceilings. Nam used fire test data based on expanding and steady plane pan fires to examine the maximum ceiling heights that would still allow the actuating of sprinklers installed on ceilings. The analysis concluded that assessing the actuating of sprinklers using pan fire tests may result in an incorrect conclusion, as typically the threshold fire size is smaller than suggested by pan fire tests.

Researchers such as Novozhilov and Harvie (1997), Ruffmo and diMarzo (2004) and Chow (1999) conducted simulations on different sprinkler sites, and researched the applicability of these models. Marshall and Di Marzo (2004) examined how sprinkler spray dynamics can be effectively modeled. The performance of sprinklers is affected by numerous factors, including the actuation of the sprinkler, formation of the sprays, water spray dispersion, size, velocity, orientation and shape of water droplets formed, and surface cooling characteristics. Marshall and Di Marzo (2004) provided mathematical models to analyze the underlying transport process for sprinkler sprays in times of fires.

Similarly, Hua et al. (2002) conducted a numerical study to examine the interaction between the water spray and a fire plume. Recognizing the limitations of existing quantitative approaches, Hua et. al (2002) introduced an approach to numerical simulation that could form a basis for the analysis of the interactions between the water spray and the fire plume. The researchers evaluated key factors such as water drop size, spray flow rate and spray pattern, and found that water sprays with a solid cone pattern and fine water droplets may be more effective than those with a hollow cone pattern and coarse water droplets.

With the use of particle tracking methods and an atomization model based on physics principles, Wu et. al (2006) conducted research on how to predict the initial spray of the sprinkler. Characterizing the sprinkler spray is an important component in assessing the performance of fire suppression systems. The atomization model allows the creation of probability distributions of the potential drop sizes and locations for the initial spray.

Chow and Fong (1992) applied field modeling techniques to study the interaction between the water spray of a sprinkler and the convective air flow induced by a fire using a system of equations that describe conservation of momentum, enthalpy and mass. The fourth-order Runge-Kutta method for predicting water droplet trajectories was used to solve the set of differential equations.

6.4 Sprinkler Droplet Size Distribution

After emitting water from the spray nozzle, water flow with a certain amount of energy is created. This water stream hits the deflector and breaks into many small water droplets which scatter in all directions. The diameter of the scattered droplets is typically within 0 mm to 5000 mm (Zhang et al. 2002).

Water droplets of different sizes have different fire extinguishing purposes. Large droplets can penetrate a fire source, while small droplets can absorb part of the heat from the fire. Zhou et al. (2012) characterized the spray characteristics of pendent fire

sprinklers by conducting experiments with a laser-based shadow-imaging system. They measured the velocity, number density and size of the water droplets both in the near and far field of the subject sprinkler. The results show that the arms of the sprinkler frame and the build of the tines and slots in the deflector have the strongest influence. They also support the hypothesis that while large drops are more able to penetrate the fire plume, small drops provide a greater cooling effect. If the sprinkler installation height is relatively high or the fire load is relatively large, this requires the scattered water stream to contain a certain amount of large droplets in order to prevent the water from being evaporated upon reaching the fire source. If the sprinkler installation height is relatively low, the travel distance of the droplet to the fire source is relatively short, it would be advantageous to have medium to small droplets. Therefore, in order to achieve the optimal fire extinguishing result, it is necessary to adjust the proportion of large and small droplets. The droplets discharged by a sprinkler can be split into two levels. The size of the droplets is related to the diameter of the sprinkler head, the shape of the deflector, type of sprinkler head, water pressure, sprinkler position, and more. For example, an increase in the sprinkler head diameter will increase the size of the water droplet, while an increase in operating pressure will decrease the size of the water droplet.

The distribution of water droplets can be expressed using the Volume Mean Diameter (VMD) or the Cumulative Volume Fraction (CVF). The VMD typically refers to the point where CVF is 50%. The CVF refers to the proportion of total droplets that are below a certain droplet volume. The detailed calculation on Volume Mean Diameter calculation appears as following:

$$d_m = 3.21We^{-\left(\frac{1}{3}\right)}d_n \tag{6-11}$$

We refers to the Weber number, while dn refers to the diameter of the sprinkler head. The Weber number can be obtained using equations (6-12) and (6-13).

$$We = \frac{\rho_\omega U^2 d_n}{\sigma_\omega} \tag{6-12}$$

$$U = \frac{Q_\omega}{\pi d_n^2 / 4} \tag{6-13}$$

In the above equations, ρ_w refers to the density of water, with unit kg/m^3; U refers to the velocity of water droplet flow, unit being m/s; and σ_w refers to the surface tension of the droplet. If temperature sets as 20°C, $\sigma_w = 72.8*10^{-3}$ N/m.

Research by Li et al. (2009) has found that the droplet size distribution follows certain rules: when dp < dm, the distribution follows the log-normal distribution function; when dp > dm, the distribution follows the Rosin-Rammler function. See equation (6-14) and (6-15):

$$y = \frac{1}{d\delta\sqrt{2\pi}}\exp\left\{\frac{-\left[\ln\left(\frac{d}{d_m}\right)\right]^2}{2\delta^2}\right\} \tag{6-14}$$

$$y = \gamma\beta\frac{d^{\gamma-1}}{d_m^\gamma}\exp\left\{-\beta\left(\frac{d}{d_m}\right)^\gamma\right\} \tag{6-15}$$

In the above equations, y refers to the particle size within the range of dp and dp+Δdp; d refers to the particle size, with unit being μm; and δ refers to the geometric deviation, with the range being 0.56~0.78.

β , γ refer to the amount associated with the nozzle, with the range being: $0.61 \leqslant \beta \leqslant 0.7$, $1.54 \leqslant \gamma \leqslant 1.78$.

Very few experiments were carried out on studying nozzle distribution. Results are inadequate in describing the water distribution for many types of sprinkler types. This thesis studied using the results of Faeth et al. (1995) on the droplet distribution in the area 3.5 m directly below a downward sprinkler with K=80 and operating pressure 0.1 MPa. The volume average particle diameter is about 1400 μm to 1600 μm.

For the side-wall long-throw sprinklers with K coefficients larger than 80, the main factors affecting the droplet size are splash plate shape, structure and bezel set versus pendant sprinklers as labelled in Figure 6.2. In addition, the sprinkler head diameter, flow and operating pressure are also important. When the operating pressure increases, the droplet diameter generally becomes smaller. When the sprinkler diameter increases, droplet size also increases. Laser-based shadow imaging system was used by Zhou and Yu (2011) to study the impact of sprinkler geometry on fire sprinkler spray formation. The study focused on the key components of a typical sprinkler including deflector, boss and frame arms. The size of water droplets is found to be affected by the width of the slot. The diameter of the deflector and the structure of the boss have minimal impact on the size of water droplets. The boss primarily determines the slot spray discharge angle. The frame arm can give a vertical spray following the direction of the

frame arm.

However, the effect of flow coefficients on droplet diameter of sprinklers is not large. Therefore, the average droplet diameter is specified as 1600 μm in the numerical simulation. Other experiments using Laser Diffraction experiments including those at Tianjin Fire Research Institute supported their assumption. With different angle of reflection, the average water spray particle size was found to be about 1500 μm to 1600 μm using the pressure and flow rate of water in the full-scale experiment of this study.

6.5 Nozzle Flow Characteristics

The sprinkler nozzle flow characteristics can be expressed as:

$$Q = K\sqrt{10 \times P} \qquad (6\text{-}16)$$

Q refers to the flow rate, with unit L/min; P refers to the nozzle operating pressure, with unit MPa; and K refers to the flow coefficient. The K value reflects the sprinkler nozzle capacity. The larger the value of K, the stronger the spray ability. Table 6-1 lists the relationship among the outlet size, flow coefficient and flow proportion.

Based on Table 6-1, when the sprinkler diameter is 12.7 mm, with the related flow coefficient being K=80, the sprinkler nozzle flow characteristics curve is shown in Figure 6.3.

6.6 Fire Sprinkler Layout Settings and Start Time

In this study, the fire extinguishing system uses an open system, with the nozzle height from the ground set at 10 m, side spray arrangement and sprinkler operating area as specified in Figure 6.4. In this area, the sprinkler distribution ability meets the requirements (as demonstrated in the experimental results in Chapter 4. The fire load (standard combustion) is placed in the sprinkler operating area.

The time for the water sprinkler system to start emitting water is determined by the early fire disaster detection time and the fire system activation time. In a medium danger level situation, the growth rate of the fire is generally 0.006 m/s. The maximum response time of the alarm system is not more than 25 s, while the time from the activation of the fire extinguishing system to the emission of water is typically 90 s. Thus, the emission of water typically happens only 120 s after the start of the fire disaster.

With regard to the temperature sensor used to activate the sprinkler and the fire extinguishing system, Heskestad and Bill (1988) provided the following system equation by McGrattan (2005).

$$\frac{dT_1}{dt} = \frac{\sqrt{|u|}}{RTI}(T_g - T_1) - \frac{C}{RTI}(T_1 - T_m) - \frac{C_2}{RTI}\beta |u| \qquad (6\text{-}17)$$

The above equation is one of the most commonly used equations in related research.

The related variables in the above equation are: u being the speed of the gas, with unit m/s; T_1 being the temperature of the connected object, with unit K; T_2 being the surrounding temperature of the connected object, with unit K; T_m being the temperature of the sprinkler, here assumed to be the same as the surrounding temperature, with unit K; B being the steam mass volume; RTI being the detection system senstivitiy; C being the heat lost coefficient when passing through the equipment; and C_2 being the experimental constant, with value 6 x 106 K / (m/s)1/2.

6.7 Heat Transfer between the Droplet Spray

Figure 6.5 shows the relationship in the heat transfer between the spray droplets and smoke.

The related variables are sprinkler radius r_d; sprinkler mass m_d; velocity V_d; temperature T_d; and smoke temperature T_g.

As the diameter of the spray droplets is relatively small, the internal heat transfer among the spray droplets can be ignored, with temperature assumed to be evenly distributed. The heat transfer process of spray droplets and flue gas can be expressed as:

$$m_d c_{p \cdot d} \frac{dT_d}{dt} = \dot{q} - \dot{m}_d h_v \qquad (6\text{-}18)$$

where q refers to the overall heat transfer within the droplet and flue gas, unit being

kW; m_d refers to the evaporation rate of sprinkler droplets, units being kg / s; h_v refers to the enthalpy of the droplet, units being kJ / kg; and c_{pd} refers to the sprinkler mass pressure enthalpy, units being kJ / kg.K.

The droplet evaporation is calculated in a semi-empirical way. If the liquid droplets are suspended in the air, its evaporation method depends on the vapor steam quality loss, evaporation loss in the mass balance equation, droplet and flue gas heat transfer, in accordance with the Priem droplet evaporation model, as stated in following:

$$\dot{m}_d = -2\pi r_d \rho_g DSh\left(Y_d - Y_g\right) \tag{6-19}$$

In the equation, M_d is the water droplet mass; D is the steam distribution coefficient as it enters the air; Y_d, Y_g are the water droplet surface and flue gas mass; Sh is Sherwood number; and p_g issmoke density.

$$Sh = 2 + 0.6 \cdot \mathrm{Re}^{1/2} \cdot Sc^{1/3} \tag{6-20}$$

Y_g and Y_d depends on equations (6-21) and (6-22):

$$X_d = \exp[\frac{h_v M_w}{R}(\frac{1}{T_b} - \frac{1}{T_d})] \tag{6-21}$$

$$Y_d = \frac{X_d}{X_d(1 - M_a / M_W) + M_a / M_W} \tag{6-22}$$

In the above equation, X_d is the steam mass proportion; h_v is the latent heat from steam; M_w is the molar mass of water; M_a is the molar mass of air; R is the gas constant; T_b is the boiling point of water; and T_d is the sprinkler droplet's temperature.

There are two ways to transmit the heat of water droplet and hot flue gas, one main transmission is convection, the other is radiation, but the temperature of flue gas flow is not high, thus the radiation produced by the flue gas can be ignored. A single droplet and smoke exchange heat formula can be expressed as:

$$\dot{q} = 4\pi r_d^{\,2} h_d \left(T_d - T_g\right) \tag{6-23}$$

Finally, the total heat energy absorbed by the water droplets from the flue gas can be expressed as:

$$\dot{Q} = \sum \dot{q} = \sum 4\pi r_d^{\,2} h_d \left(T_d - T_g\right) \tag{6-24}$$

During a fire, as smoke spreads to the protection area formed by the sprinkler water droplets at the fire site, an interaction will be created, resulting in cooling and settling characteristics (Chow et al. 2000). On one hand, water droplets will absorb the heat of the flue gas through heat transfer. On the other hand, the drag of the water droplets will create disorder in the smoke layer, resulting in smoke congestion. As smoke spreads downwards, the congested spread and wake may create a threat to the evacuating people (Li et al. 2002).

As described above, in the discharge of water droplets, a portion will have a direct

relationship with the smoke layer (You et al. 2005). The water droplet and direct effect of the fire zone will cause a portion of the water droplets to be directly evaporated during their descent. As the latent heat of vaporization of water is relatively large, it will absorb large quantities of heat, thereby reducing the temperature of the fire site, at the same time slowing down the combustion process in the fire site, thereby reducing the flame height. In confined spaces, the vaporized water will enter the smoke layer, create a large smoke-water mixture, increase the thickness of the smoke layer and compress the air layer, resulting in a significant decrease in oxygen concentration. At a certain level, this also reduces the fire burning intensity. Another portion of the water droplets will not be vaporized and will penetrate the fire site to the surface of the burning materials, directly cooling the burning materials, thus achieving the effect of rapidly reducing the power of the fire source.

6.8 Numerical Simulation on Sprinkler Pressure

As described in Chapter 5, water distribution experiments were conducted under various conditions on standard side-wall long-throw sprinklers installed in tall and large spaces. Based on this, related research were conducted and basic working parameters were selected.

Tall and large spaces are typically found in shopping malls and exhibition centres. Fire hazard is generally set to British standards for intermediate risk level (LPC 1987) by Chinese Standard GB50045-95 (2005 edition) (China National Standard 2005c), medium risk (I) level and medium risk (II) level.

Numerical simulation in a hall of 24 m*12 m*12 m (L * W * H) was carried out. There is a 2.5 m*4.0 m (W*H) exit as shown in Figure 6.6. The computational domain area is fixed as 9 m*4 m*12 m (L*W*H).

The indoor and outdoor temperature is 20℃. The regional units within the computing grid is 0.1 m * 0.1 m * 0.1 m, within which there are 43,200 grids. Five measurement points of thermocouples were setting up at the following distances from the top of the outer surface of the central combustion of 2 m, 4 m, 6 m, 8 m and 10 m. (See Figure 6.7)

The key parameter of simulation is the design fire, which is taken as having constant heat release rate. According to related study results by Wen (2014), under medium danger level conditions, within 120 s of the start of a fire, with the presence of a sprinkler system, the effective heat release rate is about 1.5 MW. In order to be more safe and conservative, when confirming the maximum heat release rate, 1.5x safety factor is considered, simulating a fire source with maximum heat release rate of 2.2 MW. This choice is consistent with the result in Chapter 4 from the three wood crib combustion experiment. See Figure 6.8.

The main system operating parameters are assumed once the sprinkler system installation type, sprinkler height, and sprinkler flow coefficient have been confirmed. Numerical simulations are to evaluate the effectiveness of the fire extinguishing systems under different operating pressures.

Based on standard fire extinguishing system design, the selected operating pressures

are 0.20 MPa, 0.35 MPa and 0.5 MPa.

6.9 Simulation Scenarios

Two modeling scenarios with sprinkler pressure 0.2 MPa and 0.5 MPa were simulated.

6.9.1 Scenario 1 with operating pressure of 0.2 MPa

Scenario 1N: No water spraying, 2.2 MW fire.

Scenario 1A: Sprinkler flow coefficient K=80, average particle size of the spray droplets 1.6 mm, sprinkler activation time 120 s.

Scenario 1B: Sprinkler flow coefficient K=115, average particle size of the spray droplets 1.6 mm, sprinkler activation time 120 s.

Scenario 1C: Sprinkler flow coefficient K=161, average particle size of the spray droplets 1.6 mm, sprinkler activation time 120 s.

6.9.2 Scenario 2 with operating pressure of 0.5 MPa

Scenario 2N: No water spray, 2.2 MW fire.

Scenario 2A: Sprinkler flow coefficient K=80, average particle size of the spray

droplets 1.5 mm, sprinkler activation time 120s.

Scenario 2B: Sprinkler flow coefficient K=115, average particle size of the spray droplets 1.6 mm, sprinkler activation time 120 s.

Scenario 2C: Sprinkler flow coefficient K=161, operating pressure P=0.5 MPa, average particle size of the spray droplets 1.6 mm, sprinkler start time 120 s.

The spray modeled scenarios predicted by FDS are shown in Figures 6.9, 6.10 and 6.11. As the main purpose of the simulation is to study the impact of the operating situation on fire extinguishment, the computing time was selected to be 400 s.

6.10 Model Results and Analysis for Scenario 1

Figures 6.12 to 6.16 show the modeling calculation results based on five designated situations under an operating pressure of 0.1 MPa.

Sprinklers of flow coefficient K=115, K=161 control fires very quickly as shown in the temperature curves of Fig. 6.12. 20 s after the fire extinguishing system emitted water, the temperature in the location 2 m above the centre of the top outer surface of the combustion object decreased from above 800℃ to below 350℃.

Thereafter, until 400 s, under the effect of the K=160 sprinkler, the T1 temperature decreased to about 200℃, and then reversed slightly rather than continued to decrease. Under the effect of the K=115 flow coefficient sprinkler, the temperature decreased to about 250℃, and then reversed to a larger degree than before rather than continued to

decrease.

With regard to sprinklers with flow coefficient K=80, Figure 6.12 shows that under an operating pressure of 0.1 MPa, the system is basically unable to control the fire.

After the fire extinguishing system emitted water, under the operation of sprinkler flow coefficient K=161 and K=115, the temperature in the location 4 m, 6 m, 8 m and 10 m away from the centre of the top outer surface of the combustion object showed a significant decrease. For the sprinkler with flow coefficient K=161, after 20 s of operation, average temperature each point (T1, T2, T3, T4) decreased to 95℃, 50℃, 45℃ and 35℃ respectively, and stabilized. At time 400 s, the temperature presented a reversal trend, but the sprinkler with K=115 is less effective than the Sprinkler with K=161. All these are shown in Figures 6.13, 6.14, 6.15 and 6.16.

Under the operation of the sprinkler with flow coefficient K=80, the temperature of each point did decrease, but basically did not achieve the fire control effect, as most clearly shown in Figure 6.13.

The modeling calculation results in Scenario 1 show that under the same operating pressure, , the fire extinguishing effectiveness of side-wall long-throw sprinklers with different flow coefficients in tall and large atria are significantly different. Considering this situation, without changing other conditions, Scenario 2 increases the sprinkler operating pressure by 2.5 times to 0.5 MPa. The purpose is to evaluate the fire extinguishing effectiveness of sprinklers with different flow coefficients after significantly increased operating pressure.

6.11 Results and Analysis for Scenario 2

Figures 6.17 to 6.21 show the impact of the fire extinguishing system in extinguishing fires under five designated modeling scenarios with different flow coefficient sprinklers (including temperature of different locations in the fire site) under an operating pressure of 0.5 MPa.

6.11.1 Analysis of Thermocouple T1 Temperature Change over Time

From Figure 6.17, after increasing the operating pressure to 0.5 MPa, the fire extinguishing ability of the flow coefficient K=161 sprinkler has a breakthrough increase. 20 s after emitting water, the average temperature in location T1 has decreased to about 100℃. For a flow coefficient K=115 sprinkler, 20 s after emitting water, the T1 average temperature reduced to below 300℃.

Thereafter, till 400 s, the ability to control fire is always very stable, with no temperature increase in location T1. However, for the sprinkler with coefficient K=115, the fire control situation did reverse. 250 s later, the temperature increased to above 200℃. At 400 s, the temperature decline trend is not obvious.

Figure 6.17 shows that under an operating pressure of 0.5 MPa, a sprinkler with flow coefficient K=80 is also unable to control fires.

6.11.2 Analysis of Thermocouples T2 to T5 Temperature Change over Time

After the extinguishing system emitted water, under the operation of sprinklers with coefficient K=161 and K=115, the temperature in the location 4 m, 6 m, 8 m and 10 m away from the centre of the top outer surface of the combustion object reduced significantly. 20 s after flow coefficient K=161 sprinkler emitted water, the average temperature in each location (T1, T2, T3, T4) declined to below 40℃. As the temperature stabilized, the trend did not change till 400 s. Under the operation of a sprinkler with flow coefficient K=115, the situation is similar to the above sprinkler, but the results are not significant.

Although the temperature also reduced with a flow coefficient K=80, there is basically no fire control effectiveness. This shows that even after increasing the operating pressure significantly, this type of sprinkler is still unable to effectively extinguish fires.

All these are shown in Figures 6.18, 6.19, 6.20 and 6.21.

6.11.3 Comparison of CFD and tests results

In comparing CFD prediction with the full-scale experiment, the steady burning stage is considered. All the initial conditions were set before CFD simulation without sharp changes of pressure at the beginning.

In full-scale experiment with sprinkler, it took time to develop the pressure at the pipe after starting the pump. Since the sprinkler height is over 10 m, the pressure would give higher water flow rate than the steady period. As a result, the fire was controlled faster than CFD at the beginning, giving differences between the full-scale experiment

and the CFD simulation result at the beginning.

Apart from the above observation, the CFD simulation results agreed well with the full-scale burning tests.

6.12 Summary

The theoretical basis for selecting FDS fire simulation software was introduced in this Chapter. The basic procedures, combustion model and radiation model were introduced. Sprinkler testing was established from distribution of sprinkler droplets, sprinkler flow characteristics, sprinkler design characteristics, fire extinguishment system activation time and the heat transported during the activation of the sprinkler. Based on this, fire source and key fire extinguishing system parameters were determined in the numerical study by combining the related factors. Appropriate boundary conditions were selected in FDS simulation. Two sets of four typical scenarios were identified for numerical studies. The simulation results indicated that sprinklers with coefficient K=161 and K=115, installed at a 10 m height, with 0.5 MPa operating pressure would give effective suppression.

Chapter 7 Experiments on Sprinkler-Fire Interaction

7.1 Experimental Studies

Full-scale burning experiments were conducted in a large hall of length 24 m and area 12 m by 12 m. There was an opening of 2.5 m by 4.0 m, as shown in Figure 7.1. The fire suppression experiment was then conducted on two side-wall long-throw sprinklers installed at height 10 m above the ground. The operation area of the sprinklers is shown in the area designated in Figure 5.14.

There are a few purposes in conducting the real-life experiment. First, validating the results produced by the mathematical simulation. Second, scientifically designing the experimental conditions to ensure that the experimental results are more scientific.

The selected sprinkler system was an open system. The system activation time is 120 s after the actual combustion of the materials. The feed pump, sprinkler piping and side-wall sprinkler positioning have similar conditions to those in Chapter 5.

From CFD simulations with FDS, sprinkler heads of flow coefficient K set at 80 (Note that K has no special unit, because K= Q/ (10P) ^ 0.5, where Q is water flow with unit L/min, and P is pressure with unit MPa) was difficult to control fires. Under operating pressures reaching 0.5 MPa, sprinklers of flow coefficients K of 115 and 161 would have better control on the fires, which means, heat release rate of burning word cribs would not increase anymore. A flow coefficient K of 161 yields the best results. From

the previous chapters on water distribution experiments, three types of sprinklers selected were with flow coefficients 80, 115 and 161. These sprinklers were operated under the operating pressure of 0.5 MPa in this fire extinguishing experiment.

7.2 Selection of Combustibles

The basis for the selection of combustion materials is that of a steady-state burning fire source with steady heat release rate, which can be easily put in the mathematical model. Based on the research conclusions in Chapter 4, the wood crib pile built using the three standard wood cribs (Figure 7.2), after 120 s of combustion, the heat release rate changed from the maximum to the stabilized state, with an average heat release rate of 2.2 MW. Furthermore, it will last a relatively long time (typically more than 500 s), the trend stabilized. Thus, three standard wood cribs were used as the combustion material for this experiment.

Even though there is no significant difference between total heat released and average heat release rate, different placement methods results in a significant difference in the heat released within a specific period, creating different difficulties in extinguishing fires (Widmann 2001). Thus, a fire extinguishing experiment should consider these types of problems. Grant et al. (2000) evaluated the current use of water sprays in suppressing and extinguishing typical compartment fires. The researchers pointed out that the key purpose of water in fire suppression and extinguishing is to remove heat from the fuel body. Thus, the heat content of the fuel is the most important determinant of the water required to put out the fire.

The wood cribs were selected as an example, with different placement methods (see Figures 7.3, 7.4, 7.5). From the research conducted in Chapter 4 and the results shown in Table 4-3 to 4-8, the time to ignite the crib and fully burn the materials is about 120 s. The n-heptane in each oil pan is 1.5 litres. The experiment in this chapter will proceed based on these requirements. Similar to the mathematical modeling process, temperature sensing points were placed at distances of 2 m, 4 m, 6 m and 8 m away from the surface of the combustion material.

7.3 Sprinkler Droplets Penetration

Under different experimental conditions, the amount of water required to effectively penetrate the fire and the upward airflow has to be understand. This requires a good interaction of water distribution facilities and fire extinguishing facilities. A collection pan was placed in the sprinkler operation area, consistent with the specifications of the water experiment. A metal structure was put on the water collection pan, wood crib on the metal structure, and combustible materials beneath the metal structure (n-heptane) in an oil pan. It was removed when the ignition time was close to 120 s. The collection pan beneath the wood crib was used to collect the hot air flow penetrating the tall and large space and water volume of the gas flame. Preliminary research was conducted on the sprinkler droplet penetration ability, as shown in Figure 7.6.

Results on above are shown in Figures 7.7 to 7.12.

7.4 Wood Crib Fires with Sprinkler of K=80

Based on mathematical modelling results under an operating pressure of 0.5 MPa, sprinklers of flow coefficient K=80 are unable to effectively put out a fire source of 2.2 MW. Fire extinguishing results proved this conclusion. Figures 7.13 to 7.15 show the fire extinguishing process using a K=80 sprinkler, with a wood crib placed as straight, stacked placements, and one on top and two below.

Wood crib (straight line placement) fire temperature change over time (Figure 7.13) shows that: at the distance 2 m away (temperature 4) from the wood crib, the temperature was over 350℃, at the distance 4 m away (temperature 3) and 6 m away (temperature 2), temperatures increased to 180℃ and 50℃ respectively.

Wood crib (stacked placement) fire temperature change over time (Figure 7.14) shows that: at the distance 2 m away (temperature 4) from the wood crib, the temperature was over 350℃, at the distance 4 m away (temperature 3) and 6 m away (temperature 2), temperatures increased to 200℃ and 80℃ respectively.

Temperature-time diagram for wood crib (one on top, two below) (Figure 7.15) shows that at a distance 2 m away from the surface of the wood crib (temperature 4), temperature reached about 300℃, at the distance 4 m away (temperature 3) and 6 m away (temperature 2), temperature reached about 50℃.

As shown in Figure 7.13, after water was discharged, the temperature reduced to

300 ℃, then with a reversal, after reaching 280℃, this status was maintained for 500 s. 900 s after fire extinguishing, the wood crib was still burning, representing the inability to control the fire.

As shown in Figure 7.14, after water was discharged, the temperature reduced to 300 ℃, then with a reversal, after reaching 280℃, this status was maintained for 200 s. Thereafter, the temperature decreased to 250 ℃, and continued till 500 s after water was discharged. The temperature did not decline. 950 s later, after the upper layer wood crib collapsed, the fire remained, representing an inability to control the fire.

Figure 7.15 shows that after water was discharged, the temperature declined slightly. 10 s later, the temperature increased, reaching 1,000℃. 280 s later, then declining thereafter. 500 s later, the temperature continued to be maintained at 500℃, representing an inability to control the fire.

7.5 Wood Crib Fires with Sprinkler of K=115

Based on the above analysis, it can be seen that even though the fire could not be controlled effectively, placing the wood cribs one on top, two below created significantly higher difficulty than the other placement methods. The one on top, two below placement created in both horizontal and vertical directions fire development superior to the other two types. Because of the limitations of the K=80 sprinkler, wood crib fire was unable to be effectively controlled. Thus, the fire site temperature

continued to increase.

When using sprinklers with flow coefficient K=115, it is possible to effectively control the fire 200 s after the activation of the sprinkler system. However, the fire extinguishing result under the straight line or stacked placement is better than that of the one on top / two below arrangement. Figures 7.16, 7.17 and 7.18 show the temperature changes at the fire site with a K=115 sprinkler under the straight line, stacked and one on top/two below placement.

7.6 Wood Crib Fires with Sprinkler of K=161

As the verification test and numerical simulation show similar results, given limited resources, K=161 sprinkler was used to conduct the most difficult fire experiment under the one on top/two bottom placement scenario. The result indicates that the sprinkler is able to effectively control the fire within 200 s of the emission of water, slightly better than the result of using the K=115 sprinkler. See Figure 7.19.

7.7 Summary

Full-scale burning experiments were conducted in a large hall. Working principles, operation height, design of conditions, and choice of fire were discussed. Positions of the fire extinguishing system, choice of sprinklers and fire extinguishing control requirements are matched with the modeling process. The results of the full-scale experiments can be used to justify the simulations.

Chapter 8 Sprinkler Water Droplet Penetration

8.1 Introduction

As discussed in the literature, for suppressing big fires at tall halls, the water discharged from sprinkler should have larger droplets to reach the fire zone. The extinguishing mechanism for sprinklers are:

- Direct action with fire.
- Cooling the smoke layer.
- Pre-wetting neighbouring combustible walls and materials.
- Displacing oxygen.

The equation of motion for a sprinkler water droplet of diameter D, velocity v, mass m and density ρ_w travelling in air of density ρ_{air} is:

$$\frac{4}{3}\pi\left(\frac{D}{2}\right)^3 \rho_w \frac{dV}{dt} = \frac{4}{3}\pi\left(\frac{D}{2}\right)^3 (\rho_w - \rho_{air})g - 6\pi\eta D v \qquad (8\text{-}1)$$

The terminal velocity v_T of droplet is then worked out by McCaffrey (1979), which shows that:

Maximum upward velocity in a fire plume

$$u_0 = 1.9\,\dot{Q}^{1/5} \text{ m/s}$$

The unit of Q is in kW.

But for sprinkler water droplets of radius a, there is a terminal velocity V_T,

$$\text{i.e.} \quad 6\pi\eta a\,(v_T + u_o) = \frac{4}{3}\pi\,(\rho_w - \rho_o)\,g\,a^3$$

$$v_T = \frac{2(\rho_w - \rho_o)ga^2}{9\eta} - u_o$$

Water droplets smaller than 2 mm diameter in a 4 MW fire will have this condition satisfied. Water cannot penetrate a plume to cool the surface of the burning object.

At this stage, the fire becomes ventilation-controlled. The severity depends on the available air supply. This is because the combustible materials are being decomposed very quickly. It is impossible for sufficient air to enter the compartment to allow complete combustion. Therefore, very hot combustible gases will spill out of the compartment and burn when they mix with sufficient oxygen. That is why long flame coming out the window can be observed.

8.2 Actual Delivered Density and Required Delivery Density

In the aforementioned analysis, it is repeatedly emphasized that when the sprinkler installation height is relatively high or the fire load is relatively large, the water discharged requires a certain proportion of large droplets to ensure that upon reaching the fire zone, the droplets will not be fully vaporized. This research pertains to the fire extinguishing technique in tall and large spaces, therefore the proportion of large droplets required exceeds that of typical large spaces. The purpose of this type of large droplets is to ensure the water droplet's ability to penetrate.

The concept of Actual Delivered Density (ADD) was proposed by Factory Mutual Research Corporation (FMRC) to investigate water penetration (LPC Laboratories Phase 1 report – Investigation of the suitability of Actual Delivered Density Apparatus (ADD) for the performance evaluation of the standard sprinklers as described in insurance service project proposal project no TE91014-19) (LPC 1999). ADD (with unit L/min m^2) refers (LPC 1999) to the unit area and unit time of water that penetrates the fire zone and lands on the combustible area. On the other hand, the Required Delivered Density (RDD) refers to the minimum delivered density necessary to control the fire disaster. When the ADD is larger than the RDD, the fire extinguishing system is able to effectively control the fire.

The ADD experiment is an important technical technique when analyzing sprinkler drop dynamics and nozzle performance, and has been used in the United States and Europe. The Loss Prevention Council Laboratories has the ADD experiment setup created based on different specifications. The U.S. experimental laboratory has focused on the application on the Fast Response, Early Stage (ESFR) special sprinklers (LPC 1987), and LPC experimental laboratory to measure standard sprinkler ADD values, establishing evaluation criteria related to sprinkler droplet penetration ability by project no. TE91014-19 (LPC 1999). Research on the relationship between ADD experiments and actual fire experiments was reported by Cheng (1997), Chan et al. (1994), Chan (1994) and Yu (2004).

Nam (1996, 1999) used computational models to study the ability of sprinklers to penetrate fires while varying the rate of water flow, size of spray droplets and spray momentum. Nam generated a large number of spray models with 275 trajectories and

specified for each a designated release speed, release angle, drop size and mass flow rate. A Lagrangian particle tracking scheme was then used to combine these spray models with free-burn fire plume models. The results demonstrate that as opposed to increasing spray momentum, increasing the size of water droplets is a more effective approach to increase the penetration ability of a sprinkler. The results also provide a means of arriving at the ideal flow rates that would maximize the penetration ability of any designated sprinkler.

Similarly, Bill (1993) used a computational model to simulate the interaction between a sprinkler spray positioned overhead and a fire plume. A Lagrangian scheme was used to calculate the droplet trajectories, and the particle-source-in-cell technique was used to calculate the interactions among moment, energy and droplet mass. The spray was modeled after the droplet size distribution, water distribution and axial momentum characteristics of a commercial sprinkler. The computational testing was conducted at two ceiling heights: 3.05 m and 4.57 m. Verification tests then conducted reveal that the model accurately predicted Actual Delivered Density for the lower ceiling height of 3.05 m, but underpredicted the ADD for the higher ceiling height of 4.57 m.

Schwille and Lueptow (2006) conducted experiments to examine the changes in the structure of a fire plume when it is being suppressed. Key characteristics such as the fire plume infrared intensity contours, plume height, plume width and plume area were measured. Schwille and Lueptow (2006) used a wide angle nozzle, narrow angle nozzle and a F980 sprinkler with different orifice sizes, nominal K factors and spray angles to generate sprays with different characteristics. A methane burner was then used to generate various desired plume sizes. The results show that increasing the

strength of the spray increases the effective width of the spray, and suggest that there is usually a portion of the plume that droplets typically will have difficulty in penetrating.

In order to conduct ADD experiments, it is important to understand the characteristics of sprinkler sprays. Ren et al. (2011) proposed a comprehensive approach to characterize sprinkler sprays. Using laser-based shadowgraphy and a particle tracking velocimetry system, the researchers were able to fully characterize the initial spray generated by two chosen sprinklers, an ESFR pendent sprinkler and a Tyco D3 spray nozzle. Spray characteristics were then made concrete with local measurements mapped onto a spherical coordinate system. The results reveal a strong relationship between sprinkler geometry and the corresponding spray pattern.

ADD experiment and related numerical models were also reported by Bill (1993a, 1993b), Nam (1996, 1999, 2004, 2005).

8.3 Water Droplet Penetrability

The mentioned ADD laboratory test setup typically uses spray fire to simulate real fires of different sizes, thereby creating conditions similar to actual fire sites. It also measures the ADD by collecting the water that can penetrate the fire zone and heat air flow.

No specialized ADD experiment setup was used in this study. A setup that fits the fire zone requirements of the fire site experiment was adopted. Through collecting the

sprinkler discharged water that can penetrate the fire zone and heat air flow and land on the combustion material, the experiment measures the ADD, and compares the results to water distribution experiments conducted under similar conditions. The related experimental conditions are reported in Chapter 7.

In order to investigate the penetration ability of sprinkler water droplets, the delivered density condition without a burning object, i.e. heat release rate is 0 kW, is set as the Local Delivered Density (LDD). The ratio of ADD to LDD is the sprinkler droplet penetrability (Jackman 1992).

$$P = \frac{ADD}{LDD} \tag{8-3}$$

8.4 Experimental Results

Based on equation (8-3), consolidating the aforementioned water collection data. The P value of sprinkler numbers 1, 4 and 6 under the operating pressure of 0.5 MPa when extinguishing fires is calculated (see Table 8-1).

The above results show the fire extinguishing abilities of penetrability and related factors. For sprinkler number 6, extinguishes fires three times, penetrability does not reach 0.40, thus with regard to actual fire disasters, it is unable to effectively extinguish fires. Sprinkler numbers 1 and 4 have penetrability above 0.90, and have a relatively good fire extinguishing ability. Next, from the perspective of the ability to extinguish different types of wood cribs, even though sprinkler number 1 is able to extinguish all

three types of fire loads, but the penetrability is only 0.75 for the one on top/two below placement, less than the penetrability of the other two types of fires. This also demonstrates the difficulty of extinguishing fires with a one on top/two below wood crib placement.

8.5 Summary

Current sprinkler fire extinguishing techniques used in large and tall halls were further discussed. The concepts of Actual Delivered Density (ADD) and Required Delivered Density (RDD) were used. Full-scale experimental setup matched with the fire requirements. Data on the droplets able to penetrate the fire plume and hot air and were able to land on the burning object were compiled to determine the actual delivered density. The experimental results were compared with similar water distribution experiments conducted under similar conditions. Penetration of water droplets and fire load characteristics matched with those observed from fire extinguishing experiments.

Chapter 9 Conclusion

9.1 Overview

The use of long-throw sprinkler in suppressing big fires in tall and large spaces was studied in this thesis through physical experiments and numerical modeling through research on automatic sprinkler systems and fire extinguishing system. Theoretical analysis on the fire scenarios, design parameters and related components such as sprinkler head selection were applied with modeling approach. Large-scale experiments were carried out with HRR measured. Experiments were conducted with and without sprinkler. The appropriate fire extinguishing modeling approach was justified. The basic requirements of automatic fire extinguishing systems were proposed with its performance evaluated by a sprinkler system testing platform. The CFD software FDS was also applied to study the interaction between sprinkler and fire load. Fire extinguishing validation research was initiated. The key factors affecting fire extinguishing effectiveness were determined and appropriate sprinkler structure and basic working parameters (flow coefficient, operating pressure, sprinkler distance, installation height) and other research objectives were proposed.

In basic testing and research work, this paper reviewed the case studies in the field with regard to HRR measurement and related situations, in order to select a widely-applicable combustion material to replace the actual combustion materials in actual places to maximize the ability to model the actual fire situation. The standard experiment combustion material was confirmed to be the standard wood crib. A 10 MW large-scale thermal system was used. Research on one, two, three, four wood

cribs placed in a straight line, stacked, and one on top/two below placements were initiated. Using these experimental conditions, the key characteristics of the experiment objects in the combustion stabilization period were obtained, thus establishing a good basis for future actual object fire research experiments. Through analysis of the fire situations in tall and large atria, the key fire extinguishing requirements were obtained and the use of side-wall long-throw sprinklers in tall and large spaces using an open system design method was initiated. Based on related standard requirements, a water distribution testing platform was established, and research were performed on sprinklers with installation heights of 6 m, 8 m and 10 m, and operating pressures of 0.2 MPa, 0.35 MPa and 0.5 MPa. Based on the water characteristics research, the technical characteristics of the three types of sprinklers were confirmed to have a good water distribution ability in tall and large spaces.

Mathematical modeling of sprinkler fires and the associated physical experimental validation are the key parts of the thesis. CFD-FDS model software with appropriate combustion and thermal radiation models can be applied for studying sprinkler-fire interactions. From the sprinkler droplet size distribution, sprinkler flow characteristics, sprinkler design and fire extinguishing activation time settings, heat removed from fire and smoke can be studied by the mathematical model established.

The threshold conditions for the FDS software was innovatively enriched to allow it to be used in side-wall long-throw systems. Two scenarios including four types of typical situations were designed to obtain the results under three large throughput sprinklers with different flow coefficients, and under different system conditions. The results indicated that sprinklers with flow coefficients 115 and 161, installed at side-

walls with installation heights of 10 m and under an operating pressure of 0.5 MPa, can effectively extinguish medium danger fires. In order to verify the experimental results and actual suitability, this thesis initiated validation research on side-wall long-throw sprinklers in tall and large atria, breaking new ground in the choice of working principles, installation height, design conditions, and fire load selection.

It can be concluded that the extinguishing system layout, sprinkler selection and extinguishing control requirements are basically in-line with those of the mathematical models. The conclusions drawn from experiments and modeling are very consistent. By using ADD and RDD in this thesis, physical fire experiments confirmed that the long-throw sprinkler system can suppress the fire in a tall hall. This was achieved by collecting the water discharged from the sprinklers that can penetrate the flames and hot air to reach the burning surface. ADD was then compared with RDD of water distribution experiments under the same conditions without a fire.

9.2 Proposed Long-throw Sprinkler Design

Experimental design parameters suitable for use in side-wall sprinkler systems in tall and large spaces are summarized as following:

- Appropriate operating pressure 0.5 MPa.
- Appropriate sprinkler installation height 6 m to 10 m, and no limit on height of object to be protected.
- Sprinkler effective operating area 6.5 m by 2.5 m with sprinkler head separated by a distance of 2.5 m.

- Sprinkler flow coefficient over 115. (No unit for K as K is given by Q/ (10P) ^ 0.5, where Q is water flow with unit L/min, and P is pressure with unit MPa.)
- Main pipe diameter over DN100 mm, Branch pipe diameter DN25 mm to DN32 mm.
- Sprinkler designed flow over 131 L/min for each sprinkler.
- Average sprinkler operating intensity over 5 mm/min.

Technical characteristics of side-wall long-throw sprinklers are discussed in Chapter 5, which illustrates the typical fire disaster scenario and evaluates the characteristics of sprinklers positioned on top versus side-wall sprinklers. Section 5.3 to 5.6 describe an experimental study conducted to evaluate the sprinkler water distribution ability of sprinklers with different flow coefficients, and with different installation heights and working pressure. Verification of standard combustion products is discussed in Chapter 3, which analyzes the characteristics of common combustible objects using heat release rate (heat released in a unit of time) and oxygen consumption calorimetry. The wooden crib was chosen as the standard combustible object for this research as it is commonly found in Class A combustible materials and exhibits stable steady state combustion characteristics. Chapter 4 describes an experimental study based on five experiments to examine changes in the placement of and the number of combustible objects (pine wood cribs). Each experiment consisted of two parts: the ignition calorimeter test to separately measure the heat release rates of the oil trays, and the wood crib calorimeter test to measure the heat release rates of the wood cribs. The results show a clear heat release rate stabilization phase lasting 6 minutes or more, and illustrate different stages of fire disasters that could be modeled by varying the

placement of and number of wood cribs. Sprinkler water droplet penetration confirmation is discussed in Chapter 8, which introduces the concepts of ADD, RDD and Sprinkler Droplet Penetrability. The Sprinkler Droplet Penetrability was then calculated based on the water collection data for various sprinklers with different wood crib numbers and placement methods.

9.3 Discussion

With rapid economic development and technological improvements, tall halls and atria have become increasingly common in commercial buildings and in architectural designs. This type of construction typically relates to a highly dense area, with higher difficulty in separating fires and significant limitations on common methods of detecting and extinguishing fires. As the indoor space in atria is relatively large, and there are numerous construction materials, tall stack piles, decorative materials of large fire load and relatively many furniture, there are numerous safety issues involved. The temperature of the fire site will increase rapidly, and the fire disaster will expand quickly with large heat release rate, early flashover. Large amounts of smoke produced will be difficult to extract, creating a dangerous situation. Once a fire disaster occurs, if it is unable to extinguish or control the fire quickly, there can be grave consequences for the building, the country and society. Thus, the extinguishing of fires in tall spaces must emphasize early detection and rapid fire extinguishing. Under ordinary scenarios, when using closed end automatic sprinkler systems, the sprinkler head is typically installed at the ceiling. With regard to tall and large spaces, however, although theoretically it is possible to place the sprinklers in a ceiling that is below 18 m, even though the sprinkler contains the ability to respond rapidly, due to the time required

for the smoke and temperature to increase at the increased height, the activation time of the closed end sprinkler might be slightly delayed than usual.

With regard to a site where the fire disaster is expanding rapidly, once the opportunity to extinguish the fire early is lost, the difficulty in extinguishing the fire increases significantly. In Hong Kong, it is common to see no sprinklers above easily combustible materials. Once caught on fire, with rapid expansion, as large volumes of smoke is produced, regardless of whether the smoke is dissipated naturally or mechanically, whether the smoke layer can maintain a relatively tall height can be a question of life and death for the people being evacuated and the firemen who are deployed on site. With regard to the distinguishing characteristics of tall and large spaces, traditional automatic sprinkler systems typically have significant difficulty in effectively landing the water on the surface of the combustion material, penetrating it and extinguishing the fire. Thus, it is important to challenge traditional notions of automatic fire sprinkler fire extinguishing techniques, and conduct in-depth research starting from fire extinguishing basic principles, product development and related techniques. It is also important to detect the temperature of the fire site early, and activate the fire extinguishing system in time. In particular, in the early stage of the development of the fire, in ensuring that the water distribution is even, it is important to increase the strength of the sprinkler and the ability of water droplets to penetrate the hot air flow, thereby creating new fire extinguishing techniques, automatic sprinkler systems and related techniques.

The conventional understanding with regard to side-wall long-throw sprinklers is that its use is relatively limited. For example, this type of sprinkler could only be used in

relatively low danger situations, and only through special verification can it be used in medium danger situations in accordance with specific rules. However, the current construction structure is multi-varied, leading to the need to constantly innovate on sidewall long-throw sprinkler fire extinguishing related techniques. With regard to the use of sidewall long-throw sprinklers in tall and large spaces, as the position of these sprinklers is difficult from those in a typically conference room or guest room, and as the sprinkler installation height is significantly higher than in typical situations, the main consideration is not the simple ability to make the wall wet.

Thus, there are challenges in providing fire suppression systems in tall and large halls. Long-throw sprinkler is a possible solution and adopted in some projects. Questions raised by the industry were addressed in this thesis. The main innovation areas reported in this thesis are:

- Proposed the fire extinguishing application method of the use of side-wall long-throw sprinklers in tall and large atria, effectively solved the limitations of common automatic sprinkler systems in tall and large spaces.

- Real-scale experiments were conducted on side-wall long-throw sprinklers in tall and large spaces, with innovative choices of operating principles, installation height, experimental conditions and fire load selection.

- Demonstrated that the CFD model FDS can be applied in studying sprinkler-fire interactions, and verified by physical experiments.

- Key design parameters are proposed for designing long-throw side-wall sprinkler systems in tall and large spaces.

9.4 Limitations

However, due to objective conditions, time and resource limitations, there are several inherent limitations of this research, mainly noted as per below:

First, there are limitations in the choice of fire extinguishing models. The multi-varied nature of tall and large atria decides the complexity of fire disasters, especially with regard to the variety of decoration materials, building products and the multiple items being stored and sold. This experiment only used fire cribs as the object of experimental research, and conducted experiments based on the fire characteristics of these wood cribs in medium fires. However, future research can focus on fires with faster growth rates, in order to expand the area of research.

Second, in tall and large spaces the construction materials, decorative materials are numerous, stack piles high, fire load large, resulting in a rapid increase in temperature in the fire site. This research has focused only on wood crib fires, and did not consider varied types of combustible objects. The next step of research would be to analyze, categorize and draw conclusions based on the fire characteristics of multiple types of combustion materials, and conduct experiments to verify these conclusions.

Third, in-depth research on the working relationship between fire sprinklers in tall and large spaces and the smoke produced by the fire has yet to be conducted. Recently,

with regard to sprinkler systems commonly installed in the ceiling of buildings, there is already some basic research having been conducted on the interaction among the sprinkler water droplet flow, the mist formed as a result of the heat and the smoke formed during the fire disaster. However, such research has focused on the mathematical modeling phase, and has not used actual fire site experiments to verify these theoretical hypotheses. There has also been very limited research on the installation and use of side-wall long-throw sprinklers in tall atria. The next step is to conduct detailed research in this direction.

9.5 Future Works

Given the increasingly multi-varied nature of the structure and function of materials in tall and large spaces, the application of automatic sprinkler systems must also be increasingly versatile. Suggested areas of focus for future research include: automatic fire extinguishing techniques and research related to the layers of materials in building walls, including the decorative layer and insulation layer. Another potential avenue for future research is the potential addition of high efficiency fire extinguishing agent in the water used to extinguish fires. With the aim of early detection and rapid fire control, future research can also focus on how sprinklers can effectively produce a flow of water droplets that not only effectively extinguish fires, but also innovate on the structure of conventional sprinklers and are of low voltage, high efficiency and water-saving.

References

Babrauskas V., Grayson J. 1992. Heat Release in Fires. New York: Elsevier Science Publishing CO., pp. 1-112.

Babrauskas V., Fleming J.M., Russell B.D. 2010. RSET/ASET, a flawed concept for fire safety assessment, Fire and Materials, 34: 341-355.

Bill, R.G. Jr. 1993a. Numerical simulation of actual delivered density measurements, Fire safety Journal, 20: 227-240.

Bill R.G. Jr. 1993b. Numerical simulation of thermal plumes, Fire Safety Journal, 21: 231-256.

British Standard Institution. 1990. BS 5306 Part 2: Fire Extinguishing Installations and Equipment on Premises. Specification for sprinkler systems, British Standard, UK.

Central People's Government of the People's Republic of China. 2009. The fire distribution situation of crowed areas in China. [EB/OL]. http://www.gov.cn/gzdt/2009-07/03/content_1356580.html

Chan T.S. 1994. Measurements of water density and drop size distributions of selected ESFR sprinklers, Journal of Fire Protection Engineering, 6: 79-87.

Chan T.S., Kung H.C., Yu H-Z, Brown W.R. 1994. Experimental study of actual delivered density for rack storage fires, Fire Safety Science - Proceedings of the Sixth International Symposium, International Association for Fire Safety Science, pp. 913-924.

Cheng Yao. 1997. Overview of sprinkler technology research, Fire Safety Science Proceedings of the Fifth International Symposium, pp. 93-110.

Cheung K.P. 2012. Concerns on installing long-throw sprinkler in tall atria, Department of Building Services Engineering, The Hong Kong Polytechnic University, Hong Kong. Available at: http://www.bse.polyu.edu.hk/researchCentre/Fire_Engineering/Hot_Issues.html

China National Standard. 2005a. China's Automatic Sprinkler System Design Standards, GB50067-2001 (2005 edition), People's Republic of China.

China National Standard. 2005b. Code of Design for Sprinkler Systems, GB 50084-2001 (revised 2005), People's Republic of China.

China National Standard. 2005c. Code for fire protection design of tall buildings, GB50045-95 (2005 edition), People's Republic of China.

Chow C.L., Chow W.K., Yuan H.Y., 2004. A preliminary discussion on selecting active fire protection systems for atria in green or sustainable buildings, Architectural Science Review, 47(3): 229-236.

Chow W.K. 1989. Smoke movement and design of smoke control in atrium buildings, International Journal of Housing Science and Its Applications, 13(4): 307-322.

Chow W.K. 1995. Use of Computational Fluid Dynamics for Simulating Enclosure Fires. Journal of Fire Sciences, 13:301-331

Chow W.K. 1996. Performance of sprinkler in atria. Journal of Fire Sciences, 14(6): 466-488.

Chow W.K. 2009a. Expert witness in court, Coroner's Court, Hong Kong.

Chow W. K. 2009b. Performance evaluation of atrium smoke exhaust systems with hot smoke tests, February (2009). http://www.scitopics.com/Performance_Evaluation_of_Atrium_Smoke_Exhaust_Systems_with_Hot_Smoke_Tests.html

Chow W.K. 2011a. Six points to note in applying timeline analysis in performance-

based design for fire safety provisions in the Far East, International Journal on Engineering Performance-Based Fire Codes, 10(1): 1-5.

Chow W.K. 2011b. Static smoke exhaust in big halls with high occupancy, Department of Building Services Engineering, The Hong Kong Polytechnic University, Hong Kong. Available at: http://www.bse.polyu.edu.hk/researchCentre/Fire_Engineering/Hot_Issues.html

Chow W.K. 2012a. Concerns on estimating heat release rate of design fires in fire engineering approach, International Journal on Engineering Performance-Based Fire Codes, 11(1): 11-19.

Chow W.K. 2012b. Lesson learnt from the Fa Yuen Street Big Fire, Department of Building Services Engineering, The Hong Kong Polytechnic University, Hong Kong (2012) – In Chinese. Available at: http://www.bse.polyu.edu.hk/researchCentre/Fire_Engineering/Hot_Issues.html

Chow W.K. 2012c. "Necessity of in-depth evaluation of long-throw sprinkler installation at tall atria storing high amounts of combustibles", International Journal of Engineering Performance-Based Fire Codes, Vol. 11, No. 1, pp. 4-10.

Chow W.K. 2012d. "Response to concerns on installing long-throw sprinkler in tall atria", Department of Building Services Engineering, The Hong Kong Polytechnic University, Hong Kong, February 2012. Available at: http://www.bse.polyu.edu.hk/researchCentre/Fire_Engineering/Hot_Issues.html

Chow W.K. 2012e. A note on fire cabin design for protecting large halls", Department of Building Services Engineering, The Hong Kong Polytechnic University, Hong Kong, February (2012). Available at:

http://www.bse.polyu.edu.hk/researchCentre/Fire_Engineering/Hot_Issues.html

Chow W.K., Chow C.L. 2005. Evacuation with Smoke Control for Atria in Green and Sustainable Buildings, Building and Environment, 40(2): 195-200.

Chow W.K., Fong N.K. 1992. Atrium sprinkler: Performance analysis, Building Service Engineering, 13: 183-196.

Chow W.K., Fong N.K. 1993. Application of field modelling technique to simulate interaction of sprinkler and fire-induced smoke layer, Combustion Science and Technology, 89:1-4, 101-151.

Chow W.K., Han S.S. 2011. Scale modeling studies on flame stretching and swirling in a room with natural vents, ASME 2011 International Mechanical Engineering Congress & Exposition, IMECE2011, November 11-17, 2011, Denver, Colorado, USA, Paper no. IMECE2011-62087.

Chow W.K., Lo H.H.W. 2008. Scale modeling on natural smoke filling in an atrium, Heat Transfer Engineering, 29(1):76-84.

Chow W.K., Shek L.C. 1993. Physical properties of a sprinkler water spray, Fire and Materials, 17: 279-292.

Chow W.K., Wong W.K. 1993 On the simulation of atrium fire environment in Hong Kong using zone models, Journal of Fire Sciences, 11(1): 3-51.

Chow W.K., Wong L.T. 1998. Fire safety in a modern atrium: site visit and visual inspection, International Association for Fire Safety Science, 3: 575-582.

Chow W.K., Yin R. 2002. Discussion of two plume formulae with computational fluid dynamics. Journal of Fire Sciences, 20(3): 179-201.

Chow W.K., Chow C.L., Li S.S. 2011. Simulating smoke filling in big halls by computational fluid dynamics, Special Issue on Advances in Computational

Fluid Dynamics and Its Applications, Modelling and Simulation in Engineering, Vol. 2011. Article ID 781252, 16 pages, doi: 10.1155/2011/781252.

Chow W. K., Liu P., Zou G.W. 2007. Wind effect on smoke exhaust systems in a large cargo hall with two compartments, 12th International Conference on Wind Engineering, ICWE12, 1-6 July 2007, Cairns, Australia, Paper T3 B4, p. 1415-1422.

Chow W.K., Cui E, Li Y.Z., Huo R., Zhou, J.J. 2000. Experimental studies on natural smoke filling in atria, Journal of Fire Sciences, 18(2): 85-103.

Chow W.K., Gao Y., Zou G.W. and Dong H. 2006. Performance evaluation of sidewall long-throw sprinklers at height, 9th AIAA/ASME Joint Thermophysics and Heat Transfer Conference, 5-8 June 2006, San Francisco, California, USA, Paper AIAA-2006-3288.

Chow W.K., Ng M.Y., Zou. G.W., Dong H., Gao Y. 2004. Full-scale burning Tests for retail shop fires: preliminary studies. International Journal on Engineering performance-Based Fire Codes, 6(3):94-121.

Chow W.K., Han S.S., Gao Y., Dong H., Huo Y., Zhang Y.M., Li S.S. 2009. Flame stretching in a room model with natural vent, ASME Summer Heat Transfer Conference, 19-23 July 2009, San Francisco, California, USA.

Chow W.K., Fong N.K., Tam T.K., Woo Y.K., 2013. News from The Hong Kong Polytechnic University", In: G. Rein (editor), International Association for Fire Safety Science Newsletter No. 34, p. 12-13, March 2013.

Chung K.C. 2005. A simplified model for smoke filling time calculation with sprinkler effects, Journal of Fire Sciences, 23(4):279-301.

Cooper L.Y. 1995. The interaction of an isolated sprinkler spray and a two-layer compartment fire environment, Heat Mass Transfer, 38(4):679-690.

Cooper L.Y., 2000, Simulation the opening of fusible-link-actuated fire vents, Fire Safety Journal, 34: 219-255.

Croce P.A., Xin Y. 2005. Scale modeling of quasi-steady wood crib fires in enclosures. Fire Safety Journal, 40: 245-266.

DiNenno P.J., Drysdale D., Beyler C.L., Walton W.D. (editors). 2002. The SFPE Handbook of Fire Protection Engineering, 3rd edition, Quincy, Mass.: National Fire Protection Association; Bethesda, Md.: Society of Fire Protection Engineers, pp. 3-13-15

Evans D.D. 1993. Sprinkler fire suppression Algorithm for HAZARD, NISTIR 5254, National Institute of Standards and Technology, Gaithersburg, MD20899, 1-16.

Faeth G.M., Hsiang L.P., Wu P.K. 1995. Structure and Break-up Properties of Sprays. International Journal of Multiphase Flow, 21: 99-127.

Gao Y., Zou G.W., Li S.S., Chow W.K. 2013. Some experimental results on internal fire whirls in a vertical shaft, Paper presented at ASME 2013 International Mechanical Engineering Congress & Exposition, 15-21 November 2013, San Diego, California, USA, Paper No. IMECE2013-62148.

Gao Z.X., Xu B.Y. 2003. Study on the relation of the sprinkler head structure and its water distribution performance, Fire Science and Technology, 22(3): 131-133.

Grant G., Brentonb J., Drysdale D. 2000. Fire suppression by water sprays, Energy and Combustion Science, 26:79-130.

Hansen R., H. Ingason. 2011. An engineering tool to calculate heat release rates of multiple objects in underground structures, Fire Safety Journal, 146:194-203.

Hauptmanns U., Marx M., Grunbeck S. 2008. Availability analysis for a fixed wet sprinkler system, Fire Safety Journal, 43: 468-476.

Heskestad G. 2006. Heat of combustion in spreading wood crib fires with application

to ceiling jets, Fire Safety Journal, 41: 343-348.

Heskestad G., Bill R.G. Jr, 1988. Quantification of thermal responsiveness of automatic sprinklers including conduction effects, Fire Safety Journal, 14: 113-125.

Hong Kong Airport Authority. 2011. Hong Kong International Airport Tenant Design Guideline, Appendix A Sample Fire Engineering Report, , April 2011 version, Issue no. 3. https://extranetapps.hongkongairport.com/iwov_extra/ListFile?path=/etra/Extranet/TSP/Procedures/Tenant+Design+Guideline.pdf&place=n

Hu Q., Yu W., 2010. Necessity and feasibility of the carrying out the CCC for seven kinds of fire control products, China Quality Certification, 2010 (9): 38-40.

Huggett C. 1980. Estimation of heat release by means of oxygen consumption measurements. Fire and Materials, 4:61-65.

Hung W.Y., Chow W.K. 2001. A review on architectural aspects of atrium buildings, Architectural Science Review, 44(3):285-295.

Jackman L.A. 1992. Sprinkler spray interactions with fire gases. PhD thesis, South Bank University, pp. 348-355.

Jones W.W., Peacock R.D., Forney G.P., Reneke P.A. 2005. CFAST-Consolidated Model of Fire Growth and Smoke Transport (Version 6) Technical Reference Guide. NIST Special Publication 1041, pp. l-70.

Kang Q., Ma B. 2010. Research on fire-safety assessment of high-rise building based on the fuzzy centralization theory//Fuzzy Systems and Knowledge Discovery (FSKD), 2010 Seventh International Conference on. IEEE, 3: 1349-1354.

Karlsson B., Quintiere J.G. 2000. Enclosure fire dynamics, Florida: CRC Press, pp. 25-46.

Korea Railroad Research Institute & SFPE Korean Chapter. 2011. Proceedings of 2011 Exchange Meeting for SFPE Asia-Oceania Chapters – Transportation Fire Safety, Seoul, Korea, 28 April 2011.

Kung H.C., Spaulding R.D., Hill. 1982. Field evaluation of Residential Prototype Sprinkler - Los Angeles Fire Test Program. Technical Report J.I.OEOR3.RA. Factory Mutual Research Corporation Norwood, MA, February 1982.

Li K.Y., Hu L.H., Huo R., Li Y.Z., Chen Z.B., Li S.C. and Sun X.Q. 2009. A mathematical model on interaction of smoke layer with sprinkler spray, Fire Safety Journal, 44:96-105.

Li Y.Z., Huo, R., Chow W.K. 2002. On the operation time of horizontal ceiling vent in an atrium, Journal of Fire Sciences, 20(1):37-51.

Liu J.H., Liao G.X., Fan W.C., Chen C.K. 2002. An Experimental Study on Burning Properties, Journal of University of Science and Technology of China, 32 (6):738-742.

Liu X., Yu D.X., Zhang J., Li, Y., Tian L.W., Jiang W.T. 2014. Combustion characteristics and influencing factor of standard combustion material used for fire test, Fire Science and Technology, 33(1):10-13.

Lo G.C.H. 2011. CPD lecture on “Fire engineering in Hong Kong”, Organized by Research Centre for Fire Engineering, Department of Building Services Engineering, The Hong Kong Polytechnic University, 15 July 2011.

Loss Prevention Council. 1987. LPC Rules for Automatic Sprinkler Installations, The Loss Prevention Council, London, UK.

Loss Prevention Council. 1999. LPC Laboratories Phase 1 report – Investigation of the suitability of Actual Delivered Density Apparatus (ADD) for the performance evaluation of the standard sprinklers as described in insurance

service project proposal project no. TE91014-19, UK.

LPS 1039: Issue 5 Requirements and testing methods for automatic sprinkler (2002).

Madrzykowski D. 2008. Impact of a residential sprinkler on the heat release rate of a Christmas tree fire, NISTIR 7506, Fire Research Division, Building and Fire Research Laboratory, National Institute of Standards and Technology, Gaithersburg, MD 20899-8661, USA, May 2008.

Madrzykowski D., Vettori R. L. 1992. A sprinkler fire suppression algorithm for the GSA engineering fire assessment system. NISTIR 4833, National Institute of Standards and Technology, Gaithersburg, MD20899, 1-35.

Marshall A.W., diMarzo M. 2004. Modelling aspects of sprinkler spray dynamics in fires, Process Safety and Environmental Protection, 82(2):97-104.

McCaffrey B.J. 1979. Purely buoyant diffusion flames: some experimental results, NBSIR79-1910.

McGrattan K.B. 2005. Fire Dynamics Simulator (Version 4) Technical reference guide. NIST Special Publication 1018 National Institute of Standards Technology, pp. 33-38.

Nam S. 1996. Development of a computational model simulating the interaction between a fire plume and a sprinkler spray, Fire safety Journal, 26: 1-33.

Nam S. 1999. Numerical simulation of the penetration capability of sprinkler sprays, Fire Safety Journal, 32: 307-329.

Nam S. 2004. Actuation of sprinklers at high ceiling clearance facilities, Fire Safety Journal, 39: 619-642.

Nam S. 2005. Fire tests to evaluate CPVC pipe sprinkler systems without fire resistance barriers, Fire Safety Journal, 40: 595-609.

Nam S., Braga A., Kung H.C., Troup J. 2003. Fire protection for non-storage

occupancies with high ceiling clearances, Fire Safety Science, 7: 493-504.

National Fire Protection Association 2002. NFPA-13. Automatic Sprinkler System Handbook. 2002 Edition, National Fire Protection Association.

Ni, Z.X., Qi, H. B., Yang, B. J. 2014. Tall Aria cloth water sprinkler system performance test and research, Water & Wastewater Engineering, 40 (11): 141-143.

Peacock R.D., Davis S., Babrauskas V. 1991. Data for room fire model comparisons. Journal of Research of the National Institute of Standard and Technology, 96(4): 411-462.

Prasad K., Patnaik G., Kailasanath K. 2002. A numerical study of water-mist suppression of large scale compartment fires, Fire Safety Journal, 37: 569-589.

Ren N., Baum H.R., Marshall A.W. 2011. A comprehensive methodology for characterizing sprinkler sprays, Fire Safety Journal, 33: 2547-2554.

Ruffino P., diMarzo M. 2004. The simulation of fire sprinklers thermal response in presence of water droplets, Fire Safety Journal, 39: 721-736.

Schwille J.A. and Lueptow R.M. 2006. The reaction of a fire plume to a droplet spray, Fire Safety Journal, 41: 390-398.

Si G. 2004. The development of 2002 edition NFPA code for automatic sprinkler system, Fire Technique and Products Information, 08(08).

Smith P.G., Thomas P.H. 1970. The rate of burning of wood cribs, Fire Technology, 6 (1): 29-38.

Song B, Yang B.J. 2008. Application and analysis of sprinkler system in storage, Fire Science and Technology, 27(7): 526-529.

Song B., Li Y. 2013. Preparation and combustion characteristic of standard combustible materials used for fire test, Fire Science and Technology, 32(7):

703-705.

Vcakatcsh S., Ito A., Saito K. 1997. Heat release rate of wood-plastic composites, SAMPE Journal, 33(5): 26-31.

Wang W., Zhan H.P., Yang D., Xu L. 2004. The design of the test-bed full-size multi-function heat release rate, Fire Science and Technology, 23(6):522-524.

Wen Min. 2014. Study of the Performance-based Fire-protection Design for Large-space Building. A Dissertation submitted for the Degree of Master. pp: 12-14.

Widmann J.F. 2001. Phase Doppler Interferometry Measurements in Water Sprays Produced By Residential Fire Sprinklers. Reprinted from Fire Safety Journal, Vol. 36, No. 6, 545-567, September 2001

Williams C. 1993. The downward movement of smoke: due to a sprinkler spray. PhD thesis, South Bank University.

Wu D., Guilleminb D., Marshall A. W., 2007. A modeling basis for predicting the initial sprinkler spray, Fire Safety Journal, 42: 283-294.

Xi D.C., Wu L.B., Fan W.C., Tan Y. 1999. Neural network approach for RHR calculation and prediction in fire science, Journal of University of Science and Technology of China, 29 (2):175-180.

Xu Q., Griffin G., Jiang Y., Preston C., Bicknell A., Bradbury G., White N. 2008. Study of burning behavior of small scale wood crib with cone calorimeter, Fire Safety Journal, 91(3): 787-790.

Yamada T. 1995. Evaluation system of code equivalency for alternative design of fire protections system in Japan – Towards the intelligent fire protection system, pp.15-23. Proceedings of the Mini-symposium on Fire Safety Design of Buildings and Fire Safety Engineering, 12 June 1995, Tsukuba, Japan – Edited by Y. Hasemi and Y. Hayashi, Building Research Institute, Ministry of

Construction, Japan.

Yang B.J. 2012. The comparison of automatic sprinkler technologies in domestic and foreign standards, Fire Science and Technology, 31(3): 265-267.

You Y.H., Chow W.K., Li Y.Z., Huo R., Wang H.B., Sun X.Q., Chen Z.B. 2005. Experimental studies on smoke control with mechanical exhaust at high level in a cabin fire. Journal of Applied Fire Science, 14(2): 105-124.

Yu H. Z., 2004. Fire performance evaluation of a K16. 8 suppression-mode upright sprinkler, Journal of Fire Protection Engineering, 14(2): 101-124

Zhang W., Hamer A., Klassen M., Carpenter D., Roby R. 2002. Turbulence statistics in a fire room model by large eddy simulation, Fire Safety Journal, 37: 721-752.

Zhao L.Z., Liu W. F., Ge M. H., Wang J. W., Cao J. F. 2008. Heat release rate test on solid combustible material, Fire Science and Technology, 27 (11): 793-795.

Zhao S.P., Zheng J., Quan Q.G. 2002. The experimental study of fire heat release rate. Fire Technique and Products Information, 12: 35-38.

Zhou X.Y., Yu H.Z. 2011. Experimental investigation of spray formation as affected by sprinkler geometry, Fire Safety Journal, 46:140-150.

Zhou X.Y., D'Aniello S.P., Yu H.Z. 2012. Spray characterization measurements of a pendent fire sprinkler, Fire Safety Journal, 54:36-48.

Figure 1.1 High combustible content in a tall hall

Figure 1.2 Smart water gun

Figure 2.1 Airport

Figure 2.2 Large integrated centres

Figure 2.3 Library

Figure 2.4 Exhibition centre

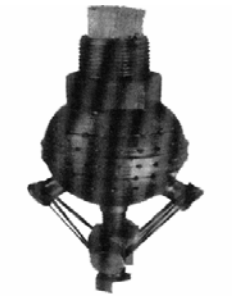

Figure 2.5 Harrison sprinkler nozzles

Figure 2.6 Grinnell - Glass bulb sprinkler

Figure 2.7 Conventional spray sprinkler, spray sprinkler, and sidewall sprinkler

Figure 2.8 Standard fusible alloy sprinkle and standard glass bulb sprinkler

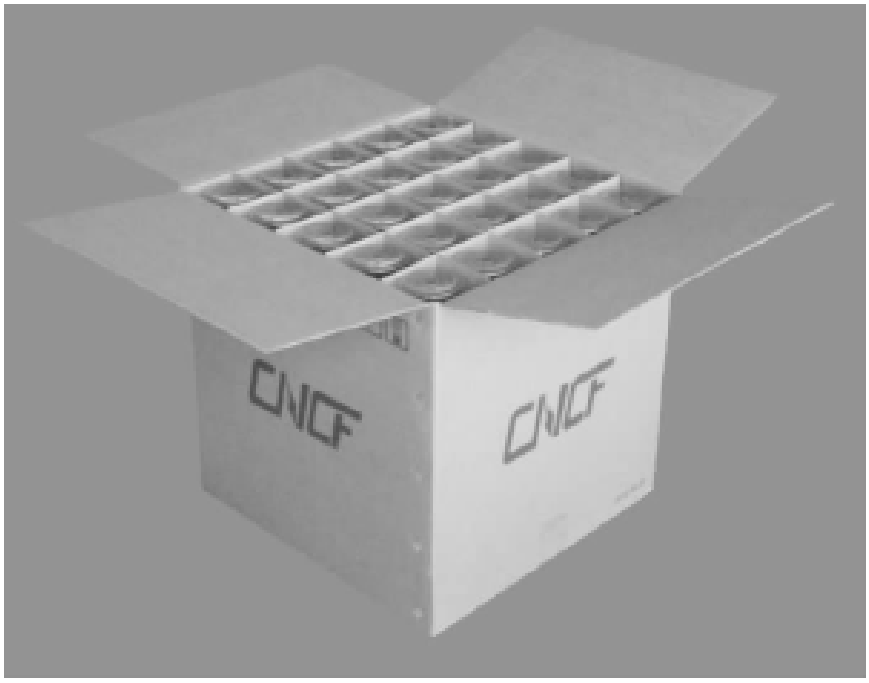

Figure 3.1 Plastic cup standard combustible object

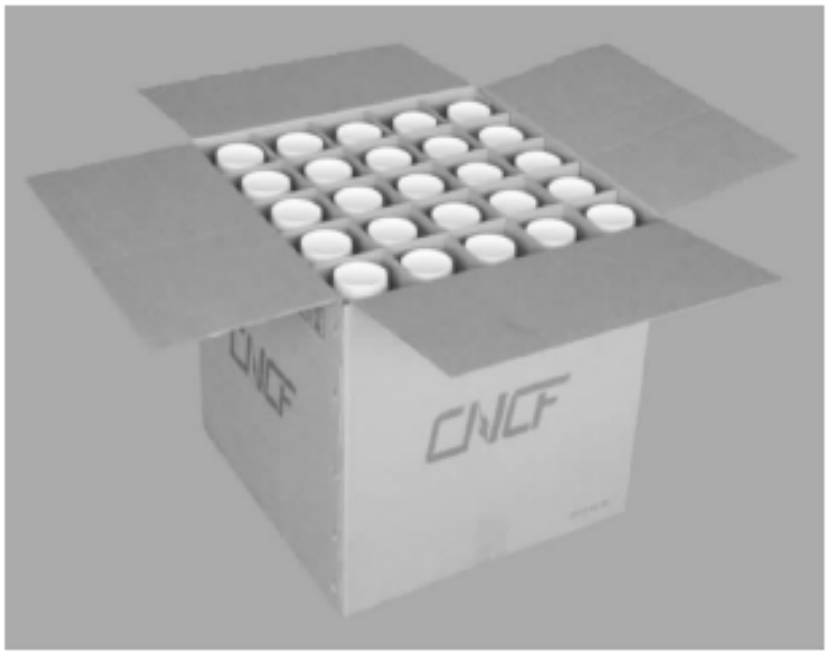

Figure 3.2 Paper cup standard combustible object

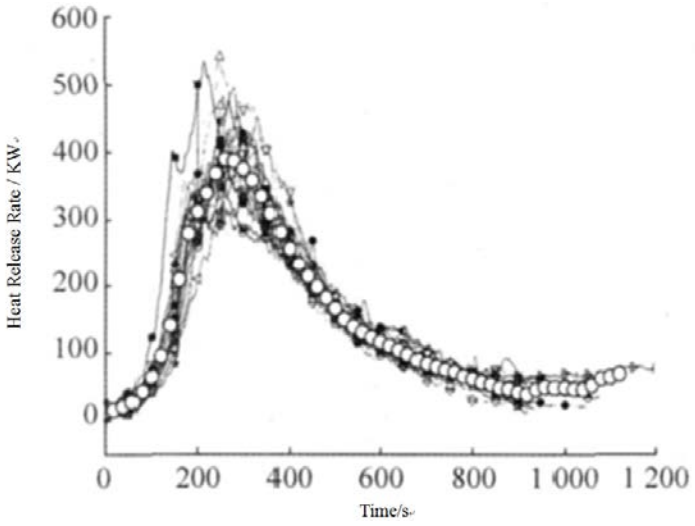

Figure 3.3 Plastic cup combination heat release rate

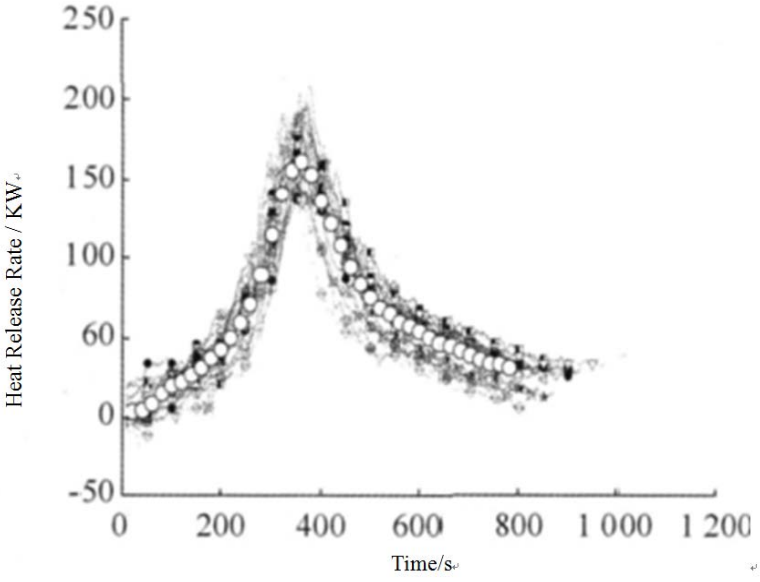

Figure 3.4 Paper cup combination heat release rate

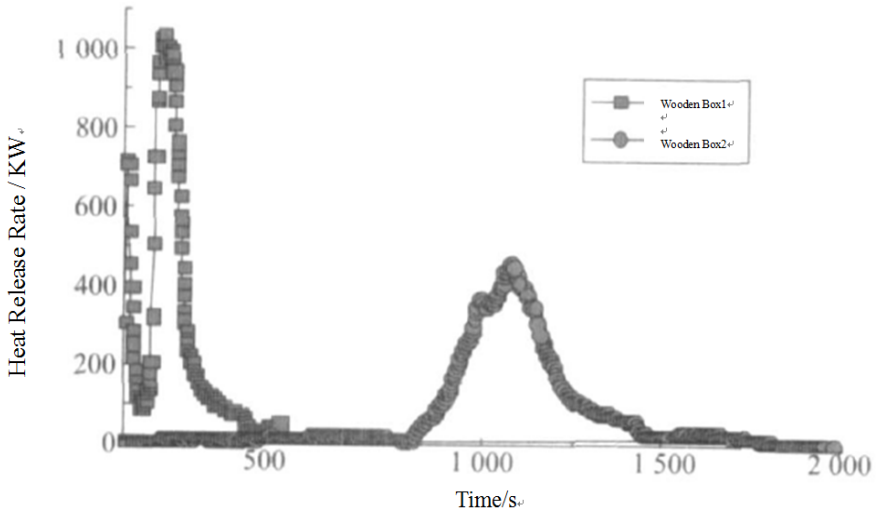

Figure 3.5 Heat release rate under different combustion conditions

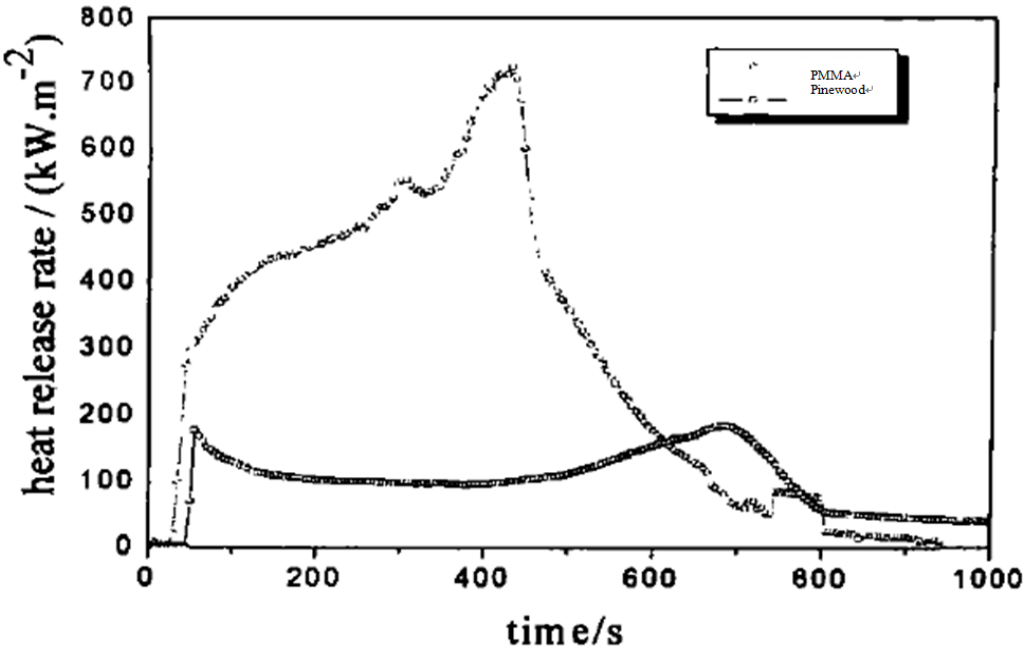

Figure 3.6 Comparison between pine wood and PMMA heat release rates

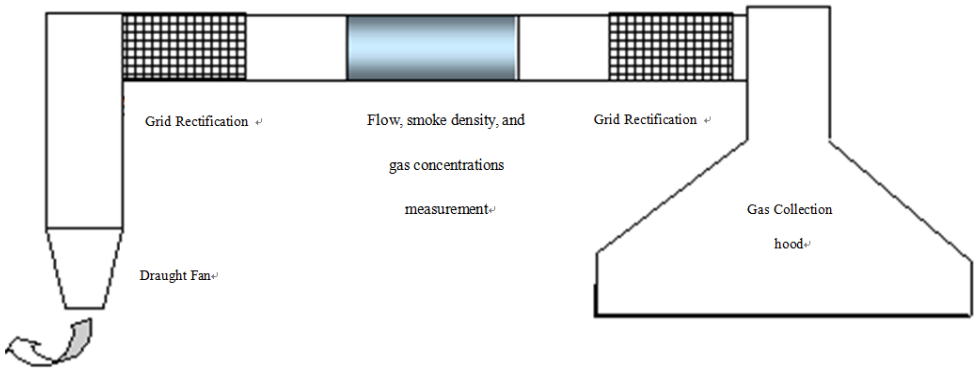

Figure 4.1 Large calorimeter

Figure 4.2 10 MW heat calorimeter system

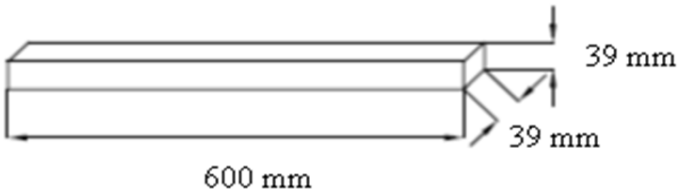

(a) Block Dimensions

(b) Appearance of wood cribs

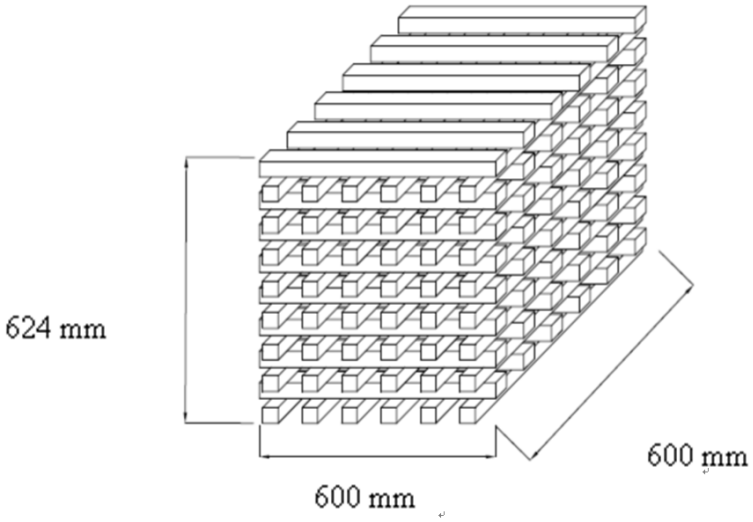

(c) Wood crib Sketch

Figure 4.3 (a) Block dimensions (b) Appearance of wood cribs (c) Wood crib sketch

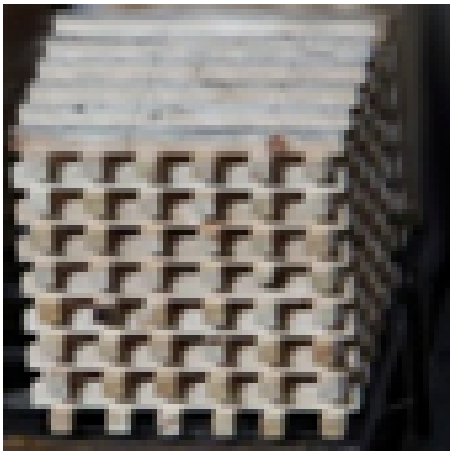

Figure 4.4 W1 1 wood crib

Figure 4.5 Overall situation of W1

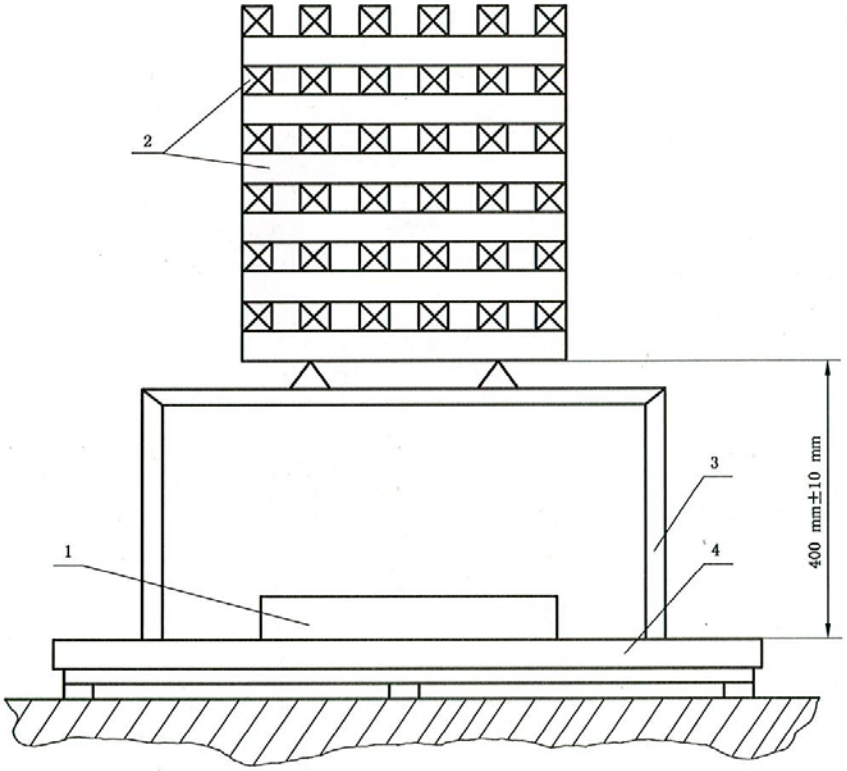

Figure 4.6 Ignition schematic diagram

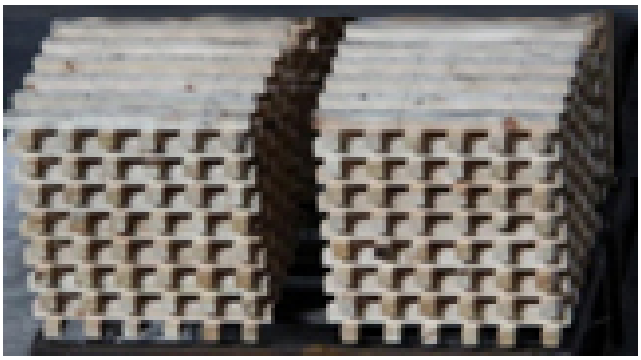

Figure 4.7 W2 wood crib placement

Figure 4.8 Overall situation of W2

Figure 4.9 W3 wood crib placement

Figure 4.10 Overall situation of W3

Figure 4.11 W4 placement

Figure 4.12 Overall situation of W4

Figure 4.13 W5 wood crib placement

Figure 4.14 Overall situation of W5

(a) Oil tray experiment stage 1

(b) Oil tray experiment stage 2

(c) Oil tray experiment stage 3

(d) Ignition of oil tray

(e) Wood cribs fully ignited

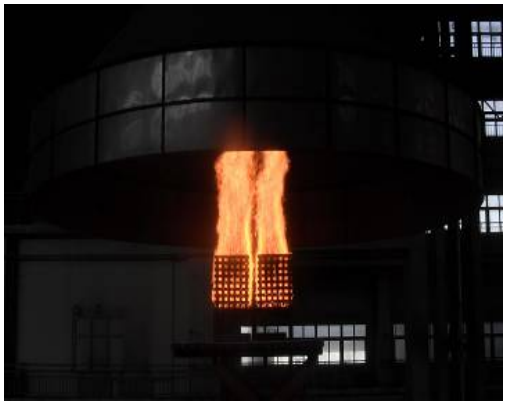

(f) Oil tray burnt out

Figure 4.15 Oil tray experiment Stage 1 to 6

(g) Burning to give largest HRR

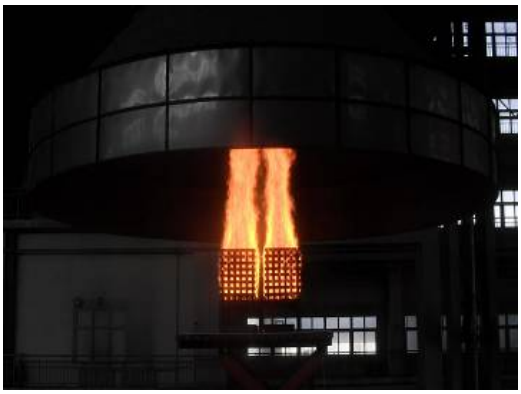

(h) Steady burning giving stable HRR

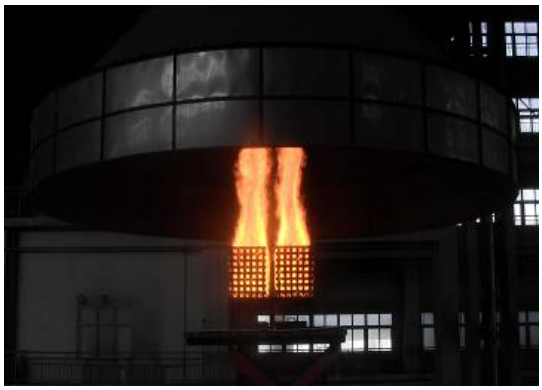

(i) End of giving stable heat release rate

(j) Decrease of heat release rate

(k) Burning completed

Figure 4.16 Oil tray experiment Stage 7 to 11

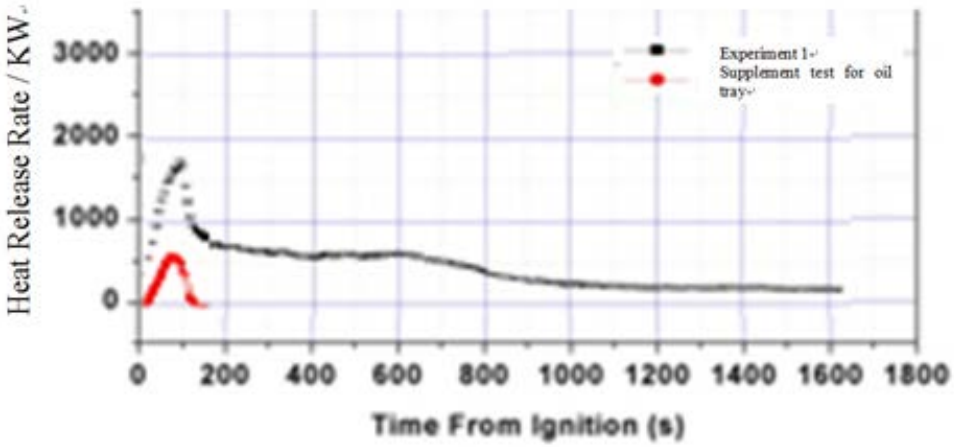

Figure 4.17 Wood crib heat release rate of W1

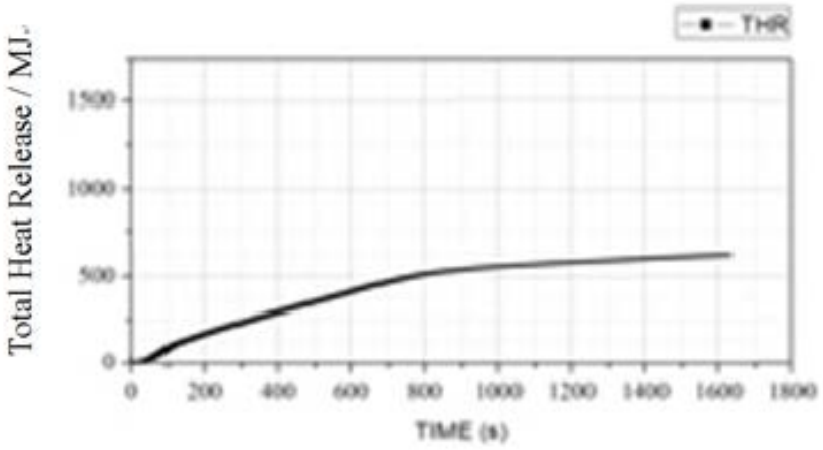

Figure 4.18 Transient heat release of W1

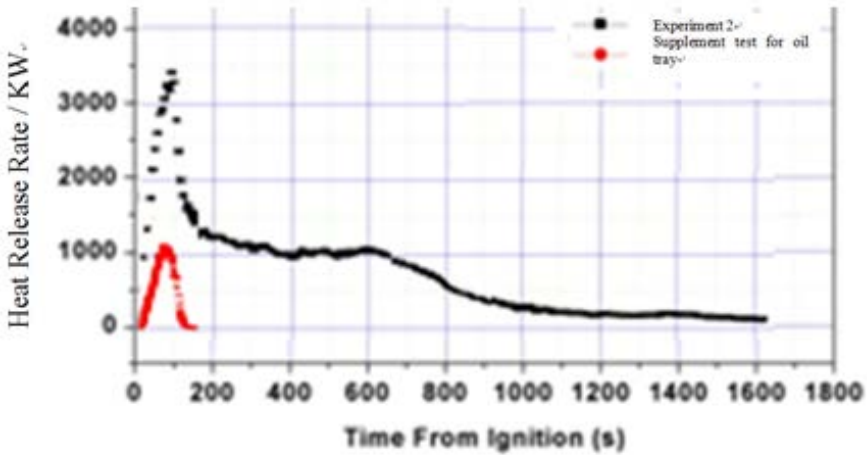

Figure 4.19 Wood crib heat release rate of W2

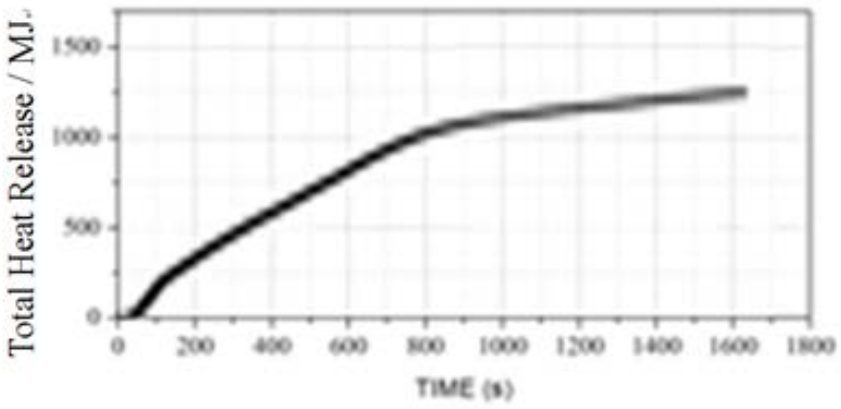

Figure 4.20 Transient heat release of W2

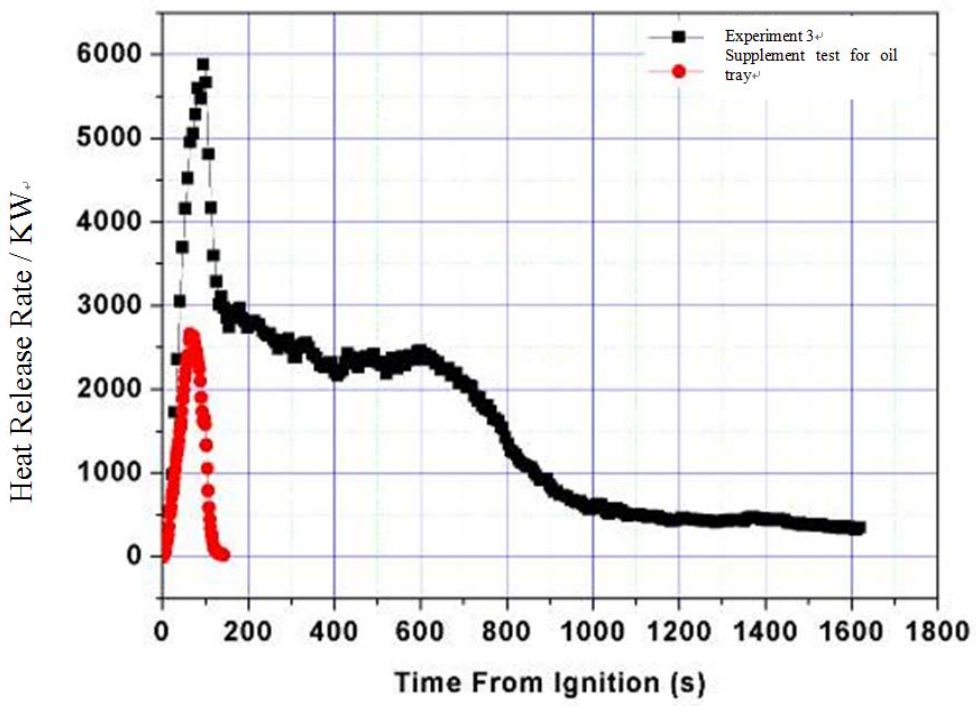

Figure 4.21 Wood crib heat release rate of W3

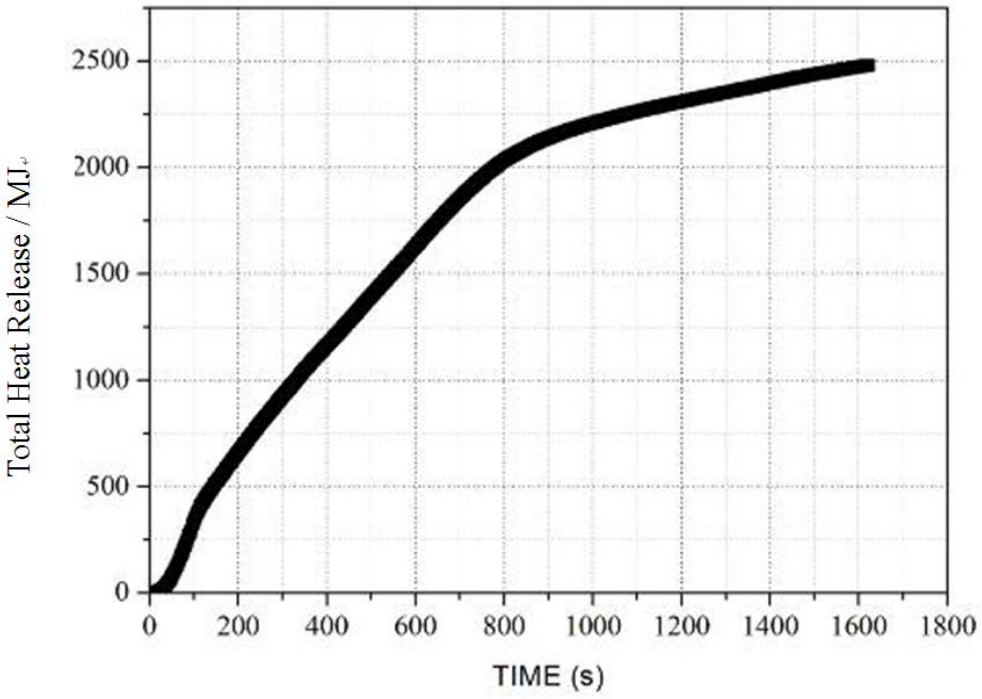

Figure 4.22 Transient heat release of W3

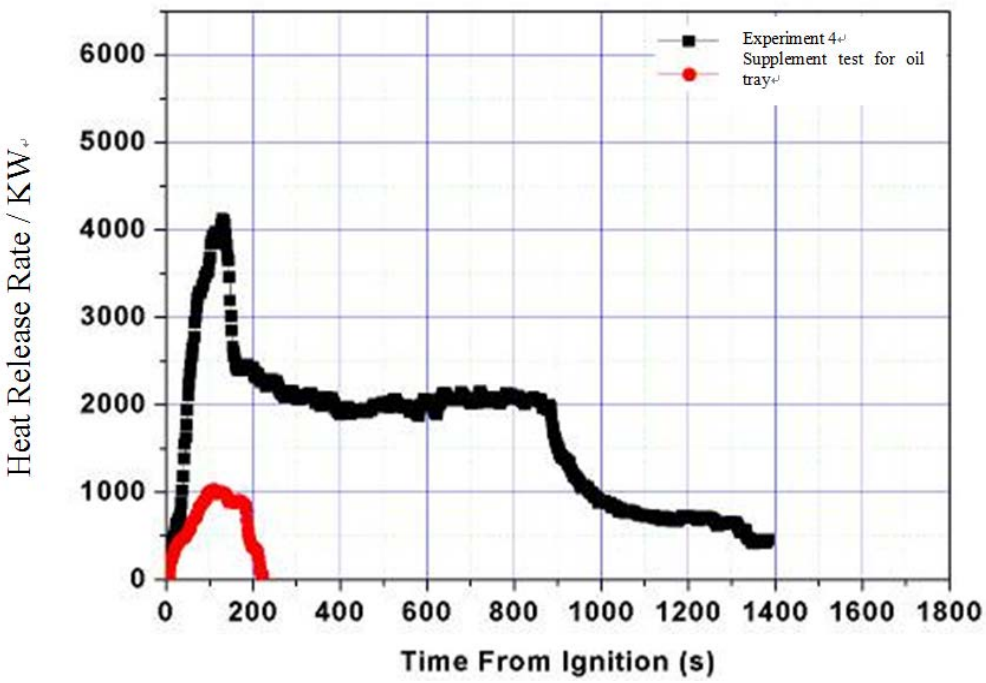

Figure 4.23 Wood crib heat release rate of W4

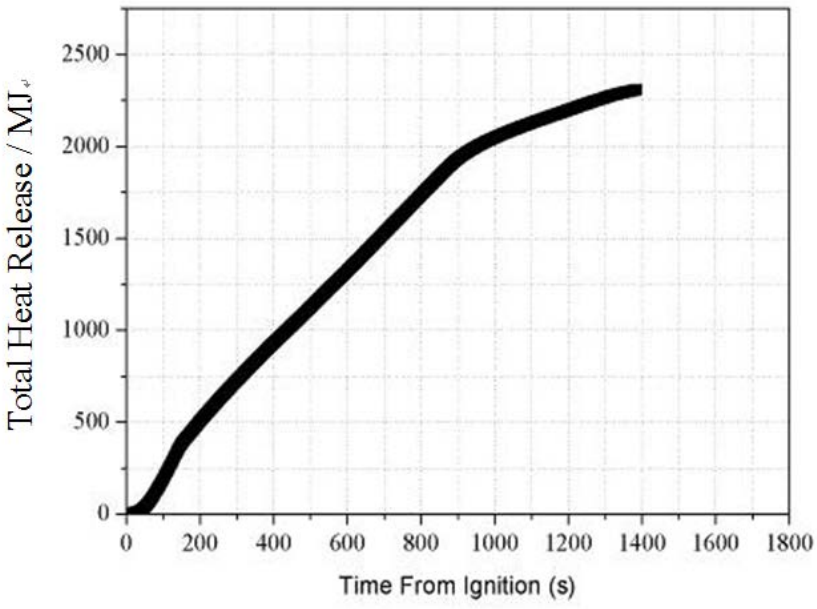

Figure 4.24 Transient heat release rate of W4

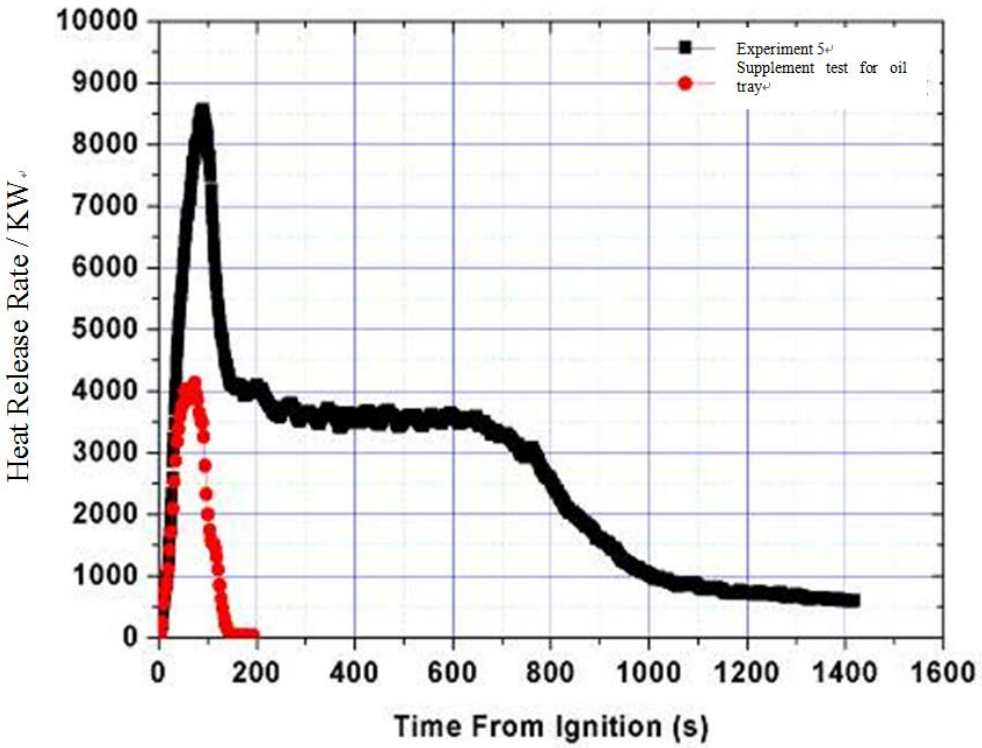

Figure 4.25 Wood crib heat release rate of W5

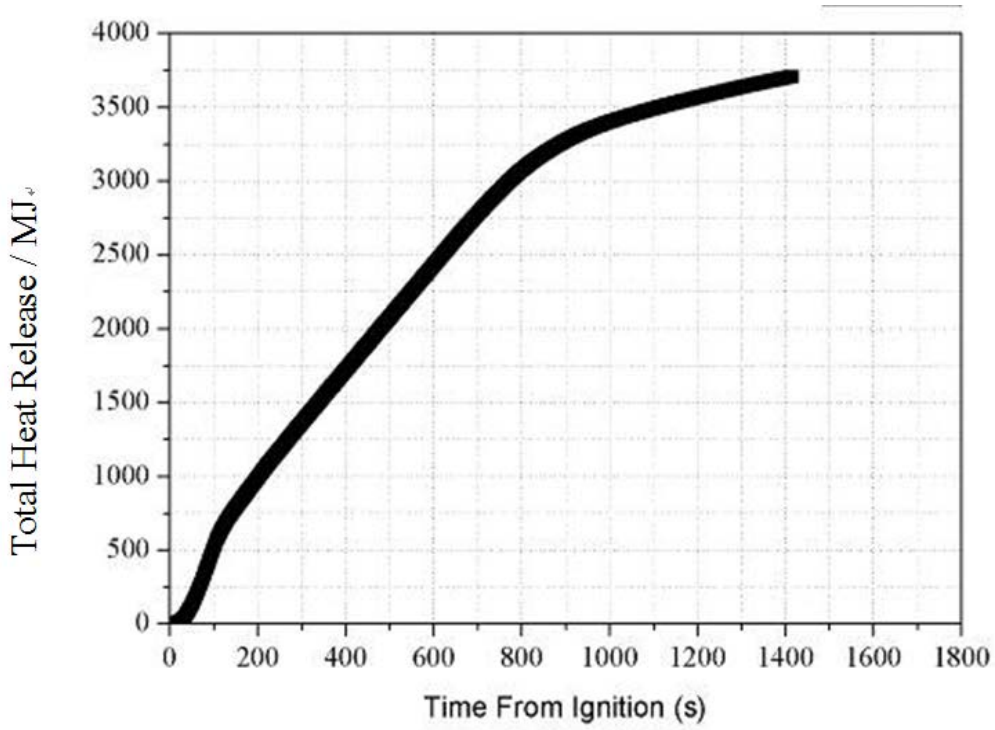

Figure 4.26 Transient heat release of W5

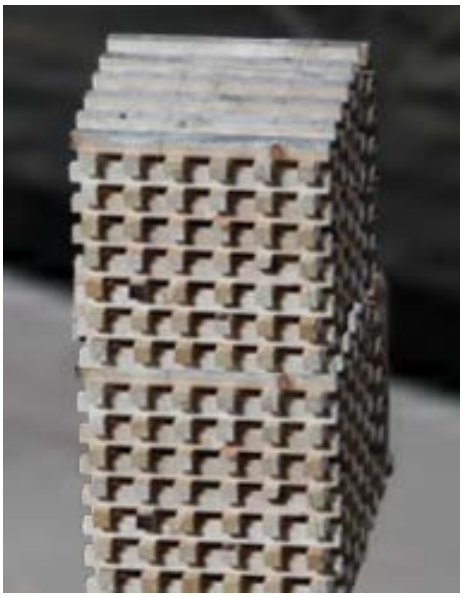

Figure 4.27 Vertical arrangement of wood cribs in supplementary tests

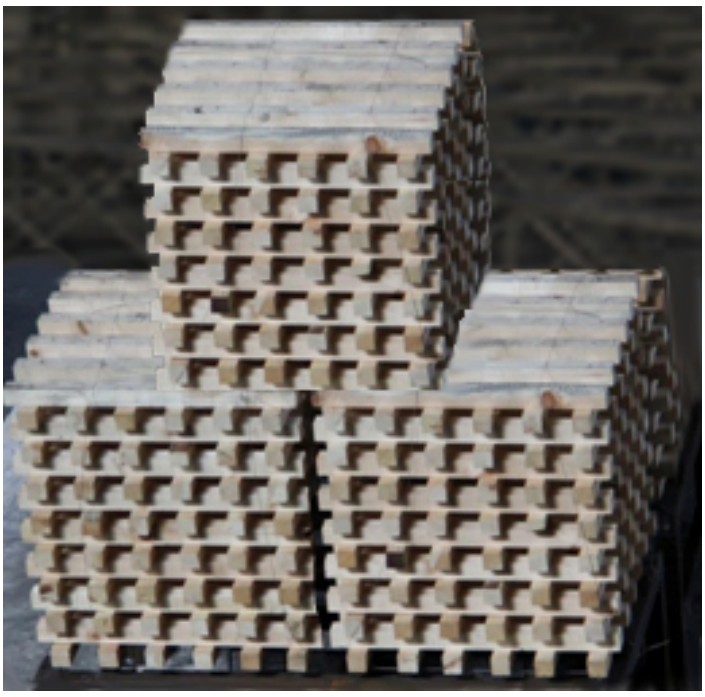

Figure 4.28 Three wood cribs arrangement in supplementary tests

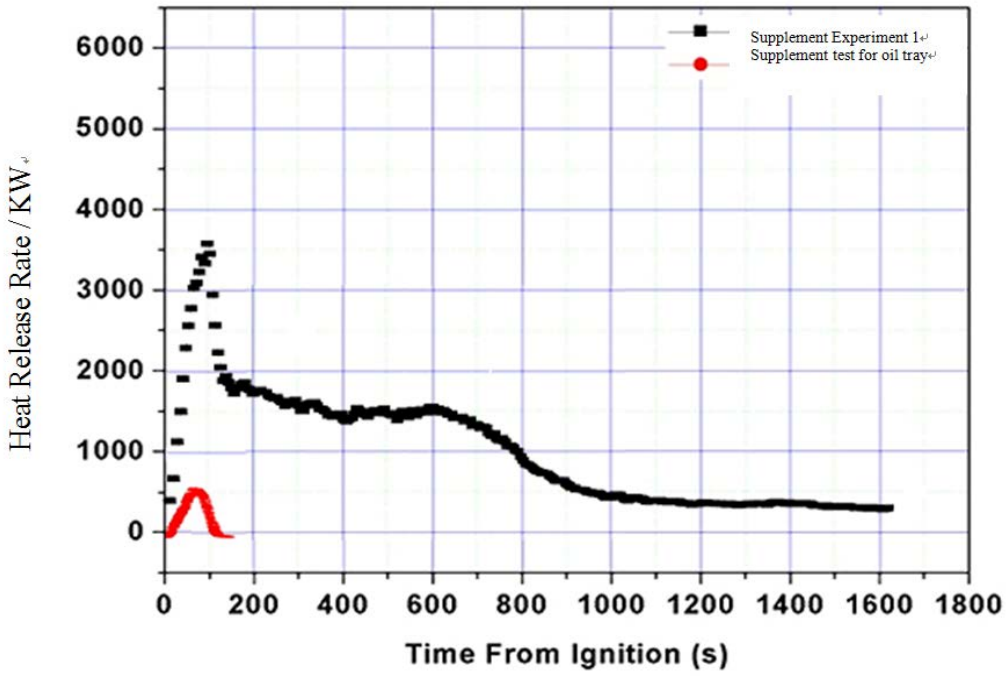

Figure 4.29 Heat release rate curve of two wood cribs stacked up

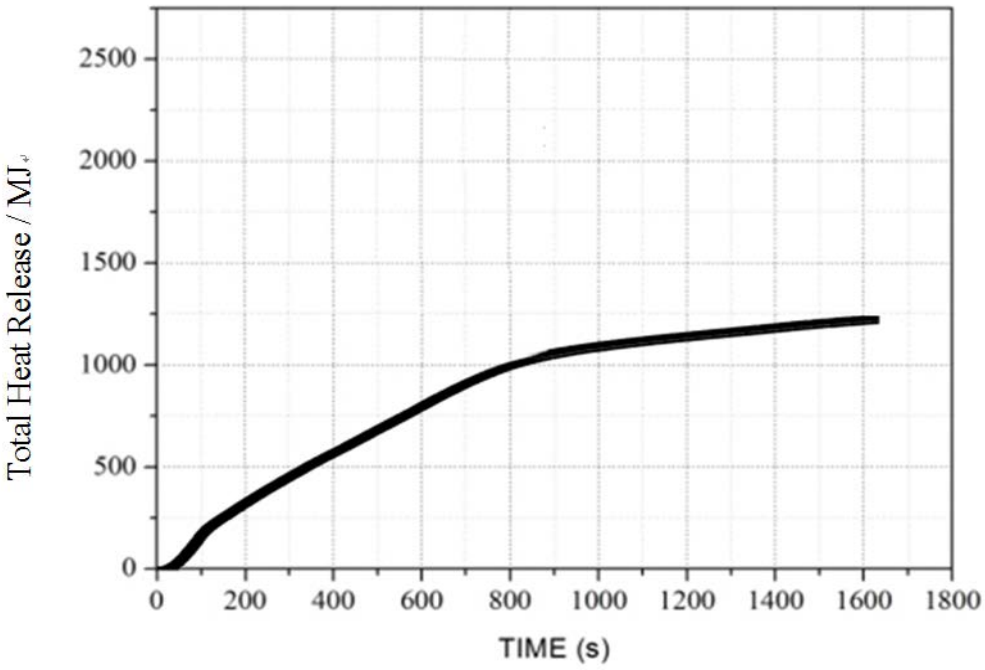

Figure 4.30 Total heat released of two wood cribs stacked up

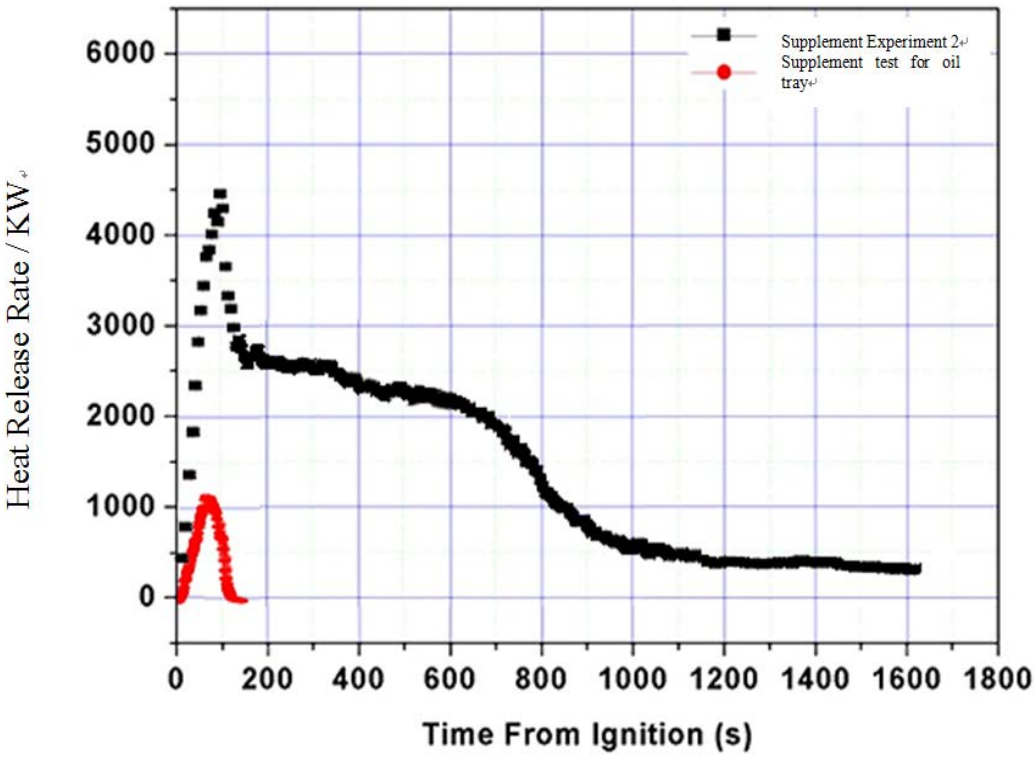

Figure 4.31 Three wood cribs placed one on top, two below heat release rate curve

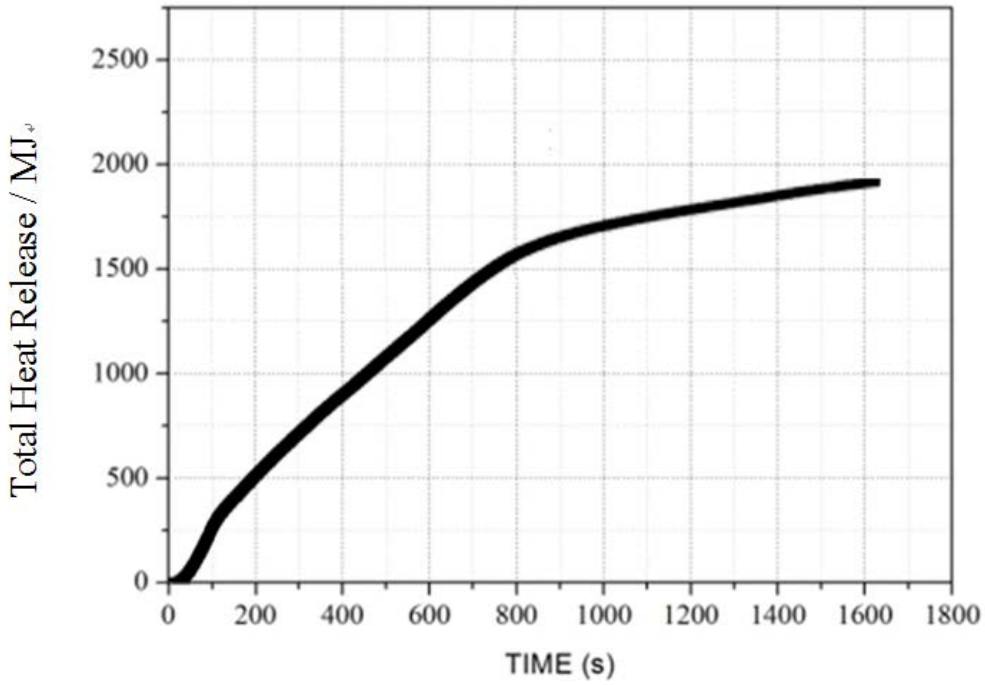

Figure 4.32 Three wood cribs placed one on top, two below total heat released

Figure 5.1 Christmas sculptures

Figure 5.2 Large blow up auspicious object

Figure 5.3 Christmas gift house

Figure 5.4 Festively designed sales area

Figure 5.5 Typical Situation 1 where there is no sprinkler above

Figure 5.6 Typical Situation 2 where there is no sprinkler above

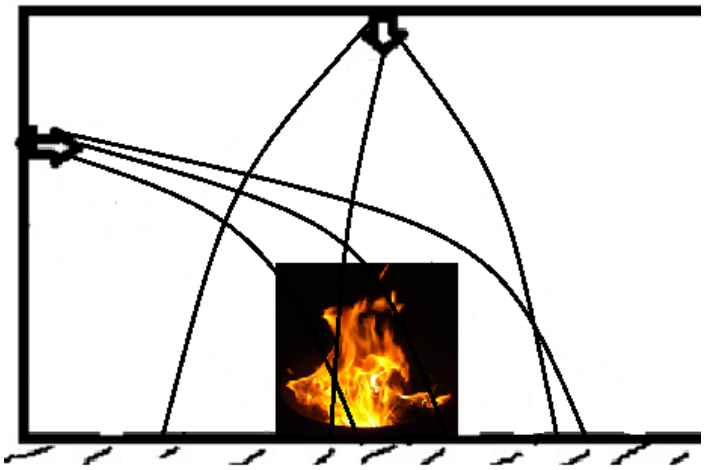

Figure 5.7 Sprinkler head positioned on top or side

Figure 5.8 Side wall large impulse spray sprinkler

Figure 5.9 LPC partial water distribution experiment positioning

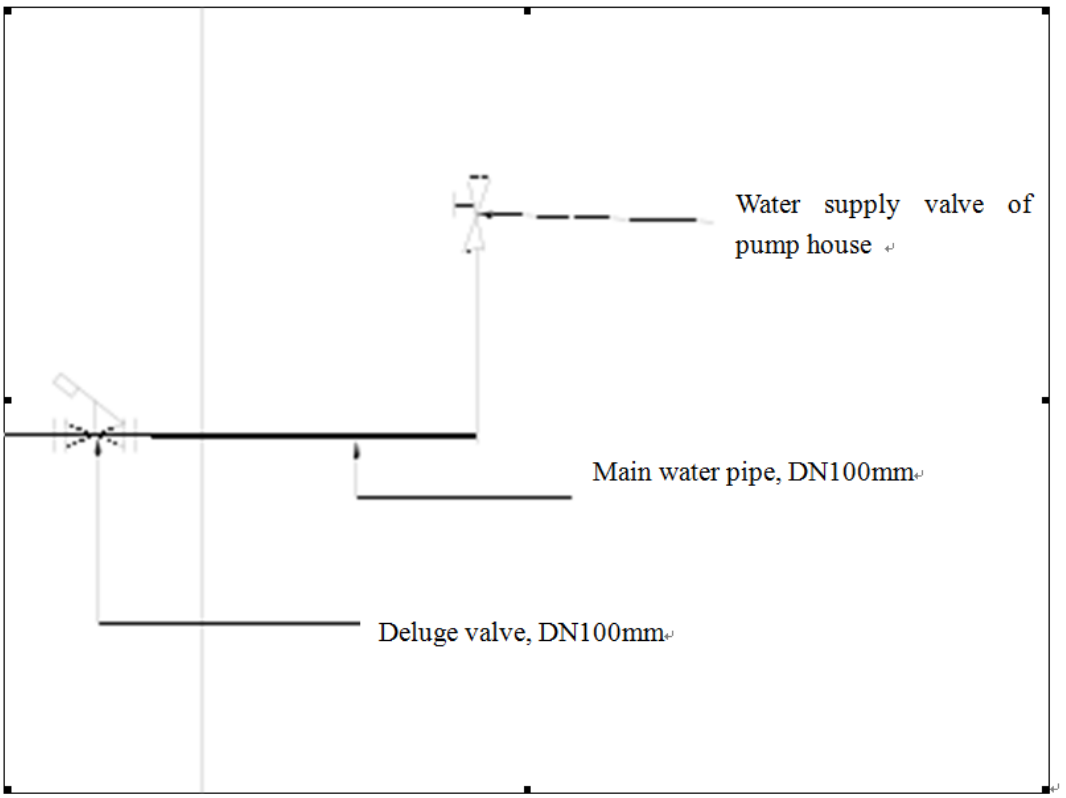

Figure 5.10 Main water supply pipe diagram

Figure 5.11 Testing sprinkler head

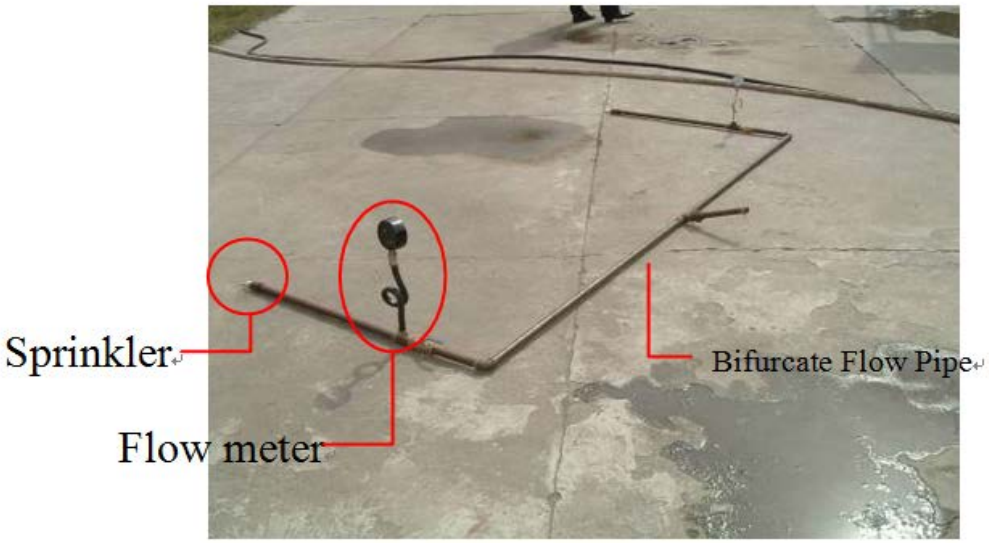

Figure 5.12 Flow pipe

Figure 5.13 Water catchment box

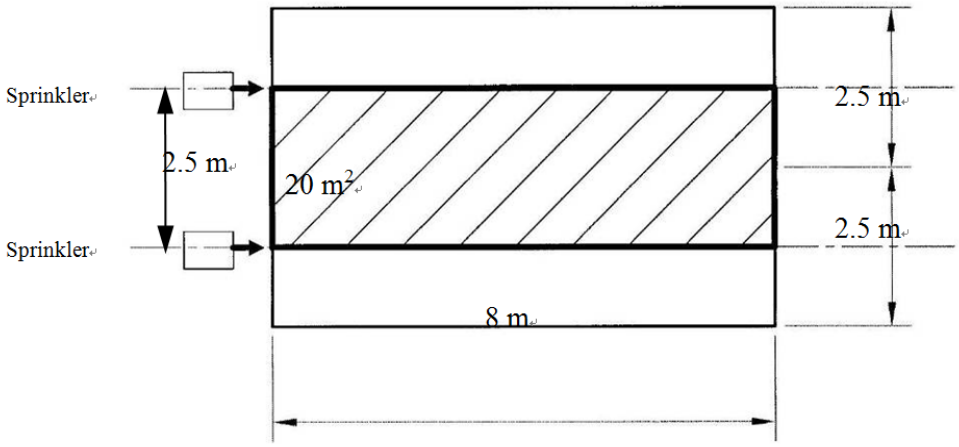

Figure 5.14 Water distribution area plan

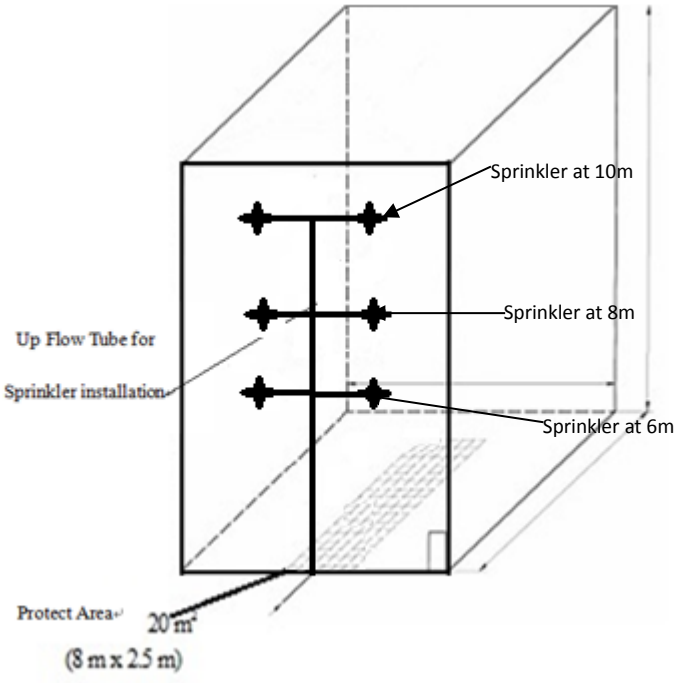

Figure 5.15 Water distribution area stacking plan

Figure 5.16 Working situation of the water distribution experiment

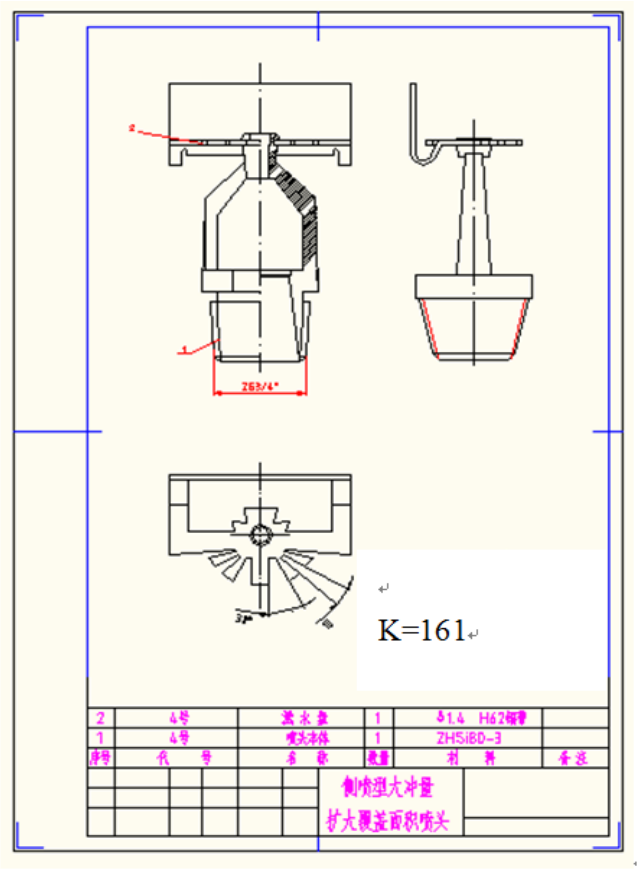

Figure 5.17 Diagrams and orifice sizes of the K=161 sprinkler

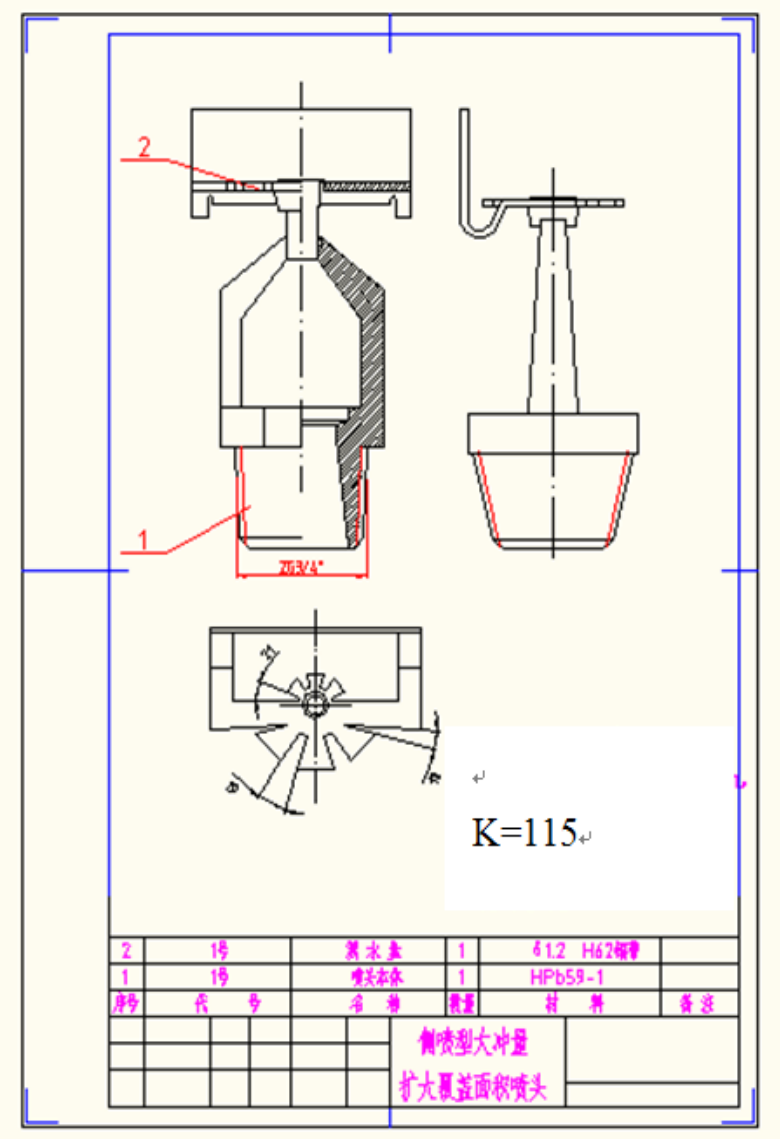

Figure 5.18 Diagrams and orifice sizes of the K=115 sprinkler

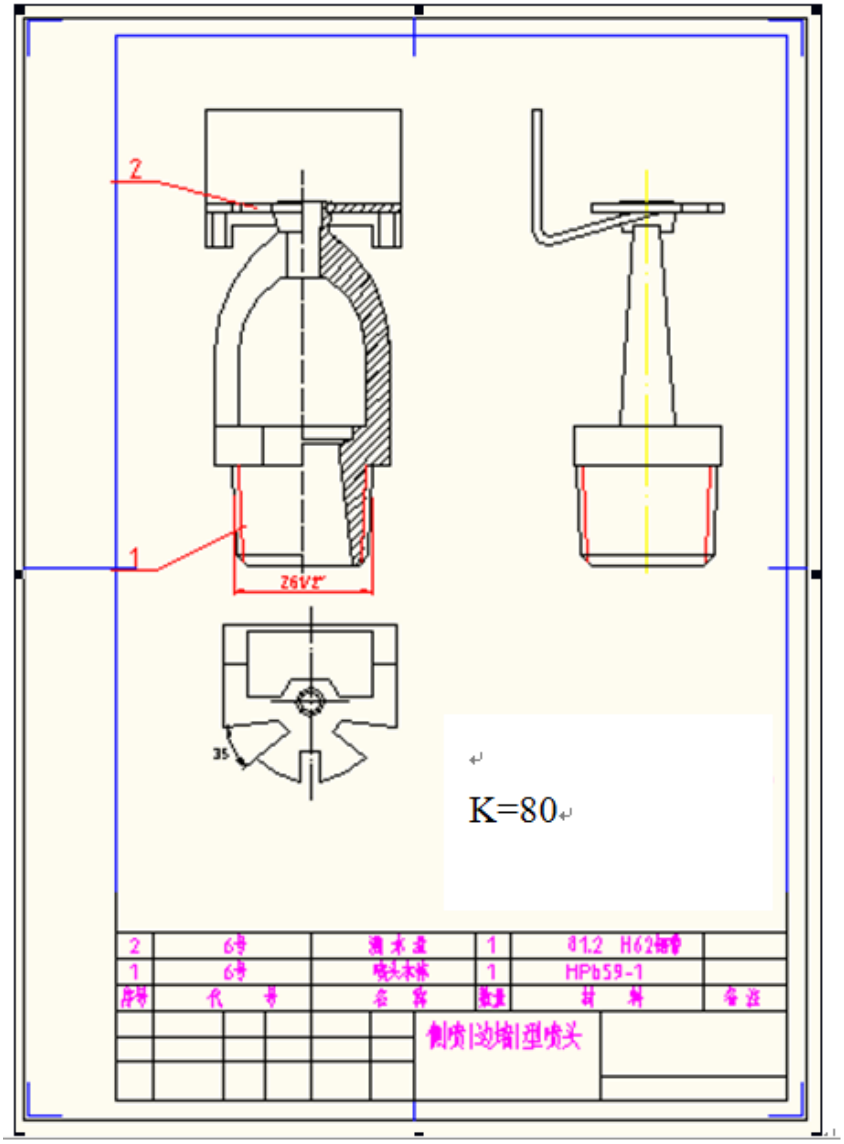

Figure 5.19 Diagrams and orifice sizes of the K=80 sprinkler

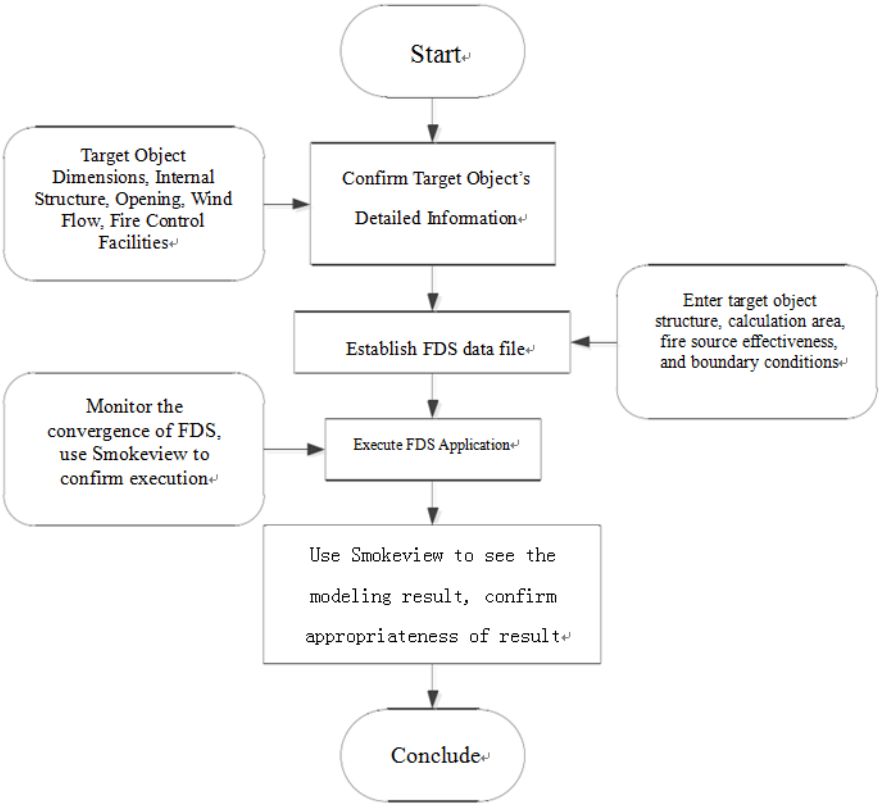

Figure 6.1 FDS application process flowchart

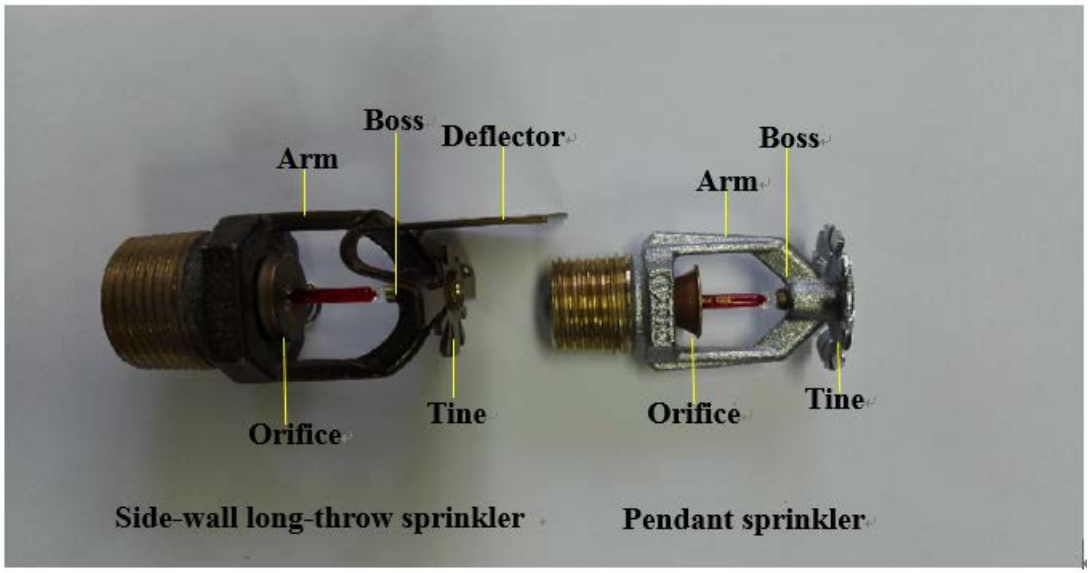

Figure 6.2 Different sprinkler structure comparison

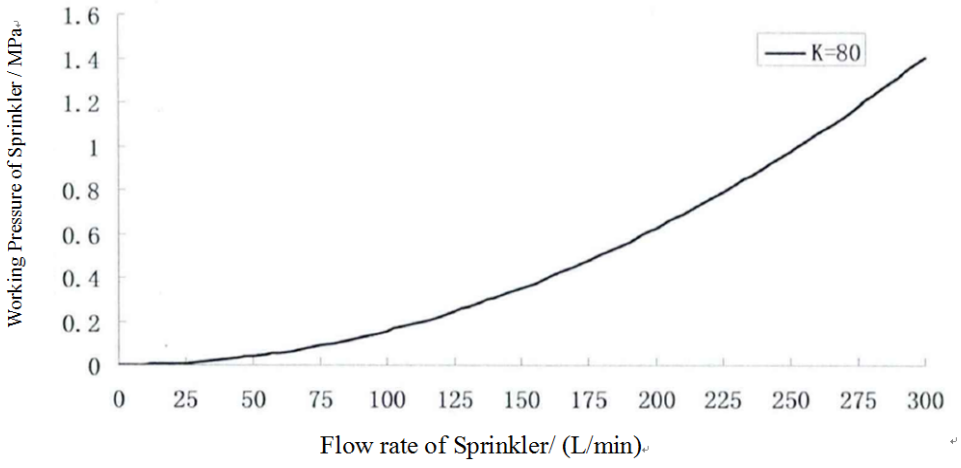

Figure 6.3 Flow characteristic curve of K=80

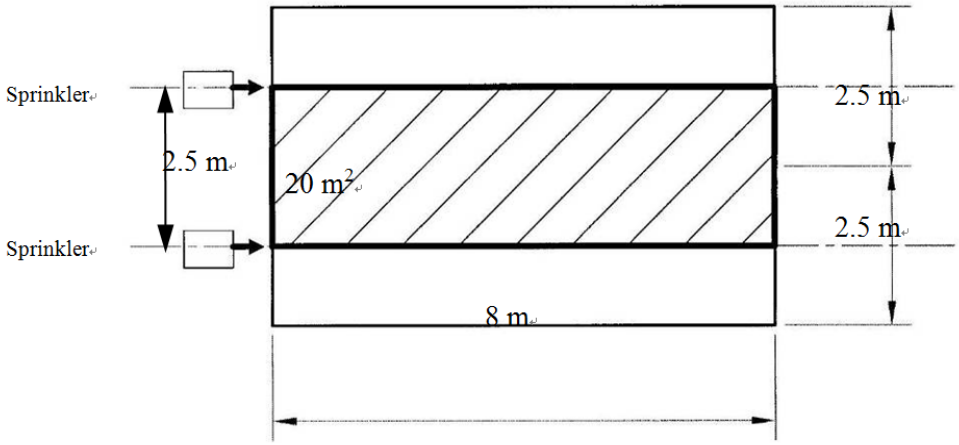

Figure 6.4 Sprinkler operating area

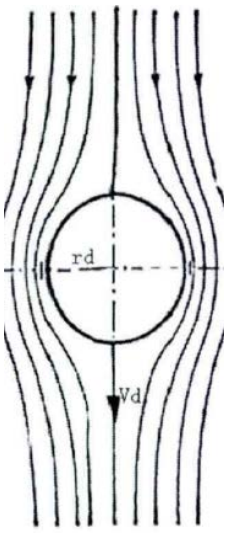

Figure 6.5 Heat transfer diagram between spray droplet and gas

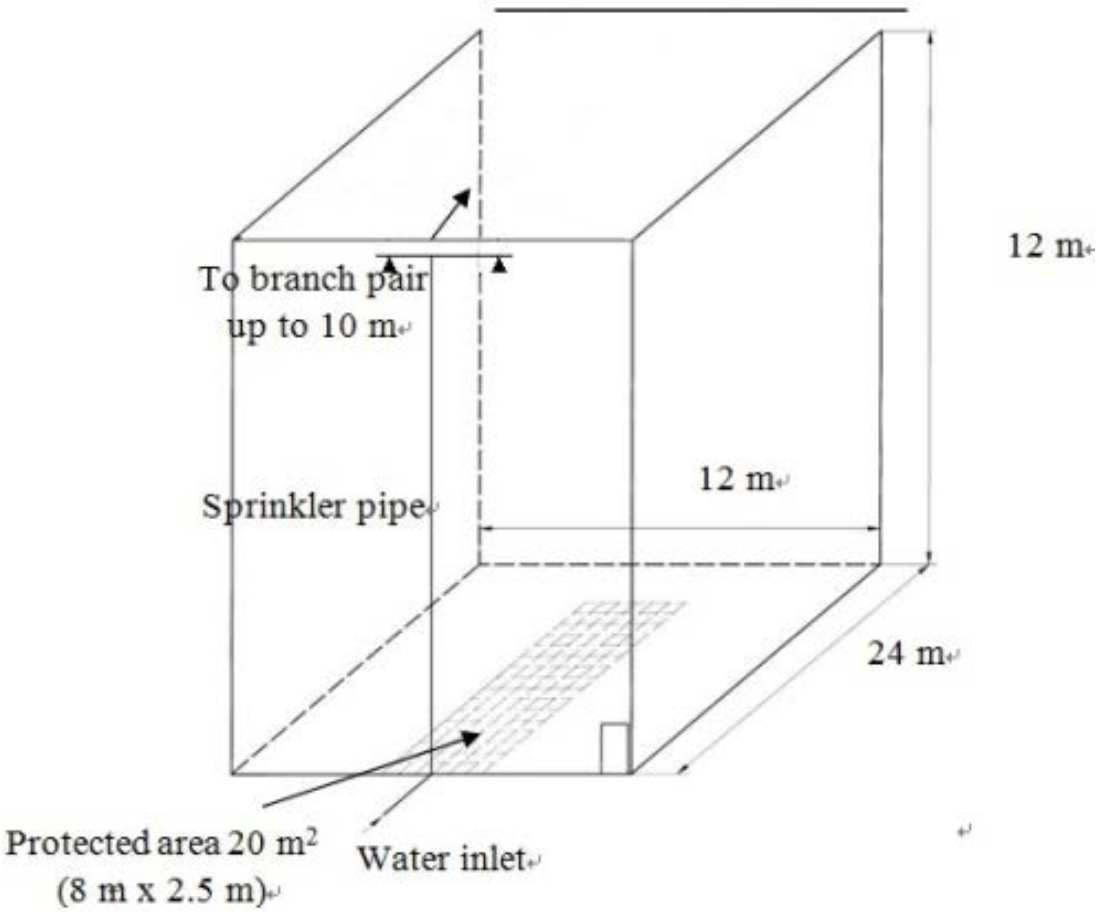

Figure 6.6 Experiment area diagram

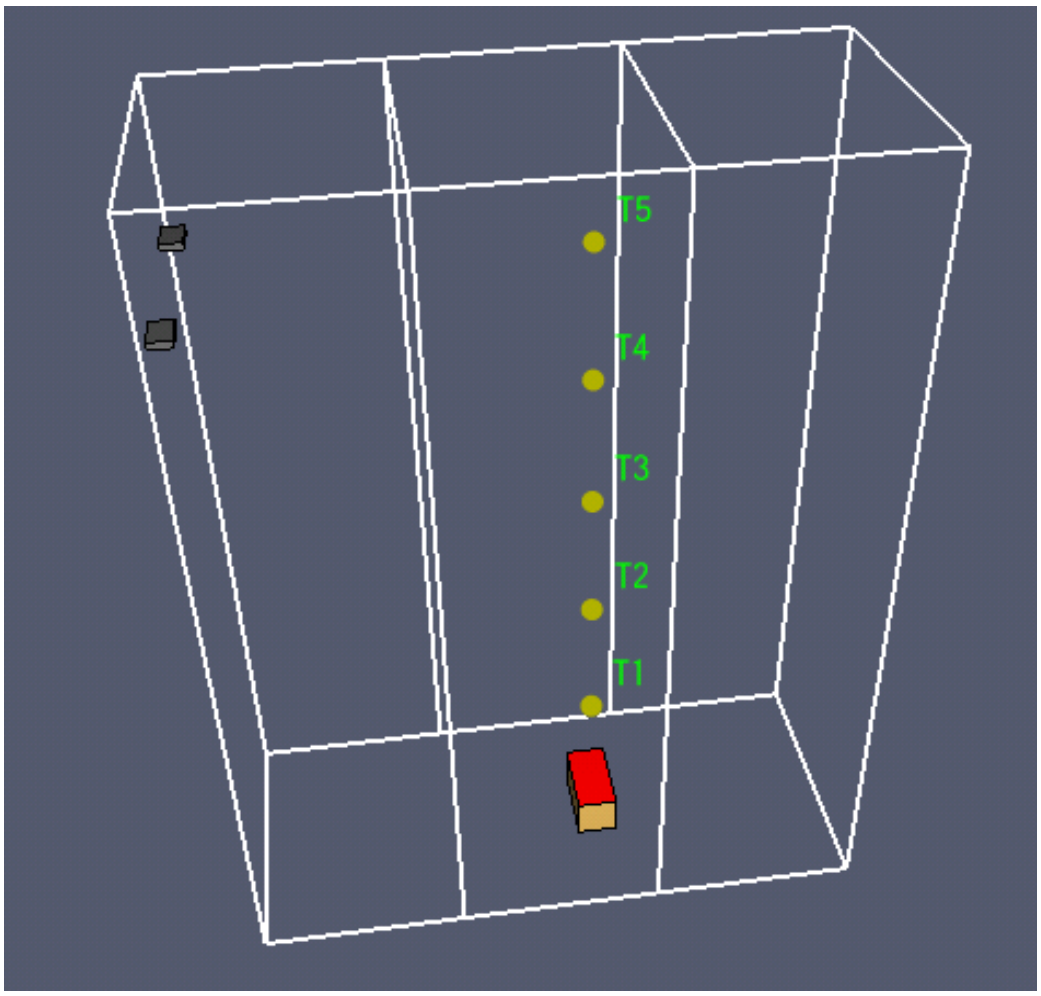

Figure 6.7 Temperature sensor set up

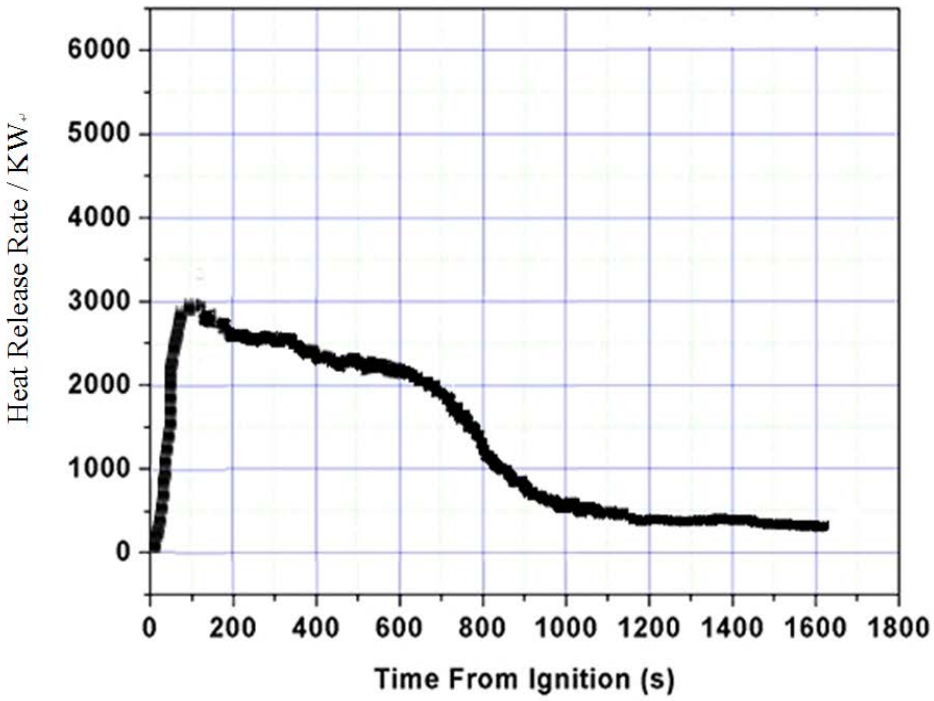

Figure 6.8 Three wood crib (stacked) heat release rate curve

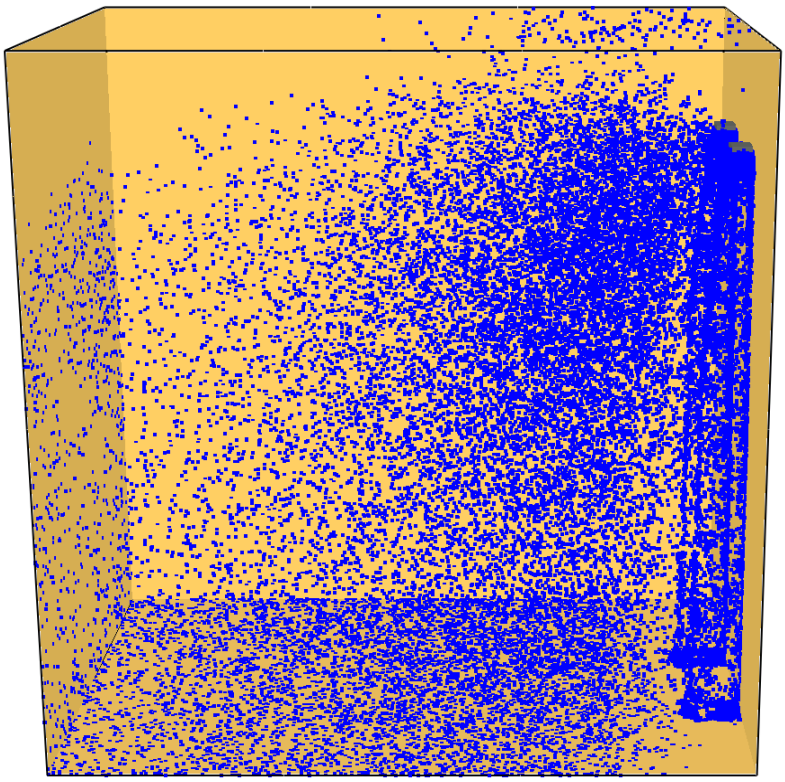

Figure 6.9 Side view of the modeled spray scenario

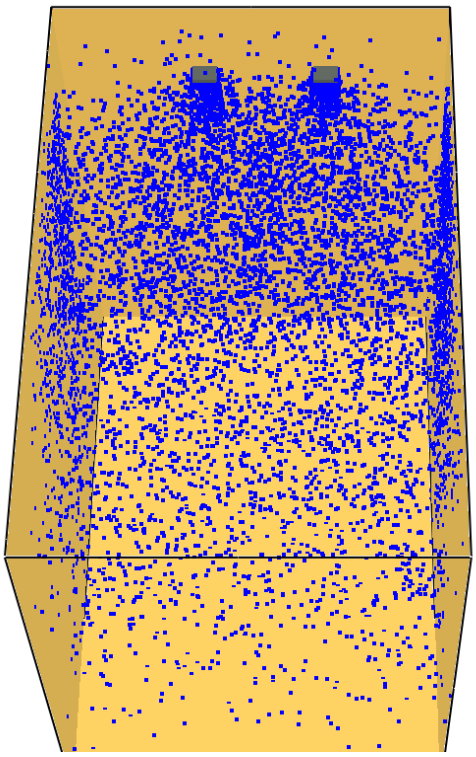

Figure 6.10 Modeled spray front view

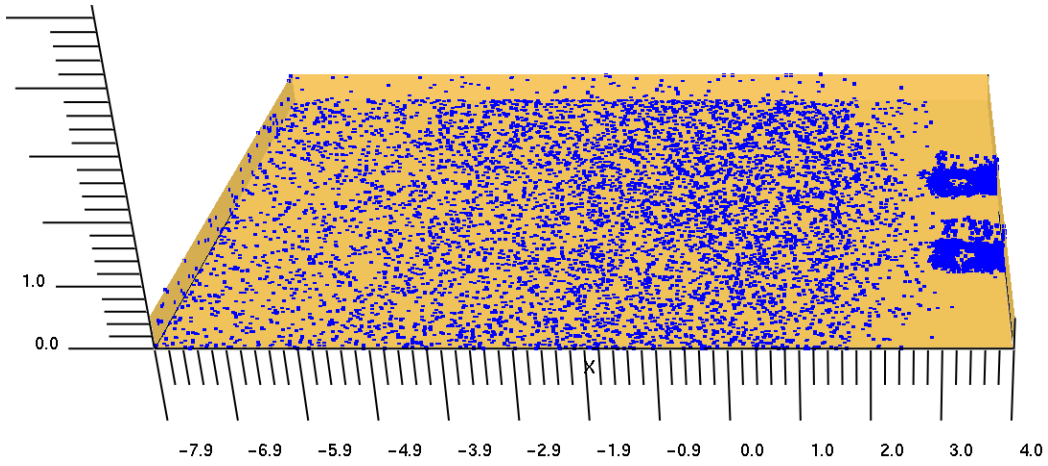

Figure 6.11 Modeled spray flat view

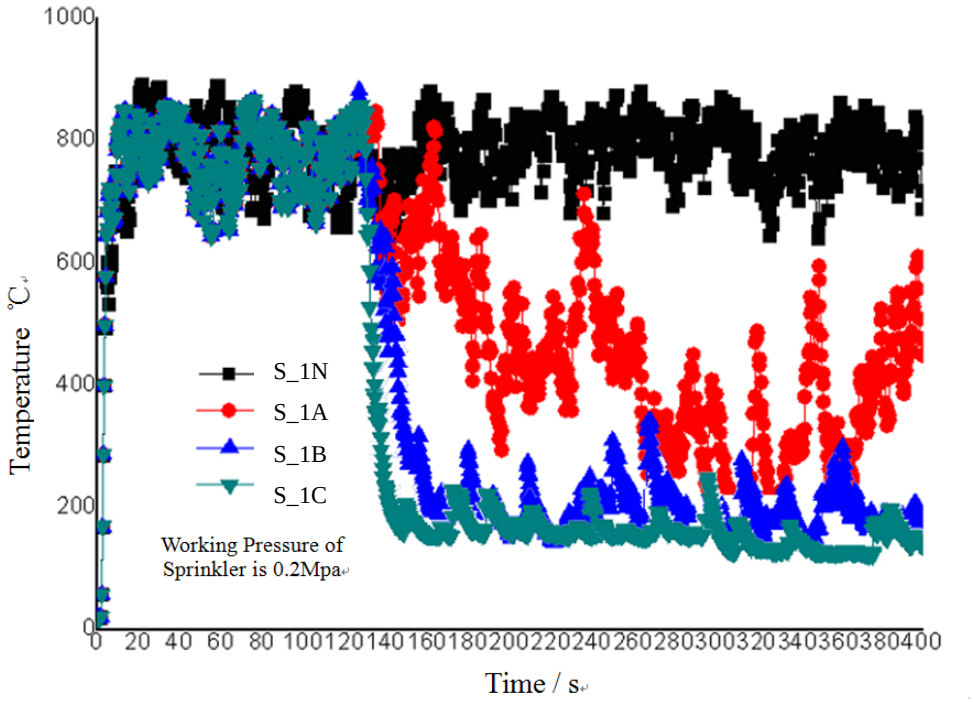

Figure 6.12 Thermocouple T1 temperature change over time of Scenario 1N, 1A, 1B and 1C

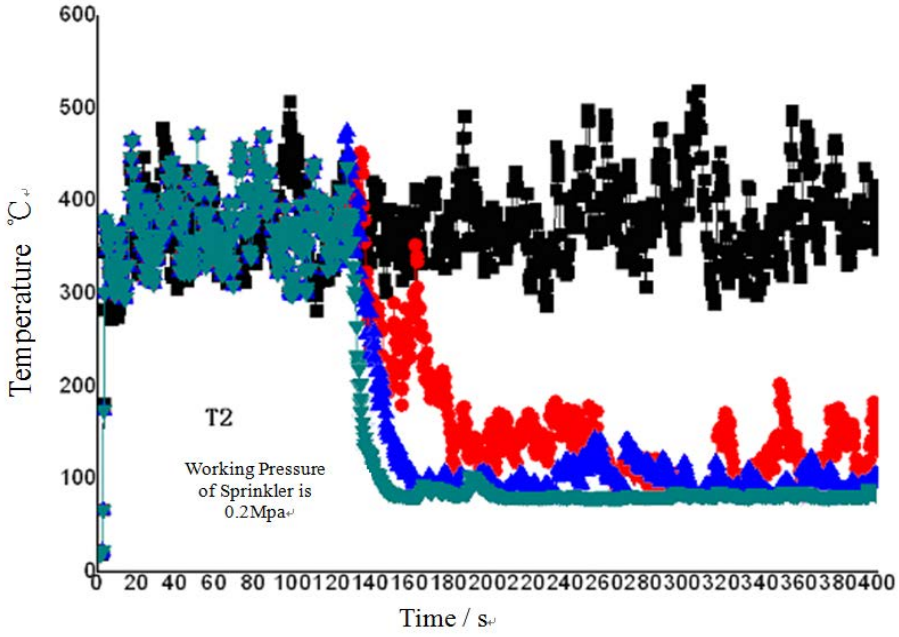

Figure 6.13 Thermocouple T2 temperature change over time of Scenario 1N, 1A, 1B and 1C

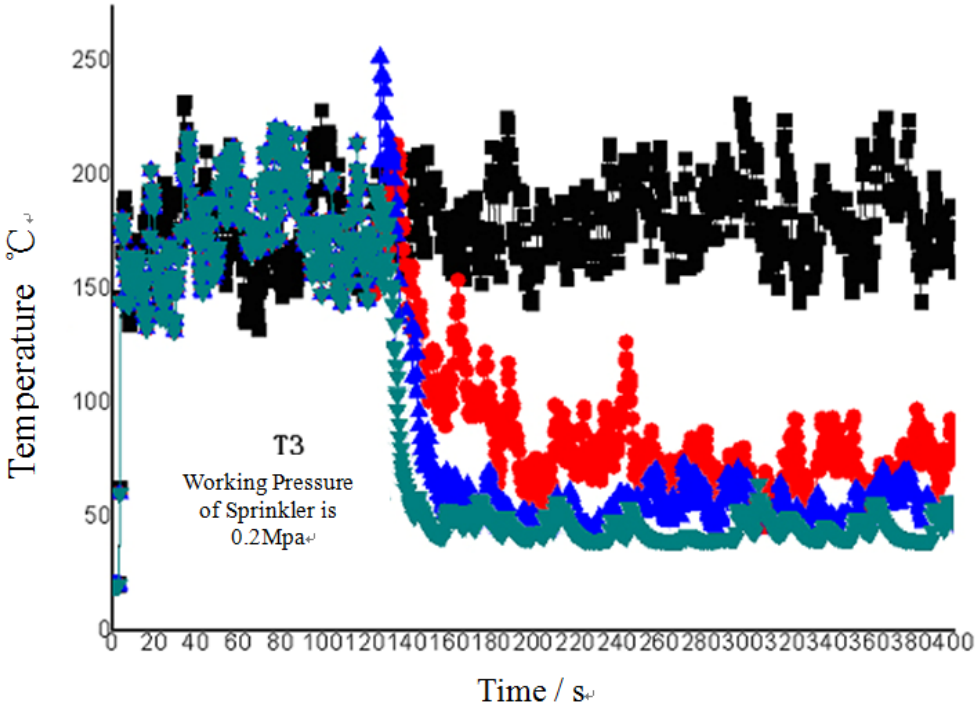

Figure 6.14 Thermocouple T3 temperature change over time of Scenario 1N, 1A, 1B and 1C

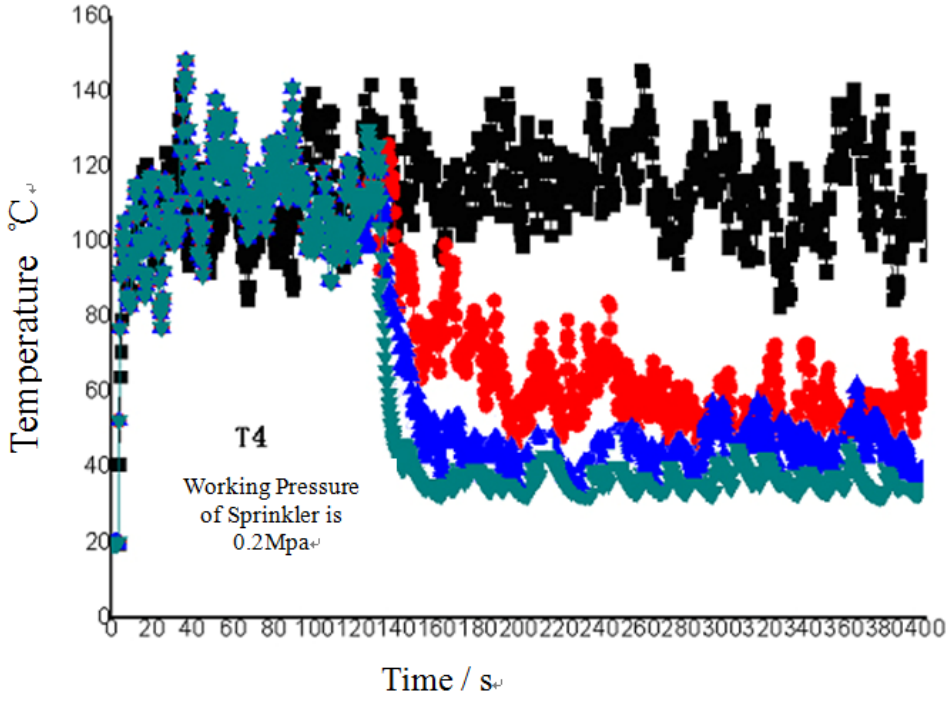

Figure 6.15 Thermocouple T4 temperature change over time of Scenario 1N, 1A, 1B and 1C

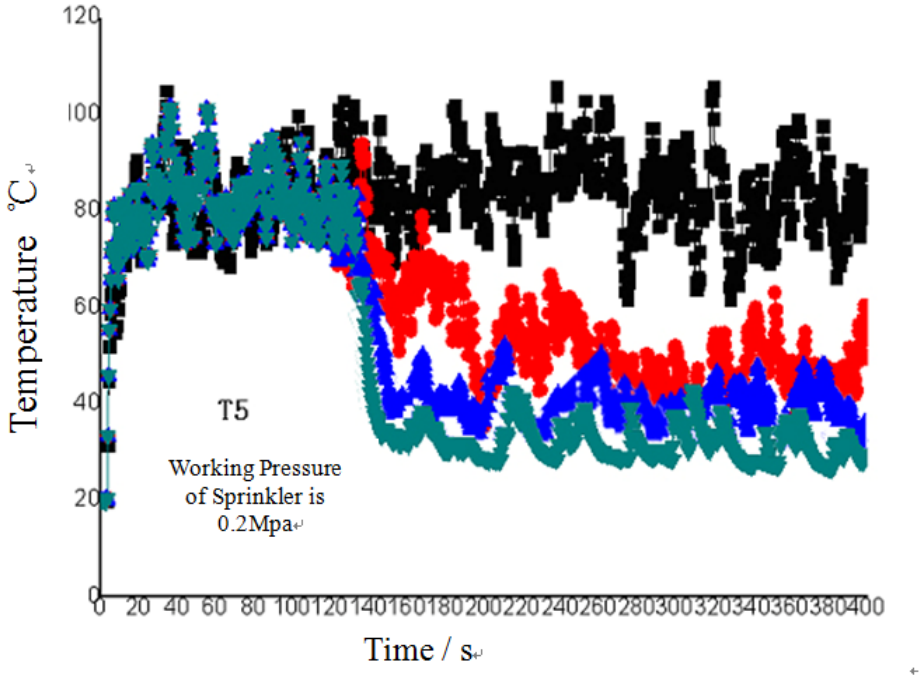

Figure 6.16 Thermocouple T5 temperature change over time of Scenario 1N, 1A, 1B and 1C

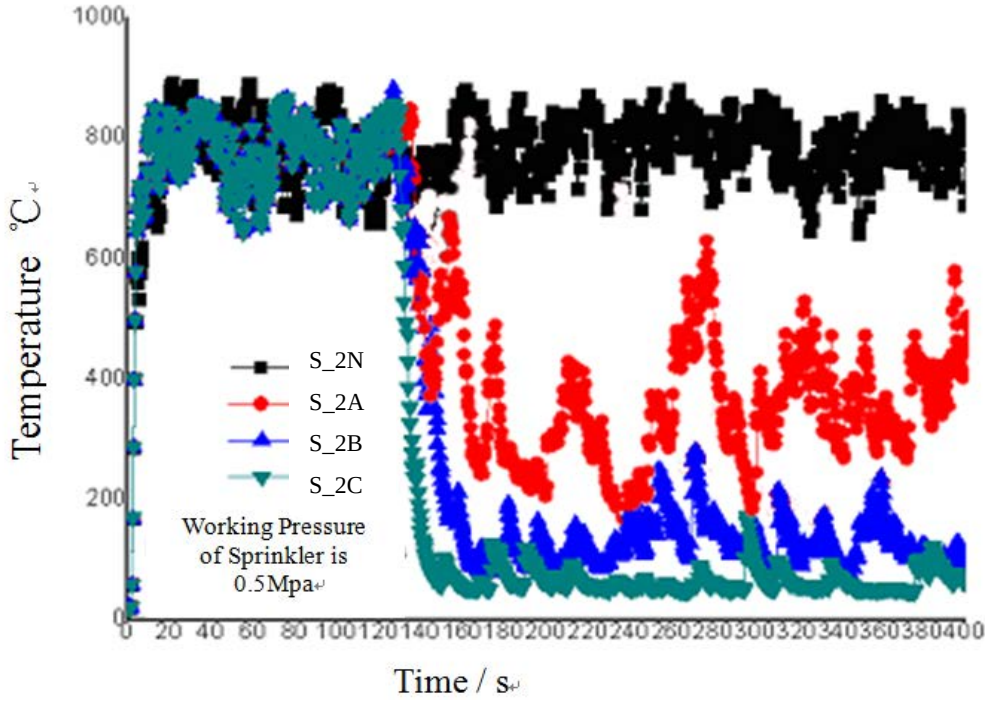

Figure 6.17 Thermocouple T1 temperature change over time of Scenario 2N, 2A, 2B and 2C

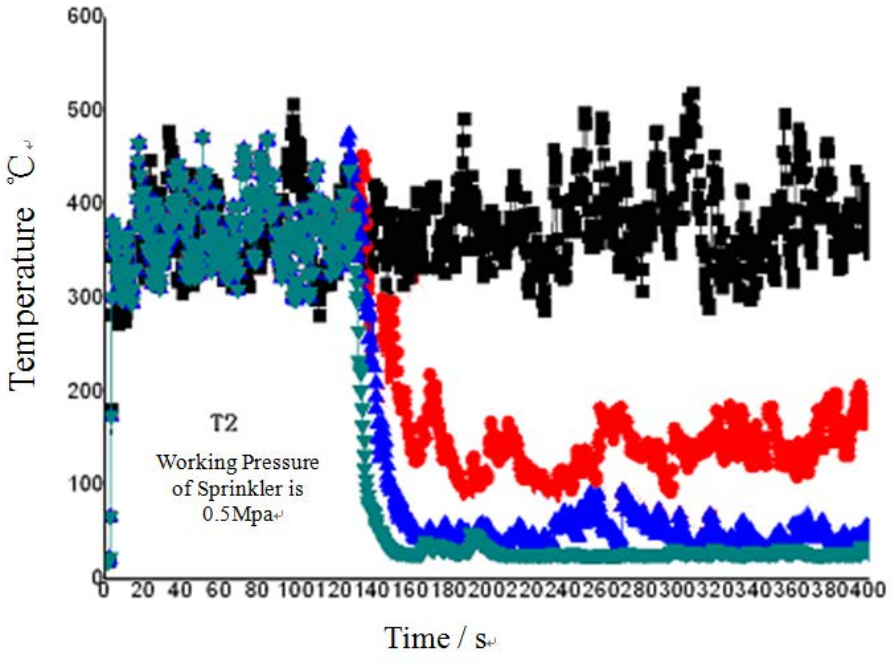

Figure 6.18 Thermocouple T2 temperature change over time of Scenario 2N, 2A, 2B and 2C

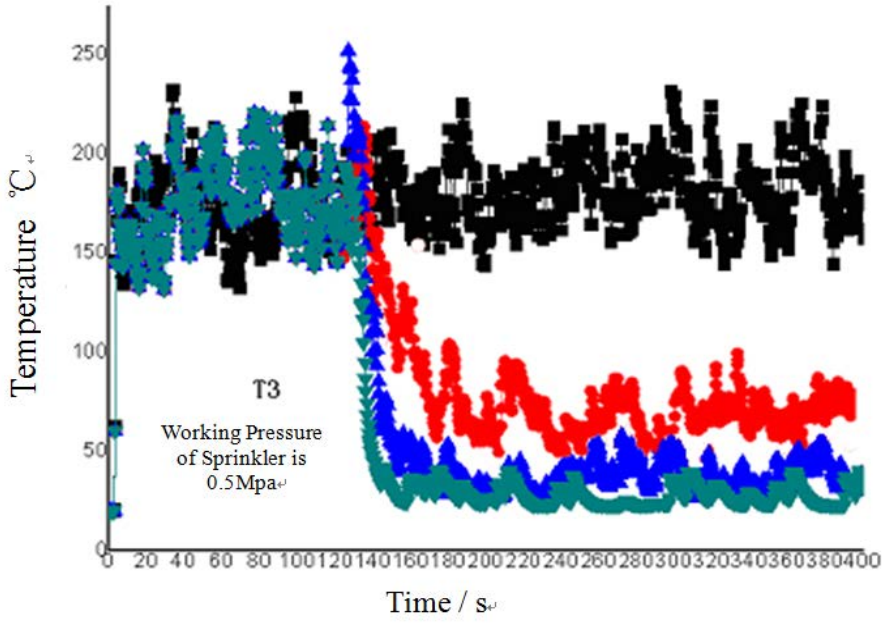

Figure 6.19 Thermocouple T3 temperature change over time of Scenario 2N, 2A, 2B and 2C

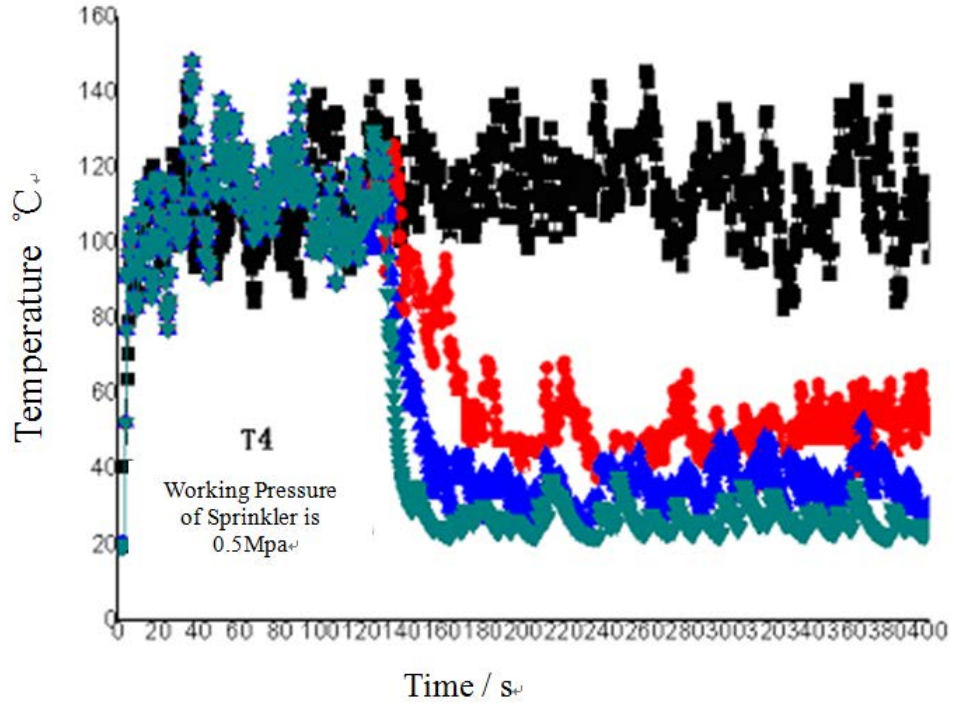

Figure 6.20 Thermocouple T4 temperature change over time of Scenario 2N, 2A, 2B and 2C

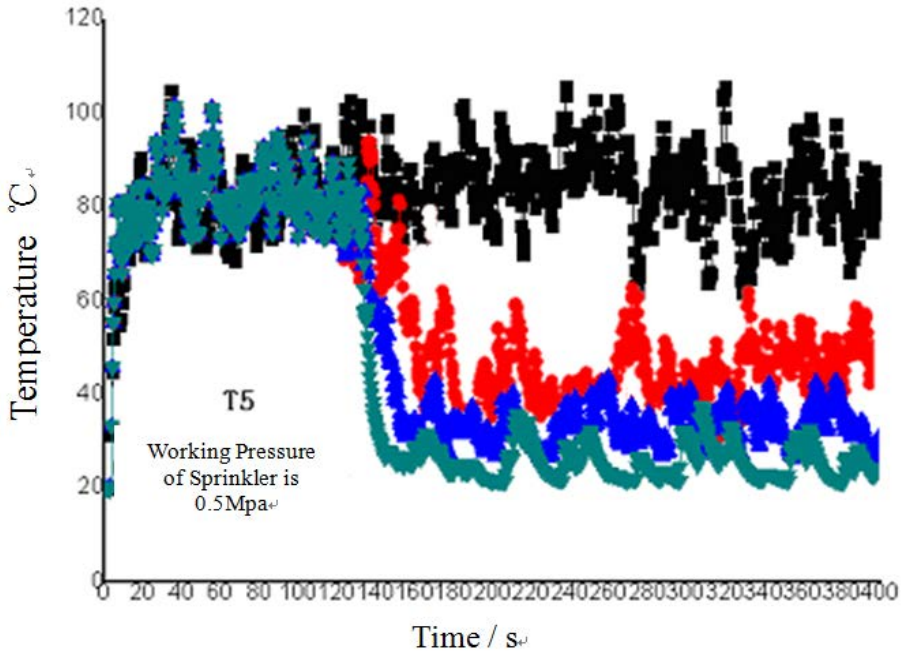

Figure 6.21 Thermocouple T5 temperature change over time of Scenario 2N, 2A, 2B and 2C

Figure 7.1 Full-scale fire experiment test venue

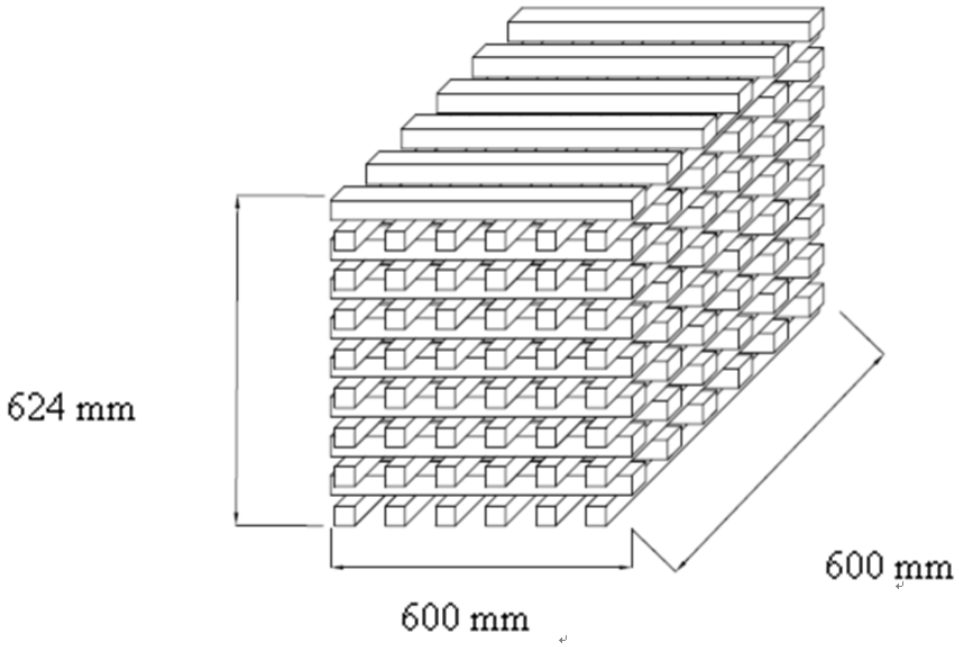

Figure 7.2 Combustion material

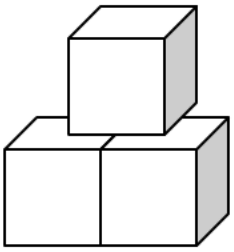

Figure 7.3 Single on top, double below

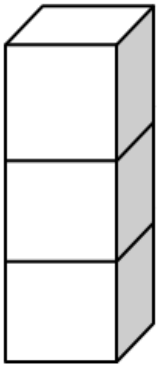

Figure 7.4 Stacked placement

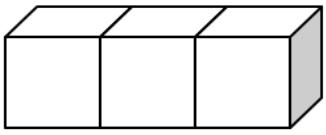

Figure 7.5 Single line placement

Figure 7.6 Wood crib and water collection pan placement

Figure 7.7 One on top, two below wood crib placement

Figure 7.8 One line placement wood crib ignition

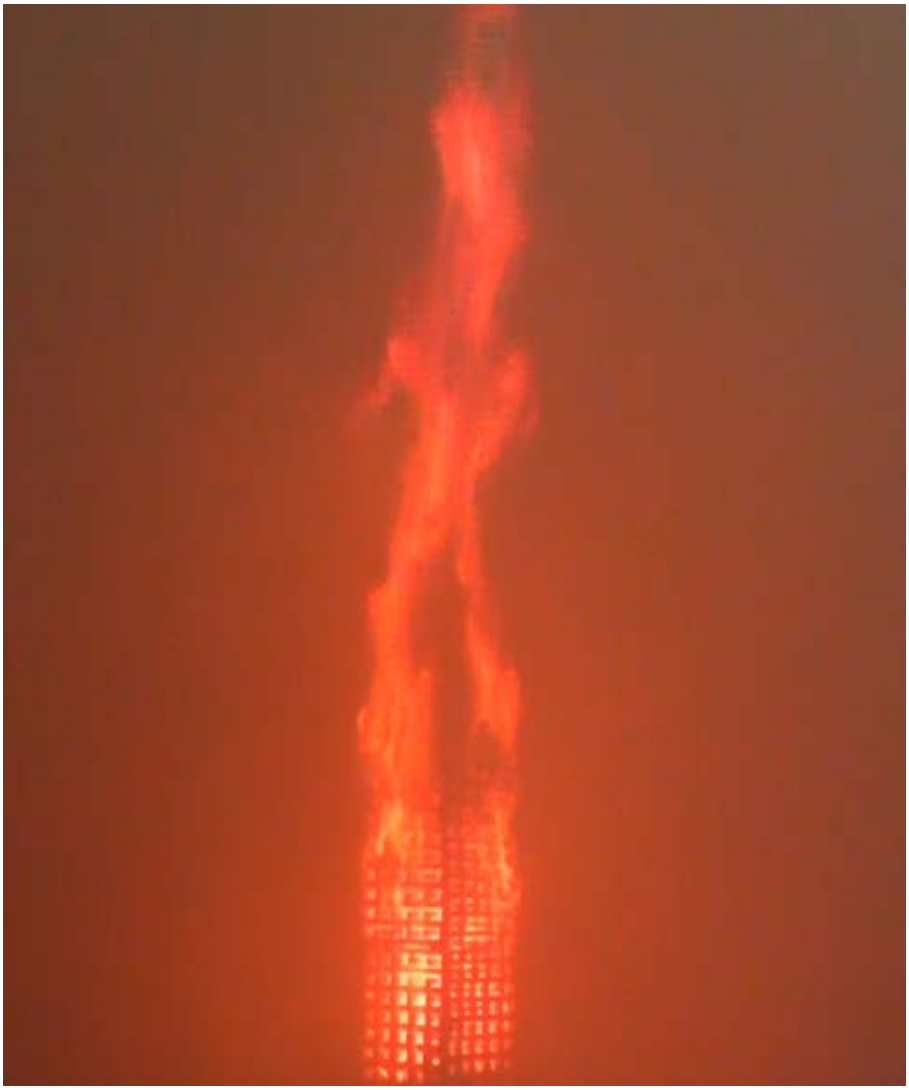

Figure 7.9 Straight placement start emitting water

Figure 7.10 Straight line wood crib fire extinguishing process

Figure 7.11 (Stacked placement) Wood crib extinguished

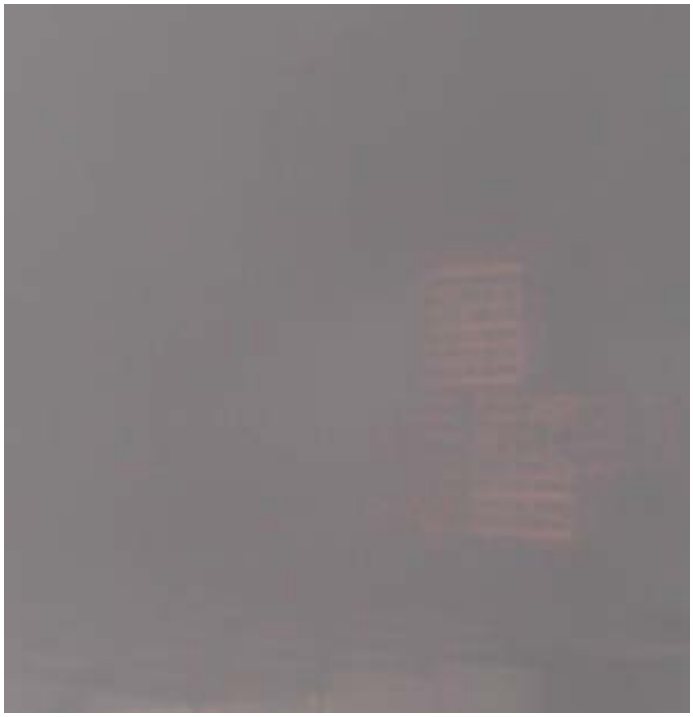

Figure 7.12 (One on top, two below) Wood crib extinguished

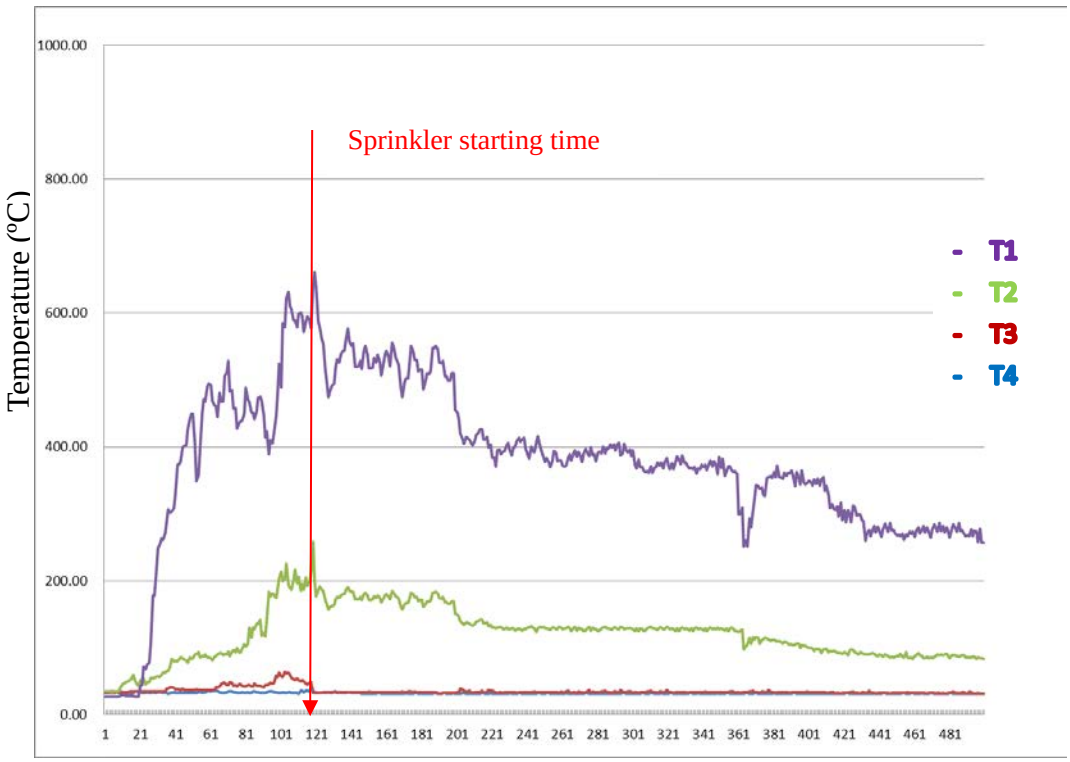

Figure 7.13 Fire site temperature change diagram (Straight line wood crib placement)

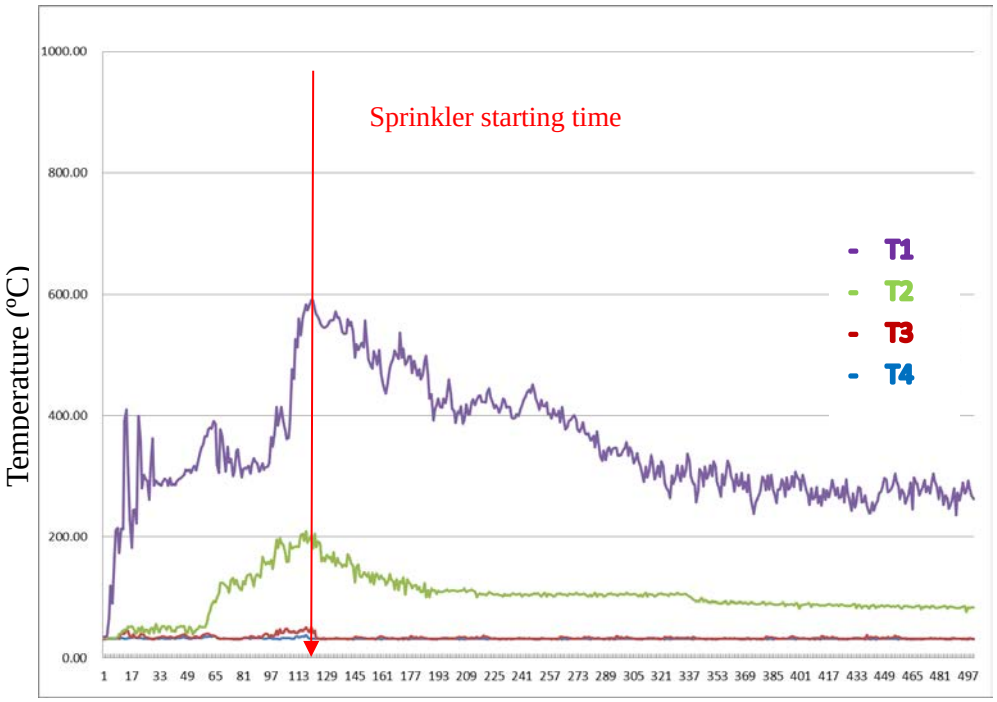

Figure 7.14 Fire site temperature change diagram (Stacked wood crib placement)

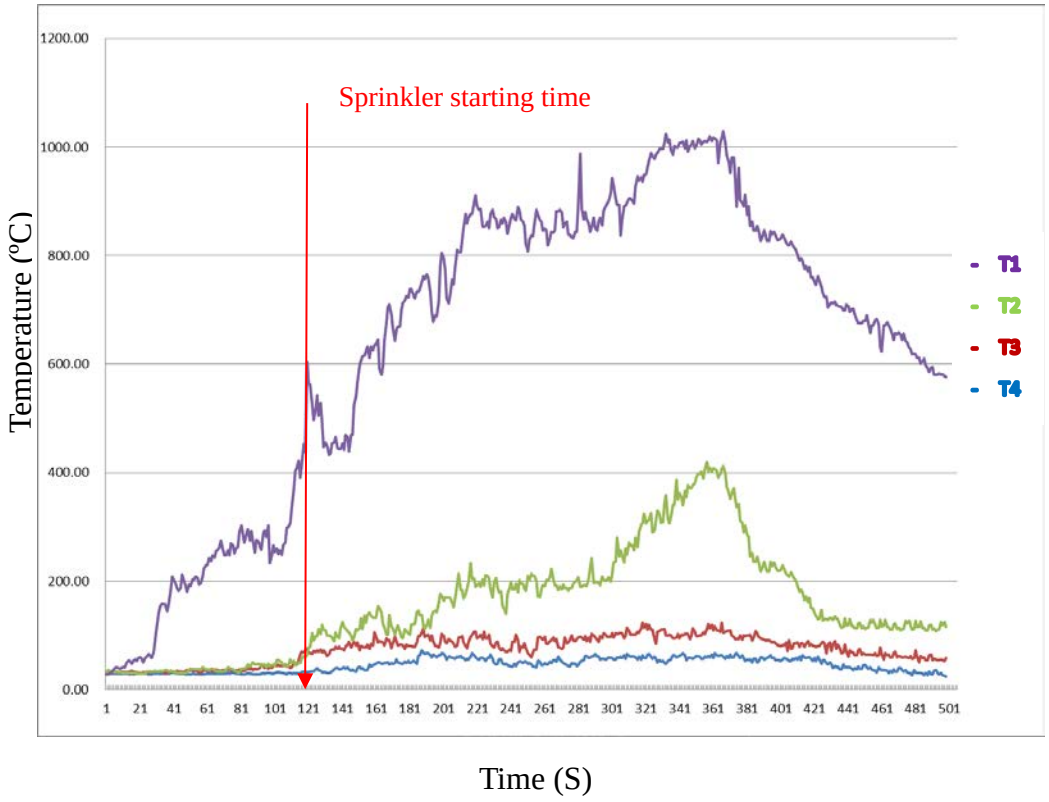

Figure 7.15 Fire site temperature change diagram (One on top/Two below wood crib placement)

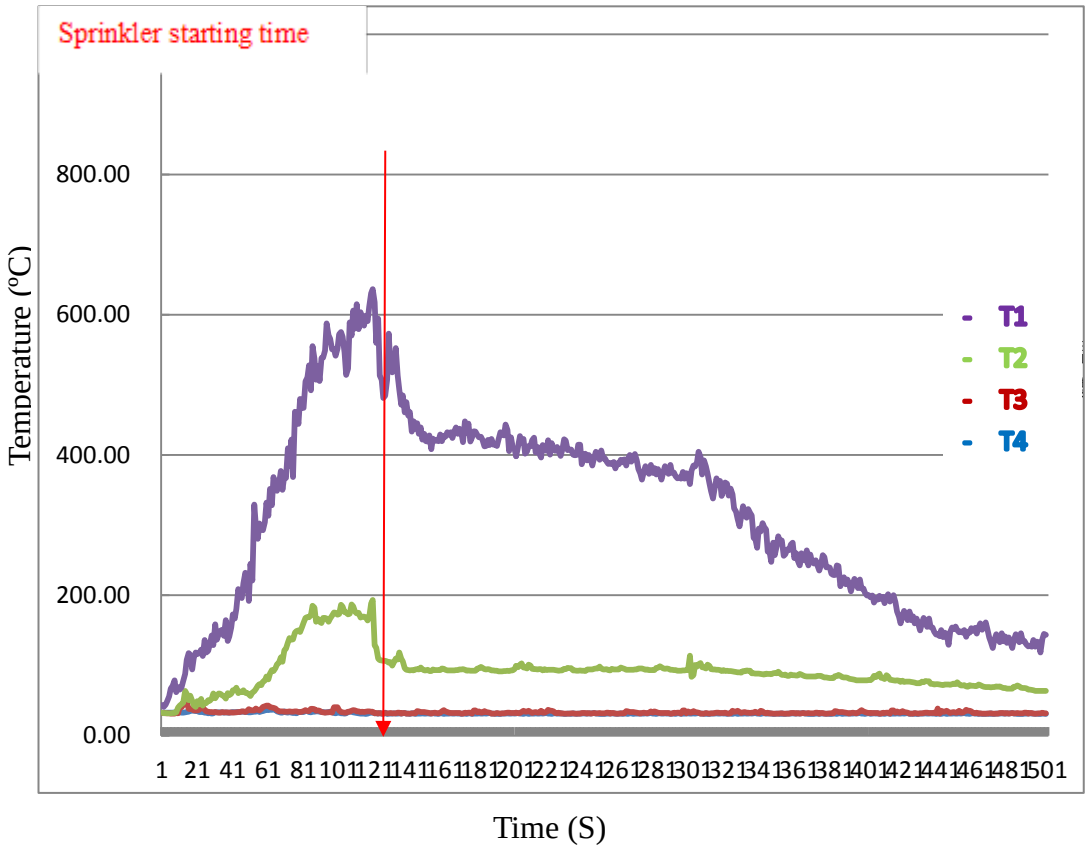

Figure 7.16 Fire site temperature change diagram (Straight line wood crib placement)

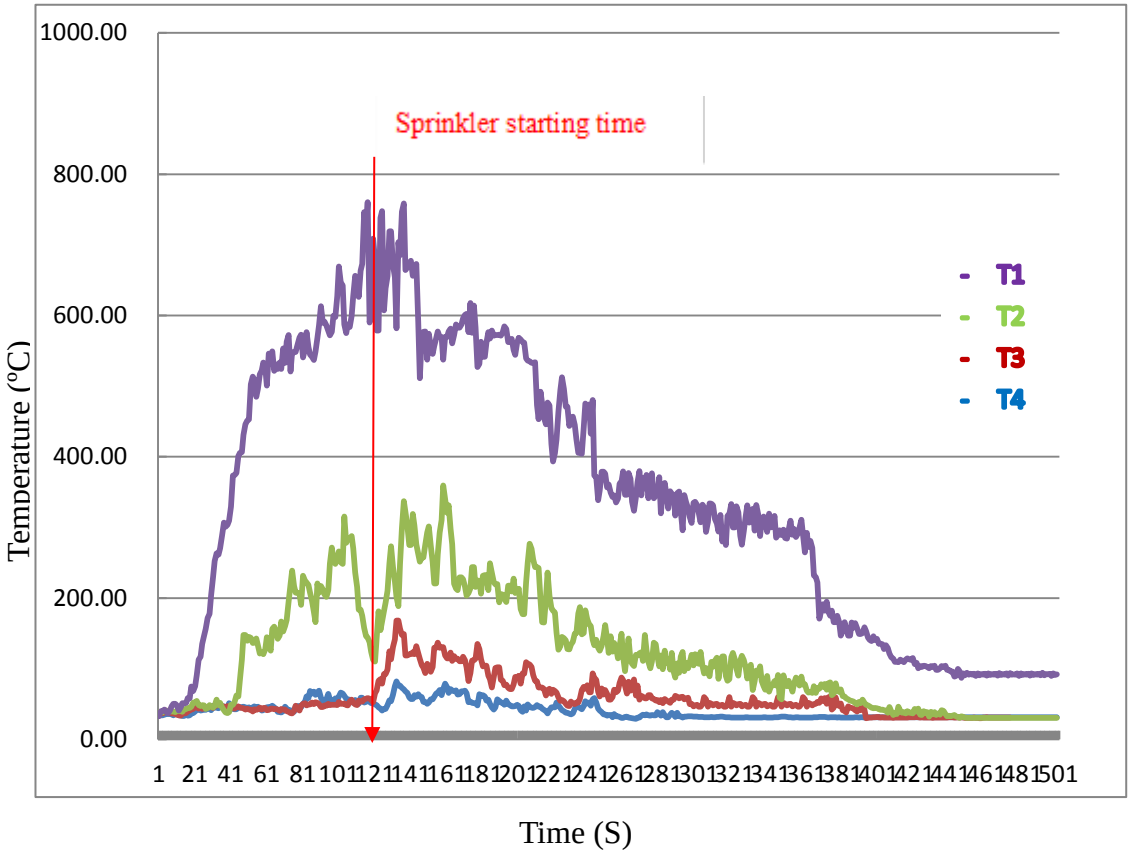

Figure 7. 17 Fire site temperature change diagram (Stacked wood crib placement)

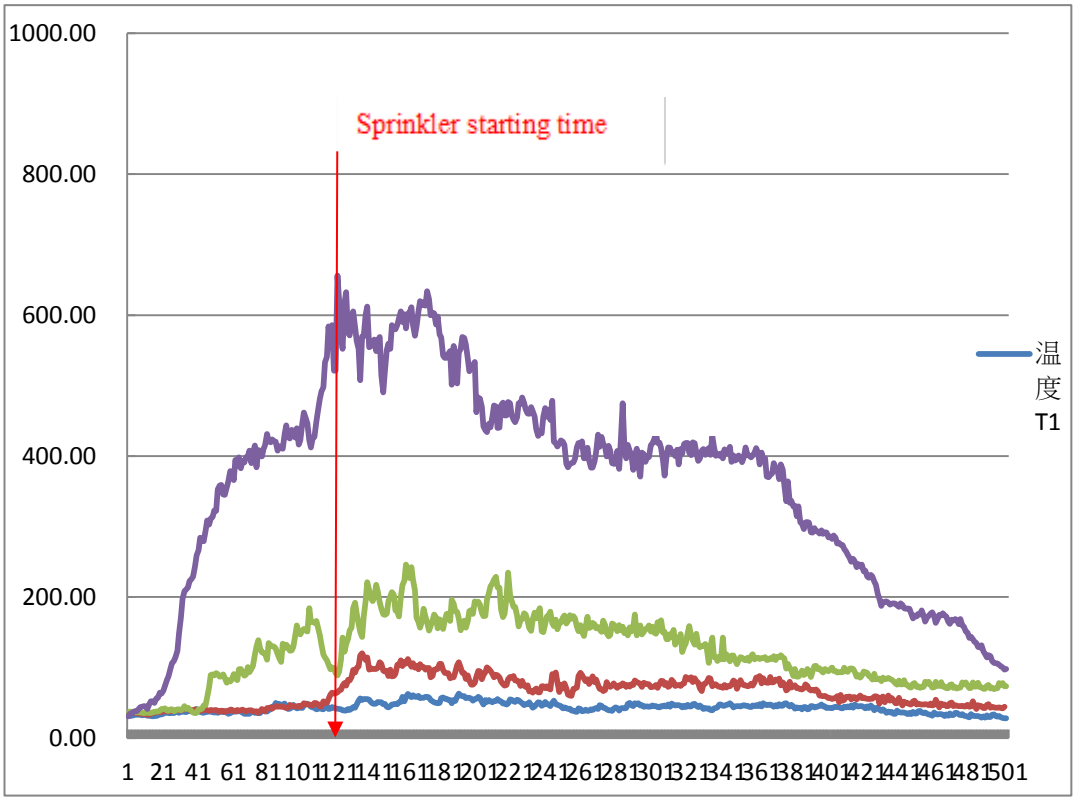

Figure 7.18 Fire site temperature change diagram (One on top/Two below wood crib placement)

e (°C)

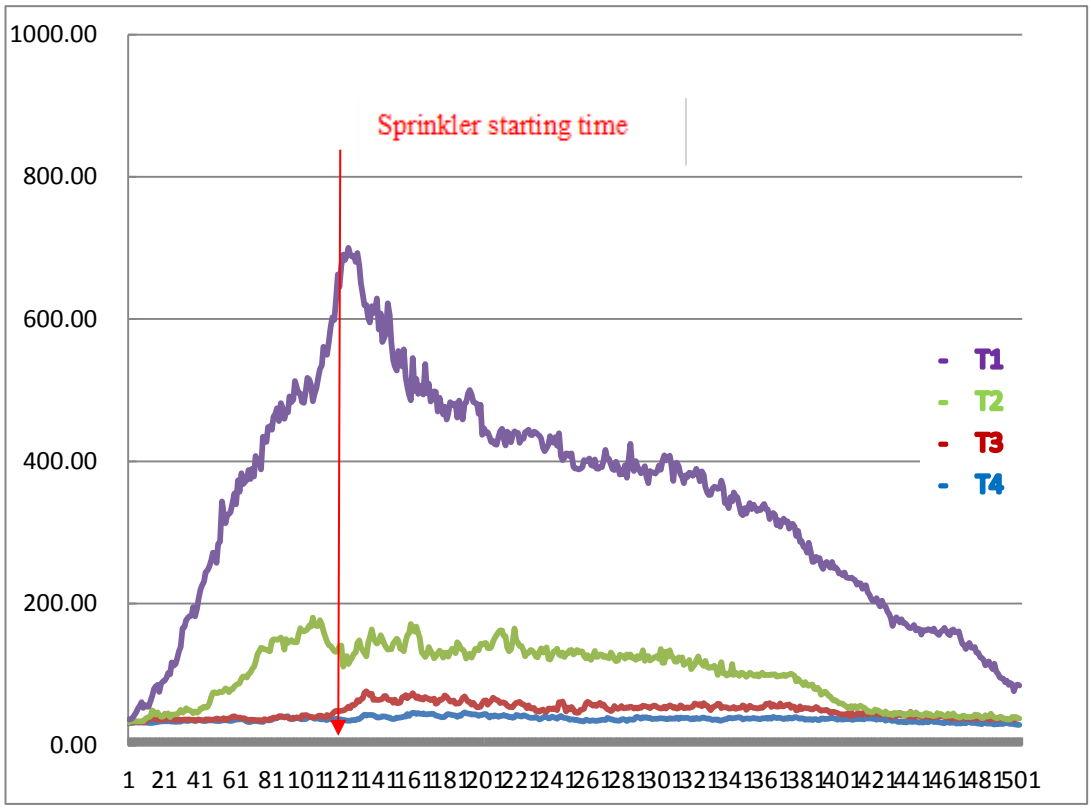

Figure 7.19 Fire site temperature change diagram (One on top/Two below wood crib placement)

Table 4-1 Parameter table

Wooden crib	Weight (kg each)	36.3, 37.8, 36.6, 36.8, 37.2 36.8, 36.9, 36.6, 36.5, 36.4 36.6, 37.2, 37.4, 36.9, 36.8 36.5, 37.3
	Water Absorption Rate (%)	9.5, 9.7, 9.9, 9.9, 10.1, 10.6 9.2, 9.1, 9.3, 10.6, 10.2, 10.1 9.3, 9.5, 9.7, 9.9, 10.3
Oil tray	Dimensions (mm)	500×500
	Water Level (mm)	30
	N-heptance (L each)	1.5

Table 4-2 Experiment results

Ignite the oil trays corresponding to the Experiment	Number of Oil trays	Number of Wood cribs and patterns	N-heptane Level (L)	Maximum Heat Release Rate MW	Total Heat Released MJ
W1	1	1	1.5	0.52	40.0
W2	2	2 flat	3.0	1.03	79.8
W3	4	4 flat	6.0	2.66	171.2
W4	2	4 stack	4.5	1.03	148.4
W5	6	6 flat	9.0	4.14	290.0

Table 4-3 W1 typical combustion process

Time	Combustion Process
0s	Ignition of oil tray
77s	Heat release rate reaches peak value of 1.73 MW (N-heptane combustion)
121s	Oil tray extinguished, heat release rate reaches 0.77 MW (Wood Crib Ignition)
650s	Heat release rate starts to decline, heat release rate reaches 0.56 MW
1620s	Wood crib fully extinguished, heat release rate averages 0.18 MW

Table 4-4 W2 typical combustion process

Time	Combustion Process
0s	Ignition of oil tray
86s	Heat release rate reaches peak value of 3.47 MW (N-heptane combustion)
139s	Oil tray extinguished, heat release rate reaches 1.39 MW (wood crib ignition)
662s	Heat release rate starts to decline, heat release rate reaches 0.94 MW
1621s	Wood crib fully extinguished, heat release rate averages 0.25 MW

Table 4-5 W3 typical combustion process

Time	Combustion Process
0s	Oil tray ignited
96s	Heat release rate reaches peak value of 5.88 MW (N-heptane combustion)
129s	Oil tray extinguished, heat release rate reaches 3.11 MW (wood crib ignition)
600s	Heat release rate starts to decline, heat release rate reaches 2.45 MW
1623s	Wood crib fully extinguished, heat release rate averages 0.35 Mw

Table 4-6 W4 typical combustion process

Time	Combustion Process
0s	Oil tray ignited
131s	Heat release rate reaches peak value of 4.12 MW (N-heptane combustion)
151s	Oil tray extinguished, heat release rate reaches 2.93 MW (wood crib ignition)
879s	Wood crib collapses, heat release rate starts to decline, heat release rate reaches 1.97 MW
1387s	Wood crib fully extinguished, heat release rate averages 0.44 MW

Table 4-7 W5 typical combustion process

Time	Combustion Process
0s	Oil tray ignited
89s	Due to excess heat（170℃）start to manually lower lift truck, 8.51 MW (N-heptane combustion)
91s	Heat release rate reaches peak value of 8.56 MW (N-heptane combustion)
139s	Oil tray extinguished, heat release rate reaches 4.41 MW (wood crib ignition)
649s	Heat release rate starts to decline, heat release rate reaches 3.56 MW
1250s	Wood crib fully extinguished, heat release rate averages 0.72 MW

Table 4-8 Large-scale crib calorimeter test results

Parameter	Experiment Number				
	W1	W2	W3	W4	W5
Environment Temperature / Humidity	21.0℃ / 29.0%	21.5℃ / 29.0%	22.0℃ / 31.0%	33.0℃ / 54.0%	31.5℃ / 52.5%
Oil Tray Environment Temperature / Humidity	33.5℃ / 63.0%				
Peak Heat Release Rate RHR (MW)	1.73	3.47	5.88	4.12	8.55
Peak Oil Pan Heat Release Rate RHR (MW)	0.52	1.03	2.66	1.03	4.14
Wood Crib Total Heat Released (MJ)	568.2	1135.8	2272.0	2158.6	3385.5
Single Crib Heat Released (MJ each)	568.2	567.9	568.0	539.7	564.3
Stable Heat Release Rate Period	7’30”	6’11”	6’15”	9’30”	7’14”

Table 5-1 Technical characteristics of sprinklers

Ability / Number	Largest Protection Area (m^2)	K Factor	Diameter (mm)	Largest Working Pressure (MPa)
1	4.9m*7.3m	115	DN20	1.20
2	4.9m*7.3m	115	DN20	1.20
3	5.0m*7.0m	115	DN20	1.20
4	4.9m*6.1m	161	DN20	1.20
5	3.0m*4.5m	80	DN15	1.20
6	3.2m*4.55m	80	DN15	1.20
7	3.0m*4.6	80	DN15	1.20

Table 5-2 Sprinkler 1 water distribution experiment result (0.35 MPa 6 m)

0.35 MPa, 6 m, unit of water height (mm)					
4	8	14	11	19	13
6	16	24	28	15	12
14	22	31	37	35	27
21	24	34	42	39	30
22	26	36	45	40	28
25	30	40	44	39	30
24	32	39	44	36	31
24	33	41	44	37	26
23	32	42	46	36	25
22	29	39	43	37	28
21	29	37	42	36	29
19	28	38	40	37	33
22	30	35	41	41	42
24	31	39	43	48	52
28	43	34	40	52	52
34	38	37	38	47	47
30	37	37	40	44	42
27	39	49	53	51	38
39	36	44	47	37	26
50	29	45	62	21	12

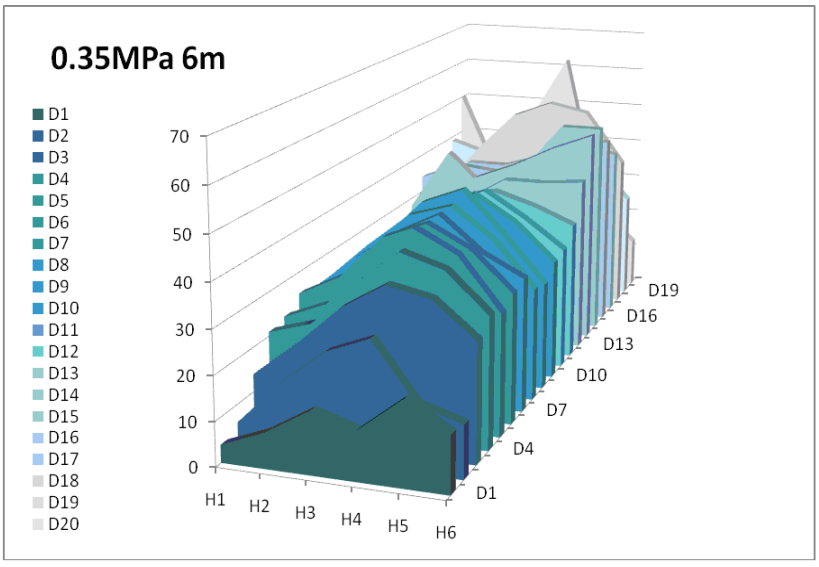

Table 5-3 Sprinkler 1 water distribution experiment result (0.5 MPa 6 m)

0.35 MPa 8 m, unit of water height (mm)					
18	23	31	33	32	20
21	28	35	37	33	21
22	27	35	38	35	23
21	24	33	38	35	24
20	24	31	35	32	25
18	23	31	34	34	27
16	21	29	39	36	29
19	24	32	38	34	22
18	24	37	38	33	22
21	30	35	39	34	23
22	32	39	40	35	23
23	37	40	41	38	30
27	37	44	45	42	33
29	39	45	45	47	38
30	42	46	47	48	40
31	43	45	47	48	39
32	43	47	49	49	39
30	45	55	53	47	32
73	43	54	47	40	29
49	38	54	53	25	20

Table 5-4 Sprinkler 1 water distribution experiment result (0.35 MPa 8 m)

0.35 MPa 8 m, unit of water height (mm)					
18	23	31	33	32	20
21	28	35	37	33	21
22	27	35	38	35	23
21	24	33	38	35	24
20	24	31	35	32	25
18	23	31	34	34	27
16	21	29	39	36	29
19	24	32	38	34	22
18	24	37	38	33	22
21	30	35	39	34	23
22	32	39	40	35	23
23	37	40	41	38	30
27	37	44	45	42	33
29	39	45	45	47	38
30	42	46	47	48	40
31	43	45	47	48	39
32	43	47	49	49	39
30	45	55	53	47	32
73	43	54	47	40	29
49	38	54	53	25	20

Table 5-5 Sprinkler 1 water distribution experiment result (0.5 MPa 8 m)

0.5 MPa 8 m , unit of water height (mm)					
19	39	61	70	48	16
18	35	58	65	45	17
18	32	53	59	39	18
16	36	51	55	37	20
19	33	48	50	38	25
20	30	47	54	37	28
19	35	49	52	40	35
20	31	48	54	41	26
22	35	45	50	44	27
22	32	46	47	43	31
23	36	47	49	44	33
25	37	50	49	45	33
27	39	48	49	52	42
31	40	48	56	60	49
32	43	49	57	71	55
33	46	53	58	62	52
38	49	57	58	60	48
42	51	58	59	55	48
83	49	58	56	42	38
51	42	65	60	30	28

Table 5-6 Sprinkler 1 water distribution experiment result (0.35 MPa 10 m)

0.35 MPa 10 m, unit of water height (mm)					
15	18	26	33	33	20
13	19	30	35	32	25
15	21	26	38	32	27
14	20	25	40	29	22
12	19	25	34	30	27
11	14	23	35	33	31
8	16	21	30	32	38
11	15	22	27	30	33
11	14	21	26	33	33
10	12	19	30	32	31
9	13	21	25	34	65
8	13	19	17	35	40
11	15	30	24	31	44
14	16	19	23	28	43
15	19	21	22	32	41
20	24	24	26	28	37
21	26	24	27	28	37
22	26	29	26	29	36
23	26	36	38	41	51
26	27	43	59	48	52

Table 5-7 Sprinkler 1 water distribution experiment result (0.5 MPa 10 m)

0.5 MPa 10 m, unit of water height (mm)					
9	20	33	52	57	33
12	19	32	58	55	38
9	18	33	48	50	42
9	19	32	37	50	46
12	16	28	38	46	46
11	17	26	36	43	52
13	14	25	34	44	59
11	15	23	31	42	48
14	16	23	30	43	47
13	18	22	28	42	50
15	15	21	28	37	19
15	15	19	24	36	54
13	16	8	23	36	55
13	17	24	24	33	50
17	23	21	25	33	48
19	24	25	28	33	44
21	27	33	36	37	41
21	26	36	39	43	43
17	29	39	44	44	53
21	23	44	72	55	59

Table 5-8 Sprinkler 2 water distribution experiment result (0.35 MPa 10 m)

0.35 MPa 10 m, unit of water height (mm)					
0	1	2	5	5	2
4	3	2	5	3	2
6	5	8	10	18	19
13	11	13	14	20	14
12	14	20	24	25	17
14	17	19	25	27	15
13	17	23	32	35	28
15	20	25	40	38	28
13	20	26	35	38	31
12	12	20	34	37	36
9	13	18	22	39	37
9	13	21	28	38	39
9	9	18	30	39	43
10	17	22	34	40	42
14	14	28	41	43	48
16	21	37	54	56	49
19	27	47	57	61	54
27	32	51	65	66	56
33	35	56	66	70	55
46	42	77	80	59	71

Table 5-9 Sprinkler 2 water distribution experiment result (0.5 MPa 10 m)

0.5 MPa 10 m, unit of water height (mm)					
0	6	1	0	6	0
1	5	6	11	5	1
10	8	7	14	18	37
8	11	9	16	27	39
15	14	15	24	37	57
11	21	18	23	41	51
15	20	20	31	40	62
11	22	24	28	39	48
10	20	24	29	42	45
14	21	23	29	40	41
8	15	25	25	33	35
14	16	18	21	28	38
10	15	21	21	27	31
10	13	21	26	31	34
15	14	20	29	30	44
15	15	24	36	35	55
24	22	28	43	43	58
25	26	40	46	51	62
31	35	42	49	53	60
30	32	59	63	50	62

Table 5-10 Sprinkler 2 water distribution experiment result (0.35 MPa 8 m)

0.35 MPa 8 m, unit of water height (mm)					
0	1	0	1	1	0
0	1	1	1	3	1
1	4	0	6	7	5
7	6	7	6	10	7
9	10	9	13	15	13
12	15	14	19	22	20
17	21	24	26	26	22
28	30	34	33	28	21
29	38	40	35	28	20
29	43	44	37	27	19
25	44	46	37	25	21
22	44	50	39	23	11
25	42	50	39	26	17
25	44	54	40	23	13
28	51	60	41	21	13
33	57	66	41	25	15
45	56	62	42	28	18
49	61	64	46	33	24
50	71	59	48	34	28
89	75	89	68	44	36

Table 5-11 Sprinkler 2 water distribution experiment result (0.5 MPa 8 m)

0.5 MPa 8 m, unit of water height (mm)					
2	4	4	4	4	5
10	6	9	7	10	6
12	12	14	16	18	18
19	14	20	29	22	13
26	30	35	37	29	13
35	40	46	44	31	11
43	54	55	43	26	18
42	59	52	42	25	12
42	58	53	39	24	14
38	53	57	44	24	12
32	47	53	40	30	17
26	42	59	43	28	19
26	41	52	46	31	19
26	42	61	58	32	21
30	53	71	72	44	23
38	58	76	85	45	25
40	62	81	82	37	25
44	66	79	69	41	29
55	65	76	64	48	38
63	58	83	67	46	45

Table 5-12 Sprinkler 2 water distribution experiment result (0.35 MPa 6 m)

0.35 MPa 6 m, unit of water height (mm)					
1	0	1	0	0	0
0	0	1	0	0	0
2	3	0	1	1	0
4	5	2	3	5	3
8	7	3	5	12	13
15	14	16	13	23	20
19	25	20	24	32	21
31	37	30	35	32	23
40	46	43	37	33	25
39	52	44	36	31	22
33	47	48	38	32	27
23	41	51	47	33	23
20	30	50	52	31	22
14	29	49	57	39	21
12	28	53	67	40	24
14	31	66	78	41	26
22	34	67	84	43	26
26	38	70	83	47	30
26	41	57	79	51	43
44	52	77	87	55	56

Table 5-13 Sprinkler 2 water distribution experiment result (0.5 MPa 6 m)

0.5 MPa 6 m, unit of water height (mm)					
1	1	0	3	0	0
2	3	1	3	3	2
2	2	3	4	5	13
10	10	9	10	19	21
20	14	17	24	32	29
30	28	25	39	46	33
49	42	73	46	47	35
53	58	54	48	44	31
57	66	59	47	40	27
52	65	65	49	36	28
37	54	64	50	36	26
26	38	59	52	35	31
18	30	55	62	43	32
17	27	64	77	51	30
17	30	82	88	55	27
25	40	85	97	58	33
32	50	90	87	59	41
36	52	82	80	59	47
38	43	69	70	55	48
55	42	70	71	49	50

Table 5-14 Sprinkler 3 water distribution experiment result (0.35 MPa 6 m)

0.35 MPa 6 m, unit of water height (mm)					
16	20	28	28	28	23
18	22	27	35	32	24
17	22	30	42	40	28
20	25	33	43	46	32
18	25	35	46	49	34
20	24	35	47	51	43
22	22	34	45	52	48
19	22	34	49	46	36
19	24	35	36	45	38
19	27	39	45	45	33
16	25	42	54	43	36
17	29	54	49	45	31
17	32	49	52	39	36
19	34	52	48	35	31
16	29	48	41	31	28
21	28	43	37	25	22
21	29	38	29	52	20
19	28	33	29	22	19
22	26	39	32	25	53
23	22	23	24	24	71

Table 5-15 Sprinkler 3 water distribution experiment result (0.5 MPa 6 m)

0.5 MPa 6 m, unit of water height (mm)					
20	28	38	44	43	25
20	32	45	49	50	39
21	33	51	52	60	49
19	30	51	57	65	57
20	26	44	59	69	58
19	25	38	62	67	64
59	25	37	54	63	74
20	25	35	53	61	52
24	25	43	51	65	52
17	25	72	53	60	50
21	23	41	49	56	55
14	27	40	53	54	46
14	26	46	56	52	42
16	28	49	55	46	37
16	31	50	54	46	31
18	33	46	49	39	30
19	25	39	45	3	26
21	24	38	37	29	24
21	27	33	36	28	27
30	27	27	31	33	92

Table 5-16 Sprinkler 3 water distribution experiment result (0.35 MPa 8 m)

0.35 MPa 8 m, unit of water height (mm)					
13	15	25	24	23	17
14	16	24	31	30	25
13	18	26	33	37	33
14	16	27	34	38	33
13	20	30	37	39	36
14	20	27	38	44	39
14	17	24	37	46	47
17	16	26	36	44	40
16	21	27	38	44	38
14	21	31	39	47	39
14	20	33	43	47	40
12	20	32	47	45	42
11	19	34	45	42	40
13	20	35	44	42	37
13	17	37	41	34	29
15	22	33	37	33	24
17	23	33	31	26	20
19	24	31	30	25	22
26	22	32	30	24	23
54	23	20	25	25	24

Table 5-17 Sprinkler 3 water distribution experiment result (0.5 MPa 8 m)

0.5 MPa 8 m, unit of water height (mm)					
10	18	25	41	45	35
11	17	24	38	46	40
11	14	27	44	50	54
12	19	21	37	51	61
16	17	19	31	49	64
15	13	20	29	46	70
15	15	20	29	46	74
15	14	16	27	43	58
12	16	21	35	45	56
14	15	24	67	41	55
12	15	27	30	41	51
13	14	18	27	38	46
14	17	21	30	41	48
13	17	21	32	46	45
16	20	21	33	52	45
18	18	24	36	47	47
19	18	25	37	45	41
21	18	26	36	35	35
29	25	29	38	33	32
72	20	21	25	32	31

Table 5-18 Sprinkler 3 water distribution experiment result (0.35 MPa 10 m)

0.35 MPa 10 m, unit of water height (mm)					
6	11	10	20	22	22
7	9	13	26	23	31
9	10	13	22	27	44
8	12	16	25	29	34
15	15	17	23	28	41
13	14	13	22	27	42
16	13	15	22	29	47
13	15	16	30	28	36
13	14	13	35	25	39
13	13	15	26	31	39
11	10	14	25	32	41
14	9	13	24	32	37
10	11	10	18	31	40
10	10	8	19	30	37
13	11	12	20	29	34
10	13	12	21	28	36
10	11	16	20	27	32
16	16	19	23	25	32
22	17	20	26	27	26
45	18	18	20	31	35

Table 5-19 Sprinkler 3 water distribution experiment result (0.5 MPa 10 m)

0.5 MPa 10 m, unit of water height (mm)					
5	7	14	23	31	38
5	9	13	21	30	35
6	10	14	19	30	39
8	10	15	19	25	45
10	12	13	24	25	37
12	12	16	19	23	37
15	15	16	17	23	37
15	15	16	16	25	27
13	15	16	9	27	24
12	15	15	22	24	27
10	14	16	16	19	18
12	16	17	22	19	25
11	13	15	21	18	19
11	13	15	17	19	21
12	13	15	16	20	27
12	11	14	18	21	29
15	15	16	19	24	33
14	16	17	26	27	32
25	19	19	26	27	30
45	20	19	23	29	35

Table 5-20 Sprinkler 4 water distribution experiment result (0.35 MPa 10 m)

0.35 MPa 10 m, unit of water height (mm)					
11	16	70	23	38	31
14	18	22	28	38	32
16	27	23	30	39	34
19	20	25	35	42	41
16	23	24	69	46	48
15	23	28	36	45	53
14	39	25	38	47	64
25	19	28	39	47	54
11	18	27	40	46	60
14	18	24	34	48	56
13	15	23	39	45	58
13	18	61	28	45	61
16	18	21	34	45	57
15	20	19	30	44	57
17	20	23	32	42	55
17	21	24	31	41	44
17	20	25	28	35	37
20	19	29	40	34	45
33	22	22	33	30	37
45	24	20	25	29	38

Table 5-21 Sprinkler 4 water distribution experiment result (0.5 MPa 10 m)

0.5 MPa 10 m, unit of water height (mm)					
7	15	21	37	60	30
11	16	25	37	71	40
12	21	29	41	82	47
13	20	27	39	52	73
16	20	28	46	47	66
14	19	24	33	40	67
14	18	22	28	43	73
10	12	22	25	40	48
9	14	20	27	37	51
12	13	8	30	43	47
11	15	19	30	43	53
19	20	25	31	45	48
17	18	20	38	40	46
15	18	26	27	38	47
20	18	22	31	36	45
19	19	23	34	36	49
19	19	24	34	40	44
22	21	26	41	36	42
46	25	5	33	35	37
36	20	22	24	28	35

Table 5-22 Sprinkler 4 water distribution experiment result (0.35 MPa 8 m)

0.35 MPa 8 m, unit of water height (mm)					
20	22	24	27	30	26
19	28	33	39	35	30
22	27	33	40	31	35
26	32	35	44	41	37
23	69	35	46	49	64
19	29	43	51	48	41
19	26	41	57	53	44
18	28	45	63	57	41
19	27	50	75	68	41
23	35	79	79	73	44
20	32	56	86	77	51
23	33	56	87	75	54
23	34	65	86	69	54
29	39	61	81	66	48
30	47	61	69	57	47
30	38	57	65	56	42
30	40	51	54	51	45
22	36	47	54	41	37
37	32	34	39	33	28
54	30	29	26	24	27

Table 5-23 Sprinkler 4 water distribution experiment result (0.5 MPa 8 m)

0.5 MPa 8 m, unit of water height (mm)					
13	47	76	85	69	36
25	41	74	81	62	37
28	44	69	99	60	38
22	40	64	70	45	29
21	32	64	69	39	29
20	33	61	72	43	29
21	36	62	79	47	34
24	38	68	92	52	21
25	40	74	107	67	30
19	34	92	121	83	41
23	44	87	126	92	51
25	50	89	121	98	61
31	54	88	108	94	66
33	54	82	101	91	72
33	56	77	90	86	71
37	52	66	76	76	69
35	49	65	72	62	60
34	44	57	65	53	56
48	43	64	52	47	67
65	44	38	40	36	42

Table 5-24 Sprinkler 4 water distribution experiment result (0.35 MPa 6 m)

0.35 MPa 6 m, unit of water height (mm)					
10	14	19	17	29	21
17	31	28	34	39	26
23	47	37	41	49	34
30	35	43	45	50	41
29	36	43	61	48	39
26	35	47	54	53	36
21	30	46	55	50	41
20	33	46	61	47	32
27	37	55	69	51	25
23	51	76	83	53	31
25	55	93	92	57	31
32	65	99	98	61	3
38	71	119	96	54	35
40	74	113	91	57	33
45	72	88	75	53	38
50	64	70	62	47	41
41	52	56	55	47	38
32	41	48	48	40	37
29	35	33	34	32	85
30	29	30	18	18	96

Table 5-25 Sprinkler 4 water distribution experiment result (0.35 MPa 6 m)

0.2 MPa 6 m TY5332, unit of water height (mm)					
4	2	0	0	6	1
6	2	5	4	5	5
18	8	7	11	21	39
26	24	17	16	24	32
23	24	23	19	25	26
27	18	17	16	22	29
22	19	15	22	25	27
26	20	24	29	34	26
28	31	28	39	40	71
30	38	38	49	49	34
33	43	51	57	55	35
25	44	52	59	51	64
33	45	53	57	50	35
34	38	51	54	46	38
33	40	47	51	44	40
27	36	46	50	44	32
31	36	46	42	39	29
27	32	41	42	36	30
24	25	31	30	27	62
23	27	16	15	21	79

Table 5-26 Sprinkler 5 water distribution experiment result (0.35 MPa 10 m)

0.35 MPa 10 m, unit of water height (mm)					
2	0	0	1	7	7
2	1	2	3	5	8
4	4	3	6	8	10
7	3	7	7	8	10
8	9	10	12	12	13
13	13	11	14	16	15
17	18	16	17	18	16
21	25	22	24	21	15
27	31	29	29	24	16
31	35	5	36	22	14
1	40	39	43	22	17
32	38	46	34	22	14
29	43	48	40	24	20
30	41	54	40	34	26
26	42	55	54	43	32
27	38	45	58	44	36
28	37	46	67	51	39
31	38	52	70	54	43
136	45	52	71	51	88
37	28	34	51	42	38

Table 5-27 Sprinkler 5 water distribution experiment result (0.2 MPa 10 m)

0.2 MPa 10 m, unit of water height (mm)					
0	1	1	1	1	2
0	4	2	0	1	4
1	0	2	2	1	7
1	4	2	3	3	5
4	4	2	4	6	8
5	6	5	7	7	7
7	7	8	8	10	16
10	9	10	9	12	12
13	13	14	15	15	15
18	24	19	15	24	21
52	35	33	21	26	22
22	34	33	38	29	25
21	33	34	30	33	29
19	23	30	36	32	30
16	22	26	40	36	35
18	23	29	38	39	37
21	26	27	37	43	37
23	22	33	46	37	33
53	20	35	40	31	28
51	17	25	27	20	26

Table 5-28 Sprinkler 5 water distribution experiment result (0.35 MPa 8 m)

0.35 MPa 8 m, unit of water height (mm)					
0	5	0	7	12	9
5	0	8	7	5	10
3	5	13	7	9	13
6	12	12	15	11	18
9	10	16	12	15	18
12	21	16	16	17	16
23	25	20	21	24	19
23	33	30	26	23	17
28	41	32	31	24	16
32	44	39	31	21	19
42	48	40	40	20	13
42	50	45	29	20	14
40	56	52	32	26	28
46	51	56	49	30	27
40	49	59	57	39	29
42	46	56	60	43	35
45	53	58	60	45	37
45	52	68	60	42	33
81	50	58	60	34	29
40	34	48	39	26	24

Table 5-29 Sprinkler 6 water distribution experiment result (0.2 MPa 8 m)

0.2 MPa 8 m, unit of water height (mm)					
0	0	0	1	4	8
1	5	2	1	5	8
2	3	3	2	5	10
3	2	1	2	5	9
5	4	6	7	6	11
6	7	5	67	9	12
6	10	8	11	10	15
10	13	11	14	13	11
14	16	16	16	14	13
17	28	22	21	19	13
22	28	30	23	19	14
23	36	35	29	20	14
25	27	38	33	23	23
24	35	39	32	26	18
23	33	37	38	28	24
24	37	37	47	37	29
27	33	35	40	31	29
27	34	41	44	31	25
35	36	50	48	29	23
48	28	25	28	25	23

Table 5-30 Sprinkler 5 water distribution experiment result (0.35 MPa 6 m)

0.35 MPa 6 m, unit of water height (mm)					
1	2	0	0	5	6
1	1	0	1	6	9
1	1	3	2	6	15
3	5	14	6	12	17
7	9	7	11	12	21
10	12	11	16	17	26
17	19	17	19	23	24
26	23	23	27	25	20
32	13	29	35	28	22
38	39	35	32	27	24
39	36	38	35	24	23
38	46	43	35	21	14
47	50	48	34	22	17
43	51	54	42	28	22
38	50	54	50	34	27
39	49	55	58	40	32
37	50	59	57	42	32
35	47	61	65	40	26
34	41	60	57	37	30
61	30	26	38	29	67

Table 5-31 Sprinkler 5 water distribution experiment result (0.5 MPa 6 m)

0.5 MPa 6 m, unit of water height (mm)					
1	0	0	1	5	6
2	0	1	3	7	15
3	1	2	3	9	24
8	3	3	7	11	33
34	9	6	12	18	33
52	15	10	15	26	61
65	21	14	23	29	42
28	24	19	26	33	33
28	26	25	32	34	32
26	26	30	37	35	30
27	32	41	42	35	29
31	41	52	45	32	24
30	49	63	47	34	25
46	60	64	52	38	28
50	66	66	54	41	37
49	62	64	58	41	38
43	56	60	60	40	34
34	44	52	44	32	32
26	32	33	35	23	30
23	22	16	33	20	40

Table 5-32 Sprinkler 6 water distribution experiment result (0.35 MPa 6 m)

0.35 MPa 6 m, unit of water height (mm)					
1	5	3	2	2	2
1	2	5	6	3	2
1	3	9	10	5	4
3	7	19	19	12	6
4	25	28	43	27	12
5	14	33	47	44	20
7	19	44	60	63	32
7	19	58	83	76	42
9	30	69	95	82	50
12	41	80	105	84	42
15	53	95	113	84	44
18	58	105	122	83	44
34	60	108	123	85	52
43	71	111	120	88	58
23	59	108	128	77	55
48	48	84	132	63	61
46	49	66	93	64	44
43	13	62	71	36	28
39	43	43	39	22	35
31	34	40	23	29	58

Table 5-33 Sprinkler 6 water distribution experiment result (0.5 MPa 6 m)

0.5 MPa 6 m, unit of water height (mm)					
5	9	12	10	10	4
12	13	19	16	13	12
16	19	28	32	23	12
15	25	37	45	39	20
9	23	19	58	58	36
6	25	71	73	80	51
3	23	59	88	95	63
11	29	63	96	108	70
8	31	78	107	110	63
10	41	98	126	111	63
18	54	117	140	102	55
21	79	134	165	90	50
37	90	139	159	79	43
60	69	138	147	75	47
58	60	108	143	67	58
48	65	83	130	61	55
53	58	62	88	54	45
54	56	57	70	37	28
37	42	44	39	22	36
27	33	42	22	26	65

Table 5-34 Sprinkler 6 water distribution experiment result (0.35 MPa 8 m)

0.35 MPa 8 m, unit of water height (mm)					
1	1	5	5	4	2
4	8	9	2	8	7
3	4	15	18	8	11
4	13	21	30	20	19
5	20	34	41	30	39
9	27	41	55	44	43
5	17	51	70	52	28
4	22	56	81	69	37
8	25	66	94	78	39
9	29	72	104	81	40
6	32	78	107	81	41
10	42	90	110	82	45
35	60	102	120	75	51
41	67	109	123	73	51
59	58	105	128	70	46
52	53	86	115	63	51
48	53	71	84	51	46
48	40	52	79	35	30
68	40	30	37	19	20
30	24	34	20	26	10

Table 5-35 Sprinkler 6 water distribution experiment result (0.5 MPa 8 m)

0.5 MPa 8 m, unit of water height (mm)					
4	9	15	21	19	11
2	5	22	37	35	20
2	11	37	46	44	27
7	12	39	64	59	35
6	87	40	77	77	39
2	17	48	85	90	52
7	26	52	98	92	56
10	24	66	109	103	51
7	29	73	115	102	52
9	38	90	128	104	53
14	47	104	140	102	53
20	53	110	142	90	50
71	49	112	130	187	48
44	42	93	133	181	53
46	40	79	124	86	61
38	43	66	97	68	61
42	49	55	93	55	50
38	48	53	95	48	36
59	56	41	47	26	23
26	29	35	30	29	14

Table 5-36 Sprinkler 6 water distribution experiment result (0.35 MPa 10 m)

0.35 MPa 10 m, unit of water height (mm)					
2	5	5	7	8	2
3	5	16	16	15	10
3	13	21	24	20	12
2	7	25	30	26	13
10	12	30	44	39	22
4	12	35	52	50	29
4	13	38	64	62	42
5	12	36	68	74	47
11	15	40	76	82	53
4	18	46	83	85	59
6	21	49	82	90	66
9	22	50	90	97	72
12	31	67	100	102	81
25	45	68	102	102	75
17	44	66	100	89	68
37	37	55	89	79	61
35	40	51	73	62	54
33	36	47	74	55	45
58	34	37	51	37	30
31	34	40	33	38	20

Table 5-37 Sprinkler 6 water distribution experiment result (0.5 MPa 10 m)

0.5 MPa 10 m, unit of water height (mm)					
3	4	13	19	17	18
4	13	24	27	35	26
3	8	32	38	43	34
7	14	60	49	59	51
4	13	29	54	68	56
2	15	29	63	76	73
3	11	38	69	82	82
3	12	44	72	82	69
2	10	43	78	81	75
4	11	45	74	86	83
6	16	46	75	87	88
7	25	47	73	90	82
17	28	36	71	94	77
24	23	34	69	86	75
50	30	32	66	80	65
28	35	67	54	71	60
24	30	37	54	59	51
20	31	37	67	62	36
49	30	32	46	40	31
15	19	27	26	33	29

Table 5-38 Sprinkler 7 water distribution experiment result (0.35 MPa 10 m)

0.35 MPa 10 m, unit of water height (mm)					
9	16	23	26	15	22
12	21	19	30	28	33
10	16	23	25	33	44
10	14	25	26	36	53
11	11	17	27	35	36
16	11	16	25	34	45
9	9	17	24	36	61
8	11	16	26	39	54
11	9	16	27	44	55
10	12	15	26	47	62
12	13	19	34	42	59
15	19	24	38	40	57
22	23	36	35	40	49
17	21	34	36	45	48
18	21	27	39	51	48
15	18	22	32	46	43
11	16	23	31	37	36
7	106	17	26	30	31
36	24	17	21	25	27
17	14	11	21	19	24

Table 5-39 Sprinkler 7 water distribution experiment result (0.35 MPa 10 m)

0.5 MPa 10 m, unit of water height (mm)					
7	9	18	33	24	37
14	6	23	59	30	65
8	12	17	28	39	75
7	11	14	56	37	80
9	11	17	27	36	83
8	11	16	26	37	58
9	7	14	24	32	56
9	11	15	22	33	47
9	11	15	22	30	44
8	15	21	31	31	41
11	15	26	34	36	42
14	23	30	35	39	43
16	21	35	139	43	46
21	26	36	141	44	51
17	24	31	40	50	52
18	22	32	36	50	53
10	13	21	32	36	43
10	14	14	23	31	38
33	24	13	14	19	29
17	18	10	15	22	30

Table 5-40 Sprinkler 7 water distribution experiment result (0.35 MPa 10 m)

0.35 MPa 8 m, unit of water height (mm)					
18	20	25	25	22	14
13	18	23	28	25	20
14	19	25	36	29	24
12	28	28	74	35	23
8	25	33	37	40	29
9	17	28	36	42	43
13	17	27	38	45	64
10	16	25	39	51	61
12	17	27	46	56	66
12	14	25	48	65	68
14	18	25	49	66	66
20	22	30	45	65	61
22	25	37	49	60	58
21	27	35	55	56	59
21	24	36	64	49	53
19	28	36	45	48	41
16	22	32	37	37	31
14	18	21	29	29	27
11	13	20	21	21	27
7	42	17	25	18	36

Table 5-41 Sprinkler 7 water distribution experiment result (0.5 MPa 8 m)

0.5 MPa 8 m, unit of water height (mm)					
11	24	33	38	34	17
21	25	34	45	40	20
13	18	42	50	43	26
10	22	30	10	53	36
14	37	27	47	59	55
10	14	30	48	67	73
8	17	26	49	75	91
9	12	28	47	79	81
9	13	31	43	80	80
11	18	35	42	70	76
15	21	31	41	64	66
19	26	35	48	60	67
22	30	43	53	65	71
24	31	47	56	64	65
31	35	41	59	63	54
24	32	40	53	54	46
17	28	34	41	42	38
14	18	29	35	32	32
8	13	64	27	26	63
13	15	15	24	22	43

Table 5-42 Sprinkler 7 water distribution experiment result (0.35 MPa 6 m)

0.35 MPa 6 m, unit of water height (mm)					
22	23	25	27	23	20
24	25	30	30	26	14
23	29	31	35	29	16
24	31	40	35	28	15
27	30	39	38	32	22
24	49	43	47	31	25
24	35	54	53	33	31
25	37	62	62	45	24
27	43	70	76	56	35
26	43	75	96	70	47
27	44	85	104	75	57
29	51	94	97	69	56
34	57	91	83	52	42
37	90	82	68	42	35
38	46	65	67	36	28
38	45	51	55	31	18
33	37	6	35	29	45
23	29	30	28	26	23
17	22	26	21	24	15
11	18	20	25	16	14

Table 5-43 Sprinkler 7 water distribution experiment result (0.5 MPa 10 m)

0.5 MPa 6 m, unit of water height (mm)					
25	35	10	44	33	10
25	135	51	51	30	13
26	39	53	51	31	15
27	37	56	57	7	15
27	36	63	62	38	20
25	43	70	73	46	28
21	35	73	82	58	36
20	35	72	100	75	40
20	41	77	107	86	53
23	53	89	100	77	61
26	65	106	96	69	50
32	67	110	95	60	42
41	75	101	85	51	36
49	44	92	70	42	29
52	60	18	67	37	32
47	153	15	58	35	39
38	45	34	38	33	8
27	34	45	29	28	25
14	26	53	22	24	20
13	18	61	22	20	16

Table 5-44 Water distribution ability under different operating pressures of a portion of the sprinklers

Water Distribution Ability Sprinkler Number	Installation Height 8m Sprinkler Operating Pressure 0.5 MPa	Installation Height 10m Sprinkler Operating Pressure 0.5 MPa	Installation Height 6m Sprinkler Operating Pressure 0.5 MPa
1	Satisfactory	Good	Good
2	Good	Satisfactory	Satisfactory
3	Satisfactory	Bad	Satisfactory
4	Satisfactory	Satisfactory	Bad

Table 6-1 Relationship among outlet size, flow coefficient and flow proportion

Discharge port diameter	Nominal Diameter	Category of port diameter	K	Flow rate %	Thread Size
12.7	12	standard	80	100	15
13.5	20	large	115	140	15 or 20
15.9		Super Lagrge	160	200	15 or 20

Table 8-1 Penetrability of three types of typical sprinkler heads

No	Operating Pressure （MPa）	Penetrability (Straight Line Placement)	Penetrability (Stacked Placement)	Penetrability (One on Top, Two Below)
1	0.5	0.94	0.91	0.75
4	0.5	／	／	0.90
6	0.5	0.37	0.38	0.37

Note: “/” Means not doing test in this situation.